CHARACTERIZATION OF RAD23, AS A SHUTTLE FACTOR

By

EVELYN IFEOMA OKEKE

A dissertation submitted to the

School of Graduate Studies

Rutgers, The State University of New Jersey

In partial fulfillment of the requirements

For the degree of

Doctor of Philosophy

Graduate Program in Biochemistry

Written under the direction of

Kiran Madura

And approved by

_____

_____

_____

_____

New Brunswick, New Jersey

October 1, 2019

ABSTRACT OF THE DISSERTATION

Characterization of Rad23, as a shuttle factor

By EVELYN IFEOMA OKEKE

Dissertation Director:

Kiran Madura

The ubiquitin proteasome pathway (UPP) is the primary proteolytic system for the spatial and temporal elimination of intracellular proteins, and is conserved from yeast to humans. Proteins that are targeted for degradation become covalently linked to a small protein called ubiquitin and are subsequently degraded by the 26*S* proteasome. Key enzymes of this pathway and their function are well characterized, but the regulation of its activities is not well understood. For instance, it is widely believed that nuclear proteins are degraded inside the nucleus despite the evidence that some nuclear proteins are degraded following their export. There were a number of discoveries regarding the site of protein turnover. *First*, the Madura group and others reported that the degradation of some nuclear proteins required export from the nucleus. *Second*, substrates were stabilized inside the nucleus when nuclear export was blocked, strongly suggesting that proteasomes do not operate inside the nucleus. *Third*, it was reported that

catalytically active proteasomes exist predominantly in the cytosol, since purified nuclei lacked proteasome peptidase activity. *Fourth*, it was determined that Sts1 plays a central role in proteasome localization. Through its interaction with Srp1 (an importin-α protein), and Rpn11 (a 19*S* proteasome subunit), Sts1 appears to localize proteasomes to the nuclear surface. *Fifth*, Srp1 was shown to harbor two distinct functions; it can act as nuclear import factor, and can tether the proteasome to the nuclear surface. These findings provide a basis for a mechanism for targeting proteasomes to the nucleus. *Sixth*, Rad23 functions as a shuttle factor that can translocate ubiquitylated proteins to the proteasome, and is known to control the stability of the nuclear protein Rad4. The shuttle factor Rad23 is present in both the nucleus and cytosol. This suggests that Rad23 might deliver nuclear substrates to cytosolic proteasomes. Using two genetic mutants, I tested this hypothesis and found that Rad23 bound high levels of polyUb substrates when it was trapped inside the nucleus. In contrast, when it was trapped in the cytosol it interacted with low levels of polyUb substrates. Whereas previous studies examined artificial substrates, I confirmed this binding pattern using the physiological substrate Ho-endonuclease (Ho), which functions in mating type switching in yeast. Therefore I propose that the function of Rad23 is to deliver nuclear substrate to proteasomes in the cytosol. The mode of nucleocytoplasmic trafficking of Rad23 remains to be discovered.

ACKNOWLEGMENTS

First and foremost, I have to thank Veli for everything. It is because of him that I feel home, that my life is so much sweeter, and that I am able to make my dreams come true. He has given me endless support; emotionally, financially and otherwise. His unconditional love helps me grow emotionally and personally. I especially thank him for his shared wisdom, positive outlook on life and his ability to make light of any situation that is less than ideal. Furthermore, I appreciate him taking me on short, or long, or far away vacations, just so that I could take my mind off PhD things for a little while and relax. I feel truly blessed to have such a wonderful person by my side to walk this beautiful earth.

Second, I want to thank my advisor and lab members. I want to thank Dr. Madura for the opportunity to come to his lab and “try out” science. He warned me that there would be times during which it would not be easy walking the path of a graduate student. I had no idea it would be that grueling at times, but he made this process enjoyable overall. His continued assistance and guidance was very much appreciate and led to me to the ultimate success. Thank you for believing in me! Also, I want to thank Li Chen, who is a true asset to the Madura lab, for “ALL” the support/advise/help one can ask for. Li was instrumental in my success as a PhD student. I also enjoyed our “Monarch butterfly side gig”, which included going on field trips to collect milkweed, caterpillars and seed pods, all while being stung by mosquitos or rained on. It brought me so much joy seeing her becoming infected with the “butterfly fever”.

Third, I want to thank my committee members, Dr. Marc Gartenberg, Dr. Beatrice Haimovic, and Dr. Smita Patel. They all contributed a great deal of time and intellect towards my thesis project. I want to especially thank Dr. Gartenberg, who displayed great patience with me. I always looked forward meeting with him, because I knew I would learn something new; yeast genetics and all, and sometimes about unrelated things, such as a resident bald eagle in Johnson Park, NJ. Nevertheless, I would appreciate it all. Thank you to Melinda Borrie, now a postdoctoral fellow in the Gartenberg lab, who was always ready to help me either trouble shoot my experiments, or brain storm some new ideas. I also appreciate the Gartenberg Lab's generosity when using their lab equipment and supplies. Also, I want to especially thank Dr. Haimovic. She has been tremendously generous with her time and support/advise. What I appreciate the most is her pushing me beyond my comfort zone. I understand today that this is where real growth occurs. I appreciate the many lunches during which she took the time to explain things that would help me progress. She is an absolutely invaluable addition to my thesis committee.

Fourth, I want to thank three very special people that I got to know during my time at Rutgers; Dr. Jerome Langer, Dr. Loren Runnels, and Dr. James Millonig. All added enormous value to my experience in graduate school, but they also contributed a great to deal to my personal growth. It is because of these three that I would do the whole "PhD thing" again. Dr. Langer were introduced to me as my first year advisor. I remember him saying that everyone needs that special person in grad school (a shoulder to cry on), and if I wanted, he could be that

person for me. I want to thank him for always being there for me either with encouraging words when I was on the verge of giving up or with a warm hug when I just needed to be reminded that life is good. I want to thank Dr. Runnels, the greatest mentor walking, for unfailingly provide assistance/advise when things turned “south”. He has great compassion for students, and I truly appreciate his efforts to create a nurturing grad school environment. In the future, I hope that there will be many more students impacted by his great mentorship. Furthermore, I want to thank Dr. James Millonig. I don’t remember how our relationship started, but I knew once I found this treasure that I had to hold on to it. Dr. Millonig gives the greatest advices and support. He unfailingly provided me with positive and encouraging words to “build back up” my confidence, and to remind of the important things in life. Dr. Millonig has a special place in my heart.

Last, but certainly not least, I want to thank my family and friends. I want to thank my mom for simply everything. My mom is the best, of course. She has always been there for me with a listening ear and the greatest advice. There is nothing better than mom trying to shine some light on your path, just so you can see a little better. I also want to thank my brother and sisters, who kept me company during hours on end phone calls discussing everything and anything. Thank you also for always willing to make the trip over the big ocean to come visit me. While visiting, they would make sure to create awesome memories. Memories, I would feed off on until their next visit. I feel blessed to have such loving siblings. Also, I want to especially thank Olufunmilola Ibironke, my dear friend and lab neighbor, who has never failed to take time out of her busy life to help me solve

any of my problems; professionally and personally. I feel blessed to have her in my life.

DEDICATION

To my mother who is kindest, most giving and strongest person there is. Knowing that your life has been nothing but easy, you never failed to make sure your children are taken care of. I owe you everything.

.

TABLE OF CONTENTS

ABSTRACT……ii

ACKNOWLEGMENTS……iv

DEDICATION……viii

LIST OF FIGURES……xi

LIST OF TABLES……xiii

CHAPTER I – Introduction

1.1 The Ubiquitin Proteasome System……2

1.2 Ubiquitin……5

1.3 E1, E2, E3 Enzymes……6

1.4 Polyubiquitin Chains……8

1.5 De-Ubiquitylating Enzymes (DUbs)……9

1.6 The 26*S* Proteasome……13
1.6.1 The 19*S* Proteasome (Regulatory Particle)……14
1.62 The 20*S* Proteasome (Core Particle)……16

1.7 Ubiquitin-like Proteins……20
1.7.1 Ubiquitin-Like Modifiers (ULMs)……22
1.7.2 Ubiquitin-Domain Proteins (UDPs)……23
1.7.3 Rad23 and its Role in DNA Repair……24
1.7.4 Rad23 and its Role in the UPP……26

1.8 Degradation of Nuclear Substrates Requires Export from Nucleus…31

1.9 Summary……37

CHAPTER II – Materials and Methods

2.1 Strains and Media……40

2.2 Ho-HA Plasmid construction……42

2.3 Protein Stability Measurements……48

2.4 Preparation and Quantification of Yeast Cell Lysate……48

2.5 Immunoprecipitation……50

2.6 SDS Page and Electrotransfer……..……..……..51

2.7 Immunoblotting…….…..52

2.8 Microscopy……..…..55

CHAPTER III – Experimental Results

3.1 Experimental Results……...…57
3.1.1 Rad23 binds high levels of polyUb substrates in the nucleus……..…59
3.1.2 Rad23 binds low levels of polyUb species in the cytosol……..…67
3.1.3 Rad23 with defective UbL and UBA domains displays the same subcellular localization as the wildtype Rad23 protein ……..….....74
3.1.4 Ddi1 shows same pattern of localization and polyUb substrate binding as Rad23 in *sts1-2* and *rna1-1*……..76
3.1.5 The localization of Rad23 affects turnover of Ho-endonuclease……84
3.1.6 The degradation of some nuclear substrates involves the nucleocytoplasmic transport system…….....89
3.1.7 Rad23 is the major shuttle factor that traffics Ho-endonuclease…….97
3.1.8 Rad23 interaction with Ho-endonuclease is altered by its subcellular location…….…….....109
3.1.9 Subcellular distribution of Ub is affected in *sts1-2* and *rna1-1*……..115

CHAPTER IV – Summary/Discussion

4.1 Summary……..117

4.2 Discussion……...120
4.2.1 Nuclear substrates are exported from the nucleus……120
4.2.2 Proteasome is predicted to be located on the nuclear surface……..122
4.2.3 Proteasome is targeted to the nuclear surface……124
4.2.4 The role of shuttle factors…….....126

BIBLIOGRAPHY……..…132

APPENDIX I……..……145

APPENDIX II……150

LIST OF FIGURES

Figure 1. Schematic of the enzymatic cascade of ubiquitylation and degradation by the proteasome……..……..……..12
Figure 2. Proteins in the UbL protein family and their main characteristic……...21
Figure 3. Schematic of domains in Rad23, Ddi1, and Dsk2 that are of significance in the UPP……..……27
Figure 4. Model of localization of UPP components……...……32
Figure 5. Previously cloned Rad14 is removed upon restriction digest using the enzymes EcoR1 and Kpn1……..…..……...44
Figure 6. PCR generated Ho fragment is cloned into previously Ecor1 and Kpn1 digested vector……..……45
Figure 7. Newly generated gene Ho-HAHA is excised using restriction enzymes EcoR1 and Xba1……..……..…..46
Figure 8. Excised, and purified Ho-HAHA fragment is ligated into empty vector containing *GAL1* promoter to generate EOP85……..……...47
Figure 9. Model of transport mechanism of nuclear substrates……...58
Figure 10. Proteasome is mislocalized in *sts1-2*……..……60
Figure 11. Rad23 is enriched in the nucleus in *sts1-2*……..……63
Figure 12. Rad23 protein levels are not affected in *sts1-2*……..…..64
Figure 13. Rad23 interaction with polyUb substrates is higher in the nucleus…..65
Figure 14. Rad23 is enriched in the cytoplasm in *rna1-1*……..……70
Figure 15. Rad23 protein levels are not affected in *rna1-1*……..……...71
Figure 16. Rad23 interaction with polyUb substrates is lower in the cytosol…..…72
Figure 17. Mutant Rad23 is enriched in the nucleus in *sts1-2* and in the cytosol in *rna1-1*……..……..…75
Figure 18. Ddi1 is enriched in the nucleus in *sts1-2*……...79
Figure 19. Ddi1 protein levels are not affected in *sts1-2*……..…..…..80
Figure 20. Ddi1 is enriched in the cytoplasm in *rna1-1*……81
Figure 21. Ddi1 protein levels are not affected in *rna1-1*……..……82
Figure 22. Ddi1 interaction with polyUb substrates is decreased in the cytosol….83
Figure 23. Matα2 accumulates in the nucleus in *sts1-2*, but localizes to the cytosol in *rna1-1*……86
Figure 24. Clb2 is stabilized in *sts1-2*……...88
Figure 25. Ho-endonuclease accumulates inside the nucleus in *sts1-2*……..…..90
Figure 26. GFP-Ho turnover not affected in *STS1* and *sts1-2* at 21°C……..…91
Figure 27. GFP-Ho is stabilized in *sts1-2* at 37°C……..……92
Figure 28. GFP-Ho accumulates in the cytoplasm in *rna1-1*……...94
Figure 29. GFP-Ho turnover not affected in *RNA1* and *rna1-1* at 21°C……95
Figure 30. GFP-Ho is stabilized in *rna1-1* at 37°C……..…..96
Figure 31. Rad23 is a major shuttle factor for Ho-endonuclease……..……..99
Figure 32. Ho is a substrate of the proteasome……...101
Figure 33. UBA domains do not exhibit substrate specificity……105
Figure 34. Rad23 binds Ho predominantly through its UBA1 domain……..108
Figure 35. Rad23 interaction with GFP-Ho is increased in the nucleus…….....110
Figure 36. Rad23 interaction with GFP-Ho is decreased in the cytosol……112

Figure 37. GFP-UbL localizes to the cytosol……....147
Figure 38. GFP-Ho is stabilized in the presence of GST-UbL……..……148
Figure 39. UBA1 domain in Rad23 primarily interacts with Ho and polyUb substrate……....149

LIST OF TABLES

Table 1. *S. cerevisiae* strains used in this study……..…….41
Table 2. Plasmids used in this study……..……..41
Table 3. Antibodies uses in this study……..……...54

Chapter I

INTRODUCTION

1.1 The Ubiquitin Proteasome System

The expression of genes is tightly controlled to permit optimal growth, and response to external stimuli. Therefore, it is of utmost importance to not only regulate the timing and levels of protein expression, but also their elimination when necessary. Thus, cellular homeostasis reflects a careful balance of synthesis and degradation that carefully controls the levels of key factors, including mRNA and protein.

All proteins are continually degraded into their constituent amino acids and replaced by new synthesis (Lecker et al., 2006). Although, it may seem wasteful to continually break down proteins, it serves an important homeostatic function (Lecker et al., 2006). The stability of proteins in different cellular compartments, such as the nucleus, mitochondria, and cytoplasm, are regulated independently, and can differ from minutes for some regulatory protein, such as cell cycle proteins, to weeks for proteins functioning in skeletal muscle, such as actin and myosin (Lecker et al., 2006). Hemoglobin in red cells can even function for months before they become replaced (Lecker et al., 2006). However, the rate of degradation and synthesis has to be regulated precisely because even a small imbalance can have deleterious effects (Lecker et al., 2006).

There are two major pathways in eukaryotes that degrade cellular proteins. One is the ubiquitin proteasome pathway (UPP), and the other is through autophagy by the lysosome (Lilienbaum, 2013). The UPP is the primary proteolytic system degrading 80-90% of the intracellular proteins, including damaged, and native proteins that are no longer required (Lilienbaum, 2013). In contrast,

autophagy by lysosomes is mainly responsible to degrade long-lived, and aggregated proteins, as well as cellular organelles, such as mitochondria (Lilienbaum, 2013). Nevertheless, both pathways are critically important for the maintenance of cellular homeostasis (Lilienbaum, 2013).

There are several examples that demonstrate the importance of a protein degradation system. For instance, the age-related decrease in proteasomal activity is marked by a deteriorating capacity to remove unwanted proteins, which is linked to disease (Lilienbaum, 2013). Another common age-related feature of a deficient degradation process is the accumulation of Ub-tagged proteins, whose failure to be degraded can cause toxicity (Lilienbaum, 2013). Diseases associated with the aggregation of ubiquitylated substrates include Alzheimer's disease, Parkinson's disease, and prion disease (Lilienbaum, 2013). In cardiomyocytes, a dysfunction in UPP is associated with a variety of cardiac pathophysiologies, such as heart failure and cardiac hypertrophy (Depre et al., 2006; Pagan et al., 2013). There are many factors that may contribute to a dysfunctional UPP, including reduced synthesis of proteasomes, chronic exposure to free radicals, and accumulation of genetic errors (Lilienbaum, 2013). UPP related pathophysiologies have been studied extensively in cancer biology. This has led to the development of therapeutic drugs that inhibit the proteasome (Almond et al., 2002). By reducing the degradation of key cell cycle regulators, proteasome inhibitors slow the proliferation of cancer cells (Almond et al., 2002). These examples illustrate the importance of a functional degradation system.

The UPP is conserved from yeast to humans, and its involvement in other important cellular processes, including DNA repair, cell cycle control, transcription, and apoptosis, has been well described (Lecker et al., 2006; Lilienbaum, 2013). It consists of a coordinated cascade of enzymatic activities that result in the attachment of the small molecule ubiquitin (Ub) to a proteasomal substrate (Hershko et al., 1983). This initial Ub is extended into a polyubiquitin (polyUb) chain. This posttranslational modification targets the substrate to the proteasome for degradation (Hershko et al., 1983). The polyUb chain is recognized by subunits within the 26S proteasome, a large, multi-subunit protein complex that degrades substrates and recycles Ub.

The Noble Prize in Chemistry in 2004 was awarded to Aron Ciechanover, Irwin Rose, and Avram Hershko for their characterization of this proteolytic system (https://www.nobelprize.org/prizes/chemistry/2004/summary/). In the late 70s, in collaboration with each other, Rose, Hershko and Ciechanover began studying the previously discovered protein of yet unknown function: Ubiquitin. They discovered that the attachment of Ub to a substrate was required for its degradation by a large complex called the proteasome. They also found that multiple Ub's were covalently linked into a chain that was essential for substrate turnover. Hershko and co-workers discovered the enzymes that conjugate Ub to artificial substrates (Hershko et al., 1983). The discovery and characterization of this mechanism led to an understanding of numerous other pathways that also involve similar targeting events.

1.2 Ubiquitin

Ub is a highly conserved 76 amino acid protein and differs in only three positions between yeast and human (Komander et al., 2012). Its C-terminus ends with a critical glycine (G) residue that is preceded by an arginine and glycine (RG) (Pickart et al., 2004). This (R-G-G) motif is essential for Ub interactions with key enzymes in the pathway, for its eventual ligation to a substrate, and in the formation of a polyUb chain (Pickart et al., 2004). The R-G-G motif is required for forming a thiolester linkage with enzymes participating in the conjugation machinery. However, Ub is linked by an isopeptide bond to substrates, and to additional Ubs in a polyUb chain. In all these covalent interactions the terminal residue G-76 participates in the covalent bond (Pickart et al., 2004; Lecker et al., 2006; Komander et al., 2012).

Ub contains several lysine residues (K-6, K-11, K-27, K-29, K-33, K-48, and K-63) that are present on its surface (Lecker et al., 2006; Finley et al., 2012). A number of these lysine residues have been shown to participate in polyUb chain assembly and other assembly variations (Lecker et al., 2006). In some instances, Ub is attached to a substrate, and remains a monomer. Substrate monoubiquitylation is believed to have a regulatory significance (Hicke et al., 1996). Specific surface residues on Ub come together to create hydrophobic patches that are recognized by Ub binding partners (Komander et al., 2012). These hydrophobic patches are essential for protein-protein interactions (Komander et al., 2012).

Because of Ub's reactive C-terminus, it is always expressed as a fusion protein that blocks the terminal residue. Ub is expressed as a chain of tandemly linked proteins, or as an N-terminal fusion to specific ribosomal subunits (Lecker et al., 2006). In yeast four Ub fusion proteins are expressed, including Ubi1, Ubi2, Ubi3 and Ubi4 (Finley et al., 2012). *UBI1, UBI2,* and *UBI3* are fused to ribosomal protein subunits and provides Ub in normal growing cells. Their fusion to ribosomal proteins can regulate the assembly of ribosomes (Finley et al., 1987). The *UBI4* gene is specifically activated during stress responses, and results in six tandem repeats of Ub (Ozkaynak et al., 1984). Ub becomes active only after cleavage from the fusion product (Lecker et al., 2006).

1.3 E1, E2 and E3 Enzymes

The attachment of Ub requires a cascade of several enzymatic reactions (Pickart et al., 2004). The first step is carried out by the Ub-activating (E1) enzyme that catalyzes the activation of the Ub's C-terminal in an ATP dependent manner (Lecker et al., 2006). In the budding yeast, there is only one known E1, encoded by the *UBA1* gene expressing an abundant 114 kDa protein (McGrath et al., 1991). Uba1 uses ATP to form a Ub-AMP intermediate with the C-terminal glycine in Ub. This step initiates the formation of an intramolecular thiolester linkage with a Cysteine (C) residue in E1 (McGrath et al., 1991).

The activated thioester-bound Ub is transferred to an active site cysteine residue in a Ub-conjugating (E2) enzyme (Lotz et al., 2004). E2 enzymes are

generally smaller than E1, with an average size of 21kDa. The catalytic Cysteine residues in E2 enzymes are highly conserved (Lotz et al., 2004; Lecker et al., 2006). In yeast, there are 11 unique E2s that can conjugate Ub to substrates. The large number of E2 enzymes can extend the range of substrate-targeting specificity (Lecker et al., 2006).

The transfer of Ub from the E2 to a substrate involves an isopeptide bond (Lecker et al., 2006; Herrmann et al., 2007). This step can be catalyzed directly by the E2 enzyme or by an associated Ub (E3) ligase (Lecker et al., 2006). E3-ligases are the key factors in substrate recognition, and they make up the largest group of proteins involved in the ubiquitylation process (Lecker et al., 2006; Finley et al., 2012). There are close to 100 E3-ligases in yeast. (Finley et al., 2012). It is believed that the formation of distinct E2-E3 complexes greatly increases the specificity of substrate-targeting (Pickart et al., 2004; Lecker et al., 2006).

E3's can be grouped into two general structural classes: HECT domain E3s and RING domain E3s (Finley et al., 2012). Most E3s belong to the RING family of E3-ligases. Only five HECT domain E3s have been identified in yeast (Finley et al., 2012). RING domain E3s enable Ub to be transferred from the E2 to the lysine acceptor residue in the substrate (Finley et al., 2012). Thus, the E2 directly facilitates the formation of the isopeptide linkage with the substrate, whereas the RING domain E3s activate E2 for ubiquitylation of the substrate (Finley et al., 2012). In contrast, HECT E3s possess a Cysteine residue in their active site that receives Ub from the E2. The Ub is then attached to the substrate directly by the HECT E3 (Finley et al., 2012). HECT E3s have a modular structure in the

approximate 350 residue catalytic domain. The N-terminal lobe of the HECT domain is involved in interacting with the E2s, whereas the C-terminal lobe binds substrates (Finley et al., 2012). Once Ub has been conjugated to a substrate the polyUb chain is assembled in a mechanism that is poorly understood.

1.4 Polyubiquitin Chains

The assembly of a polyUb chain requires conjugation of multiple Ubs *via* specific lysine residues (Finley et al., 2012). The type of linkage (and length) exerts distinct regulatory signals, although most depict a degradation signal (Finley et al., 2012). Studies of the polyUb chain structure revealed that the different types of linkages created distinct chain conformations (Finley et al., 2012; Komander et al., 2012). The topology of polyUb chains is expected to differ when (1) a chain is formed with a homogenous linkage to a specific lysine residue, (2) a polyUb chain is formed using different lysine residues (mixed linkage), (3) a branched polyUb chain, and (4) an unanchored polyUb chain (Komander et al., 2012). The topology of polyUb chains will determine if neighboring Ubs can form electrostatic interactions to form a stable “compact” structure. Other linkages favor an “open” conformation (Komander et al., 2012). It is estimated that ~ 30% of linkages occur through K-48, 28% through K-11, and 16% through K-63 (Finley et al., 2012). The K-48 linkage chain, as well as the K-11 and K-6 linkage adopt a compact conformation in which a hydrophobic patch centered on Ile-44 are aligned to form a targeting surface for protein interactions (Hicke et al., 2005). In contrast, a polyUb

chain assembled through K-63 adopts an open conformation in which the hydrophobic patches in Ub are not clustered (Komander et al., 2012). Binding partners of these open conformation chains may exploit the flexibility and distance between chain moieties instead of recognizing a distinct stretch of hydrophobicity on Ub's surface, (Komander et al., 2012). It is poorly understood how the length and topology of the polyUb chains is controlled. However, there is some evidence that the E2 enzymes take on that role in conjunction with binding partners, such as E3 (Komander et al., 2012). It is thought while the E3 is responsible primarily for substrate recognition, the E2 enzyme recognizes distinct surface lysine residues on Ub (Komander et al., 2012). Not every E2 can recognize the same lysine residue. Therefore, a specific E2-E3 complex may be required for the selection of the appropriate lysine to generate a particular topology (Komander et al., 2012). Once the chain has been assembled, its interaction with regulatory proteins that bind polyUb chains are likely to mediate the functional effect of a specific chain. Specifically, substrates conjugated to polyUb chains assembled *via* a K-48 linkage are guided to the proteasome for degradation, whereas a K-63 chain controls ribosome efficiency, and internalization of cell surface receptors (Spence et al., 1995).

1.5 De-Ubiquitylating Enzymes (DUbs)

De-ubiquitylating enzymes (DUbs) are required for the processing of Ub fusion proteins that are the only source of Ub in the cell (Finley et al., 2012). DUbs

are responsible for releasing the Ub from the precursor fusion, as mentioned above, although it is not known which DUbs play a key role in this process (Finley et al., 2012).

DUbs are also required for reversing substrate ubiquitylation (Komander et al., 2012). DUbs make up a large and diverse protein family that recognize distinct polyUb chains linkages, and topologies (Tanaka et al., 1998; Komander et al., 2012). The twenty DUbs in yeast are categorized into four families: (1) the Usp family with 16 members (2) the Otu family with two members (3) JAMM family with one member and (4) Uch family with one member (Finley et al., 2012). Each family exhibits a different selectivity and function in the de-ubiquitylation process. Some DUbs function in chromatin remodeling, such as Ubp8, and others function specifically on the endosome, for instance Ubp4 (Finley et al., 2012). All DUbs are Cysteine proteases that specifically hydrolyze the amide bond immediately after the C-terminal Gly-76 residue in Ub (Glickman et al., 2002). Although the Dub's hydrolyze the Ub linkage in an identical chemical mechanism, they interact with their substrate in different ways (Clague et al., 2019). For instance, some DUbs interact with substrates *via* a specific domain in the DUb that is distinct from the catalytic domain (Clague et al., 2019). Other DUbs show selectivity for a specific polyUb chain topology (Clague et al., 2019). Some Dubs can dismantle all but the last (substrate-linked) Ub in a polyUb chain (Clague et al., 2019). The resulting monoubiquitylated substrate is recognized by a distinct DUb (Clague et al., 2019).

DUbs plays an important role in controlling the concentration of free Ub, and the stability of substrates (Glickman et al., 2002). One important function of DUbs

is to recycle Ub by removing Ub from the target protein as it is being processed for degradation (Finley et al., 2012). The key DUbs in yeast that release Ub from substrates that have arrived at the proteasome are Rpn11, Ubp6, and Doa4 (Swaminathan et al., 1999; Amerik et al., 2000; Leggett et al., 2002; Chernova et al., 2003; Hanna et al., 2003; Hanna et al., 2007; Kimura et al., 2009). While Rpn11 and Ubp6 remove Ub from substrates at the proteasome, Doa4 removes Ub from membrane proteins that are internalized by multivesicular bodies and targeted to the lysosome (Finley et al., 2012). Both, Rpn11 and Ubp6 may release Ub as intact chains, rather than sequentially dismantling the polyUb chain (Glickman et al., 2002). However, there are DUbs, such as Ubp14, that only dismantle unanchored chains (Glickman et al., 2002). Interestingly, the DUb Doa4 can do both, remove chains that are attached to substrates, and disassembly an unanchored chain (Glickman et al., 2002). In addition, some DUbs specialize in cleaving monoubiquitin from substrates, while others may modify existing chains by cleaving within the chain (Clague et al., 2019). Overall, the unique substrate specificity of DUbs underscores their remarkable functional diversity (Finley et al., 2012).

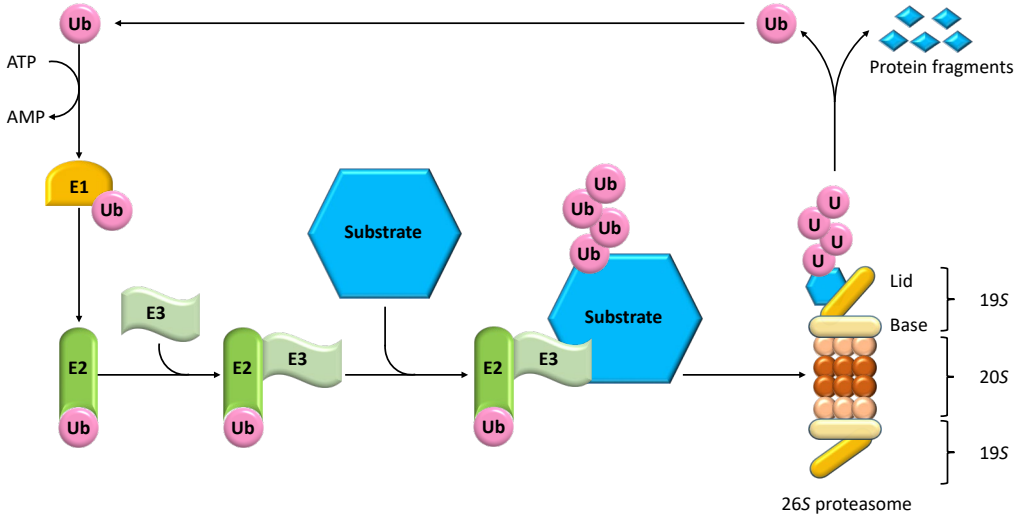

adapted from Rahimi, 2012

Figure 1. Schematic of the enzymatic cascade of ubiquitylation and degradation by the proteasome. Ub is activated by E1, the Ub-activating enzyme, in an ATP-dependent manner, and then transferred to an E2, the Ub-conjugating enzyme. E2 associates with an E3-ligase, and together they transfers the activated Ub moieties to a substrate bound E3. PolyUb chain extension occurs, which is recognized by the 26S proteasome where the protein becomes degraded, but the Ubs are recycled (Rahimi, 2012).

1.6 The 26*S* Proteasome

The proteasome is a large multi-subunit protein complex that serves as a major site for intracellular protein degradation. The proteasome can be found in all archaea and eukaryotes, and in certain bacteria (Darwin, 2009). Although the bacterial and archaeal proteasomes are much simpler than eukaryotic proteasome, the structure of this protease complex has been conserved over the course of evolution (Humbard et al., 2013). In eukaryotes, many proteins have been shown to be degraded in a Ub-proteasome dependent manner. In contrast, Ub and the Ub-conjugating system do not exist in bacteria or archaea, thus the targeting of substrates involves a different mechanism. Although, recently a Ub-like protein called Pup (prokaryotic Ub-like protein), was found to target proteins for proteasomal degradation in *mycobacterium tuberculosis* (Pearce et al., 2008). This strengthens the idea that post-translational modifications are an evolutionarily conserved mechanism that marks proteins for proteasomal degradation.

The fully assembled 26*S* proteasome is an approximately 2.5 MDa complex that consists of at least 33 individual subunits (Glickman et al., 2002). It is a complex protease, and all subunits are highly conserved (Glickman et al., 2002; Finley et al., 2012). The 26*S* proteasome comprises two major subcomplexes: (1) the 20*S* core particle (CP), also called the catalytic particle because it contains all the hydrolytic activities, and (2) the 19*S* regulatory particle (RP) which is a non-catalytic component that recognizes substrates conjugated to a polyUb chain (Glickman et al., 2002; Finley et al., 2012). An intact proteasome (26*S*) consists of a single 20*S* subunit that is bound to two 19*S* particles at each end.

1.6.1 The 19*S* Proteasome (Regulatory Particle)

Once the polyUb substrate has been targeted to the 26*S* proteasome a series of events ensue at the 19*S* subunit. Some of the major functions of the 19*S* particle are (1) substrate recognition through specialized receptors, (2) substrate unfolding through the action of resident ATPases, (3) Ub recycling by resident DUb enzymes, and (4) substrate translocation into 20*S* particle (Glickman et al., 2002). The 19*S* subunit also controls the opening of the translocation channel into the 20*S*.

The 19*S* particle consists of at least 19 distinct subunits, and has a total mass of 1MDa (Glickman et al., 1998b). The 19*S* can be partitioned into a base subcomplex with at least 10 subunits, and a lid subcomplex containing nine subunits (Glickman et al., 1998a).

The lid houses several subunits of the Rpn type, which stands for **R**egulatory **P**article **N**on-ATPase (Glickman et al., 2002). For instance, Rpn6 plays a pivotal role in stabilizing the interaction between 19*S* and 20*S* by interacting with key residues of the ATPase subunits in the base (Lander et al., 2012; Pathare et al., 2012). PolyUb chain recognition is accomplished by Rpn13, one of the two known polyUb chain receptors in the 19*S* subunit (Husnjak et al., 2008). The other one is Rpn10, which interacts with polyUb chains through an Ubiquitin-Interacting-Motif (UIM) (Elsasser et al., 2004; Verma et al., 2004; Mayor et al., 2007). In contrast, Rpn13 requires a Pleckstrin homology (PH) domain for binding polyUb chains (Husnjak et al., 2008). Rpn10 and Rpn13 are located on opposite sides of the substrate translocation channel at the 20*S*, but may interact with the same

polyUb chain (Lander et al., 2012; Sakata et al., 2012). The function of Rpn10 as polyUb chain receptor can be regulated (Isasa et al., 2010). It was reported that monoubiquitylation of Rpn10 inhibits its interaction with polyUb chains *via* its UIM motif, and can cause its release from the proteasome (Isasa et al., 2010).

Additionally, Rpn10 can stabilize the interaction between lid and base (Glickman et al., 1998b; Saeki et al., 2000). The first 190 amino acid residues in Rpn10 contain a VWA domain, which appears to stabilize the interaction between the lid and the base (Glickman et al., 1998a). In the presence of high concentration of sodium chloride (NaCl), the lid dissociated from the base in yeast cells lacking Rpn10, consistent with a role in stabilizing the 19*S* complex (Glickman et al., 1998a). However, Rpn10 is expressed at stoichiometric excess compared to other proteasome subunit and only ~ 10% is present in the proteasome. The function of the free form of Rpn10 is not known.

The removal of the polyUb chain, after a substrate has been delivered to the proteasome, is critical for successful degradation. Intriguingly, the removal of the polyUb chain is closely coupled to substrate unfolding and translocation into the 20*S* subunit. Substrate deubiquitylation is mediated by resident DUbs, including Rpn11 and Ubp6 (Amerik et al., 2000; Leggett et al., 2002; Chernova et al., 2003; Hanna et al., 2003; Hanna et al., 2007). Ubp6 is located distant from the translocation channel, and removes Ub in an ATP-independent manner (Finley et al., 2012; Lander et al., 2012). In contrast, Rpn11 is located close to the translocation channel, and its activity is closely coupled to the energy dependent unfolding step (Finley et al., 2012; Lander et al., 2012; Worden et al., 2017).

Six ATPases, which assemble into a hexameric ring, form the base of the 19*S* particle, and coordinate substrate unfolding and translocation (Tomko et al., 2010). These six ATPases belong to the AAA family, and are termed Rpt1-6, which stands for **R**egulatory **P**article **T**riple A) (Finley et al., 2012). These ATPase subunits, as well as Rpn1, Rpn2 and Rpn10, form the base subcomplex of the 19*S* RP (Lander et al., 2012). Substrate unfolding is essential because the translocation channel into the 20*S* CP is only 13 angstroms in diameter, which is too narrow for native proteins to traverse (Glickman et al., 2002). The mechanism of unfolding and translocation remains to be fully understood.

1.6.2 The 20*S* Proteasome (Core Particle)

After substrate recognition, de-ubiquitylation coupled to unfolding, and translocation, the substrate is now inside the 20*S* CP. The 20*S* subunit is a barrel shaped structure made up of four stacked rings, each consisting of seven subunits (Groll et al., 1997). The outer rings consist of α-subunits (α1 – α7), and the two inner rings are comprised of β-subunits (β1 - β7) (Glickman et al., 2002; Finley et al., 2012). In eukaryotes, the seven α- and β-subunits are related but not identical, whereas in the prokaryotic proteasome, the seven subunit ring is comprised of identical subunits (Darwin, 2009). Therefore, the prokaryotic 20*S* is comprised of two homoheptameric rings of β-subunits sandwiched between two homoheptameric rings of α-subunits, whereas the eukaryotic 20*S* particle consists of four heteroheptameric rings (Darwin, 2009).

In prokaryotes and archaea, the proteolytic activity lies within the β-subunits (Darwin, 2009). However, since all β-subunits are identical, there are 14 peptidases of only one type. In contrast, in the eukaryotic proteasome, the peptidase activity is located in subunits β1, β2 and β5; thus the intact proteasome contains six peptidase sites (Groll et al., 2005). These threonine proteases have the active site in their N-terminal threonine amino group (Groll et al., 2005). However, each protease has different substrate specificity. The β1 subunit has trypsin-like activity; hence it cleaves after basic residues (Groll et al., 2005). The β2 subunit has caspase-like activity that cleaves after acidic residues, and β5 has chymotrypsin-like activity and cleaves predominantly after hydrophobic residues (Groll et al., 2005). The multiplicity of protease activities favors complete hydrolysis of substrates.

All proteolytic subunits of the 20*S* are synthesized as inactive precursors (also called propeptides) that are processed during their assembly into the 20*S* CP (P. Chen et al., 1996; Arendt et al., 1997; Groll et al., 1997). The β-subunits active sites face the inner cavity within the 20*S* barrel, thereby restricting their action only on accurately targeted substrates (Groll et al., 2000; Kohler et al., 2001). The two outer α rings form the translocation channel that can be regulated to control substrate entry into the 20*S* CP (Groll et al., 2000; Whitby et al., 2000; Bajorek et al., 2003). In a free 20*S* subunit, access into the proteolytic chamber is occluded by the N-termini extensions from all seven α-subunits (Groll et al., 2000). These extensions form an asymmetric structure that obstructs entry into the 20*S* particle (Groll et al., 2000; Whitby et al., 2000). However, the α3-subunit differs from the

other α-subunits because its N-terminal domain extends across the translocation channel, while also interacting with every other α-subunit (Groll et al., 2000). In order for a substrate to enter the chamber the α-subunit extensions have to be displaced. This can be controlled by the assembly of the 19*S* subunit to the 20*S* proteasome, and can also be mimicked by a denaturant such as sodium dodecyl sulfate (Larsen et al., 1997; Glickman et al., 1998b; Smith et al., 2007). Another significant role for the 20*S* subunit is to serve as docking station for the 19*S* RP. The junction between each α-subunit in the 20*S* particle creates a pocket that interacts with C-terminal extensions in ATPase subunits in the 19*S* particle (Tian et al., 2011).

Eukaryotic 20*S* CP assembly proceeds through a series of steps and involves five dedicated chaperones (Ramos et al., 1998; Finley et al., 2012; Kunjappu et al., 2014). The assembly is believed to begin with the formation of the seven membered α-ring, which is facilitated by the chaperone complex Pba1-Pba2 in yeast (Kusmierczyk et al., 2011). The α-ring serves as a template for the assembly of the β-ring, and requires the chaperone complex Pba3-Pba4 (Kusmierczyk et al., 2008). Once the $\alpha_7\beta_7$ structure (also called “half-proteasome”) is formed, two such half-proteasomes are combined, and β-subunits propeptides are removed, leading to a mature 20*S* CP (Kunjappu et al., 2014). In yeast, the Ump1 chaperone binds the half-proteasome and promotes their dimerization into the mature α7β7β7α7 complex (Ramos et al., 1998). Loss of any of these chaperones result in proteasomal abnormalities (Ramos et al., 1998; Kusmierczyk et al., 2008; Kusmierczyk et al., 2011).

After the chaperone guided 20*S* CP assembly is complete, it serves as the template on which the 19*S* RP is assembled by a distinct family of chaperones. Four chaperones that function in this process include Nas2, Nas6, Rpn14, and Hsm3 (Funakoshi et al., 2009; Kaneko et al., 2009; Le Tallec et al., 2009; S. Park et al., 2009; Roelofs et al., 2009; Saeki et al., 2009). Each of the 19*S* particle chaperones binds to the C-terminal domain in an Rpt protein (Finley et al., 2012). The base of the 19*S* subunit, which consists primarily of the hexaheteromeric ATPase ring, is assembled from three precursor modules (Finley et al., 2012). Each module consists of an Rpt pair that is bound to at least one chaperone (Funakoshi et al., 2009; Kaneko et al., 2009; Saeki et al., 2009). The Rpt1-Rp2 complex is chaperoned by Hsm3 bound to Rpt1, whereas the Rpt4-Rpt5 module has Nas2 on Rpt5 (Funakoshi et al., 2009; Saeki et al., 2009; Tomko et al., 2010). The Rp3-Rpt6 module has Nas6 bound to Rpt3 and Rpn14 associated with Rpt6 (Saeki et al., 2009; Tomko et al., 2010). The mechanism of proper base assembly has not been described, but the C-terminal tails of Rpt4 and Rpt6 play a key role (S. Park et al., 2009). The deletion of a single amino acids from their C-termini leads to a defect in 19*S* particle assembly (S. Park et al., 2009).

Interestingly, a distinct type of proteasome, termed the “immunoproteasome” has been described in mammals (Goldberg et al., 1992; Kunjappu et al., 2014). Upon interferon-γ signaling the three β-subunits harboring peptidase activity are replaced by distinct βi-subunits, also called Low molecular Mass Proteins (LMPs) (Goldberg et al., 1992; Bochtler et al., 1999). Each of these βi-subunits is genetically homologous to their corresponding β-subunits; thus the

β1i/LMP2 replaces the β1-subunit, β2 is substituted by β2i/LMP10, and β5 is swapped with β5i/LMP (Goldberg et al., 1992; Bochtler et al., 1999). In addition, upon interferon-γ signaling the 19*S* is replaced by the 11*S* regulator, also called PA28, which binds to the α-ring to activate the 20*S* CP (Whitby et al., 2000). Immunoproteasomes generate peptides that are more suitable for binding MHC Class I molecules, which appear on the surface of antigen presentation cells (Kloetzel, 2001; Yewdell et al., 2001).

In summary, polyubiquitylated substrates can interact with several subunits in the 19*S* RP. The dismantling of the polyUb chains is coordinated with substrate unfolding and translocation into the 20*S* subunit. The six ATPases that provide the energy for protein unfolding are located near the translocation channel into the 20*S*. Following entry into the catalytic chamber the substrate is hydrolyzed to amino acids and small peptides.

1.7 Ubiquitin-Like Proteins

The Ub-fold is a conserved structural motif that is widely distributed in proteins. However, most of these ubiquitin-like proteins do not function in proteolysis (Pickart et al., 2004; Herrmann et al., 2007). Only a small number of ubiquitin-like proteins consist solely of the ubiquitin-fold, and are classified into two groups: (1) Ubiquitin-like modifiers (ULM) and (2) Ubiquitin-domain proteins (UDP) (Pickart et al., 2004) (Fig. 2).

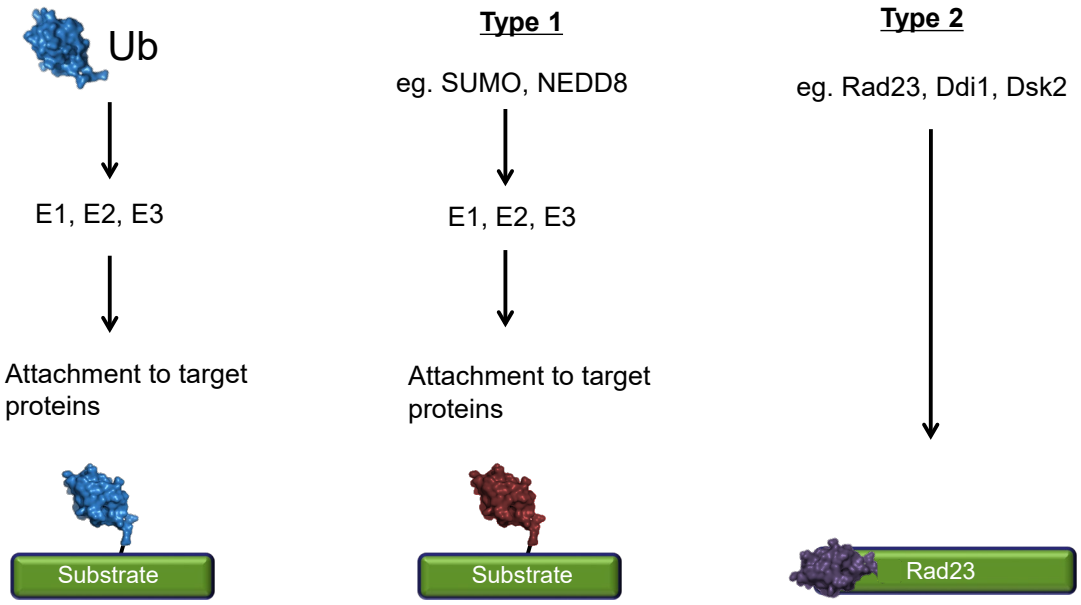

Figure 2. Proteins in the UbL protein family and their main characteristic. Ub requires E1, E2, and E3 enzymes for its activation and conjugation to a substrates. Type 1 UbL proteins resembles Ub in that they share the characteristic Ub-fold and require E1, E2 and E3 enzymes for the activation and conjugation to a target protein. Type 1 enzymes differ from those E1, E2s and E3s that Ub requires. Type 2 UbL are different in that the characteristic Ub-fold is a domain as part of the protein itself, thus they do not require conjugation factors.

1.7.1 Ubiquitin-Like Modifiers (ULM)

The ULM family include proteins such as Ub, Nedd8, and Sumo in *Saccharomyces cerevisiae* (Pickart et al., 2004). However, in mammals there are at least eight additional members, including FAT10, ISG15, and Ufm1 (Herrmann et al., 2007). ULMs share the characteristic Ub-fold, and their c-terminal tail also ends with a glycine residue for ligation to target proteins *via* an isopeptide bond (Kerscher et al., 2006). Each ULM has a unique set of substrate conjugation factors (Welchman et al., 2005). These enzymes are also grouped into E1, E2, and E3 enzymes, but they differ from those of Ub (Welchman et al., 2005). ULMs are also expressed as precursor proteins, just like Ub; thus they require cleavage from their fusion products for maturation (Tanaka et al., 1998). The cleavage is performed by UbL-specific proteases (ULPs) that resemble DUbs (Kerscher et al., 2006).

The conjugation of ULMs to substrates serves a regulatory role (Welchman et al., 2005). For instance, SUMOylation can facilitate protein-protein interaction, either by creating a new interaction surface, or by altering the conformational state of the target protein (Ulrich, 2005). SUMO is the only ULM known to assemble into chains, although its function is poorly understood (Ulrich, 2005; Kerscher et al., 2006). Initially, SUMO and Ub were thought of as distinct homotypic signals with divergent functions. In fact, it was assumed that the conjugation of SUMO or Ub to a substrate exerted opposite effects (Ulrich, 2005; Kerscher et al., 2006; Guzzo et al., 2013). However, the recent discovery of chains containing both SUMO and Ub adds another level of complexity that is not understood (Guzzo et

al., 2013). The synthesis of these chains depends on the activity of SUMO-targeted Ub-ligases (STUbLs) that ubiquitylate polySUMOylated substrates (Guzzo et al., 2013). SUMO-Ub hybrid chains were originally identified as a targeting signal for degradation by the proteasome (Guzzo et al., 2013). More recent studies revealed that SUMO-Ub hybrid chains can also mediate the recruitment of DNA repair factors to sites with DNA lesions (Guzzo et al., 2013). Taken together, these observations suggest that Ub and ULM modifications provide versatile ways for regulating protein function (Kerscher et al., 2006).

1.7.2 Ubiquitin-domains proteins (UDP)

The Ub-fold has been exploited extensively during the evolution of protein structure (Dantuma et al., 2009). This characteristic fold is found in many proteins that promote protein-protein interactions. Unlike the ULM family of proteins, the Ub-fold in Ubiquitin-domain proteins (UDPs) is generally a domain that makes up a portion of the larger protein, and is not conjugated to other proteins (Elsasser et al., 2004). Consequently, UDPs do not contain a reactive C-terminus. Instead, this characteristic Ub-like domain (UbL), which is almost always positioned at the extreme N-terminal, is an essential part of the protein that facilitate protein-protein interaction (Watkins et al., 1993). It was later discovered that the UbL domain can also interact with the proteasome (Schauber et al., 1998).

Specific UDPs can also harbor either one or two Ub-associated (UBA) domains through which they can bind Ub or polyUb chains. UBA domains are small domains of ~ 40 amino acids (Dieckmann et al., 1998). They adopt a very specific

fold that is made up of three tightly packed α-helices separated by two flexible regions (Dieckmann et al., 1998; Mueller et al., 2002). However, the main residues involved in making contact with Ub are found in the first and third helix (Mueller et al., 2004). Mainly the hydrophobic residues surrounding Ile44 in Ub are responsible for binding the UBA domain, as well as other Ub-binding domains (Hicke et al., 2005). UDPs were later referred to as shuttle factors, and it was proposed that they function in the UPP, because they can bind the proteasome through their UbL domain and polyUb substrates through their UBA domains.

1.7.3 Rad23, a connection between DNA Repair and the UPP

Rad23 was initially studied in its role in the DNA Nucleotide Excision Repair (NER) pathway (Madura et al., 1990; Watkins et al., 1993; Guzder et al., 1995). NER is one of many pathways that functions to maintain genome integrity. NER is required for the removal of large and diverse helix-distorting lesions that can interfere with replication and transcription (Boiteux et al., 2013). These DNA lesions include UV-induced cyclobutane pyrimidine dimers (CPDs) and pyrimidine (6-4) pyrimidone photoproducts (6-4PPs) (Cadet et al., 2005; Friedberg et al., 2006). In humans, at least seven complementation groups are linked to NER, and defects cause xeroderma pigmentosum (XP), a disease that is characterized by extreme sensitivity to UV light (Friedberg et al., 2006).

NER consists of two main subpathways: (1) transcription-coupled repair (TCR), which removes DNA lesion at actively transcribed genes to quickly resume transcription; and (2) global genome repair (GGR), which repairs DNA lesions in

heterochromatin, and in the non-transcribed strand of transcriptionally active genes (Giglia-Mari et al., 2011). Five distinct biochemical steps make up the NER pathway: (1) damage recognition, (2) DNA strand-incision, (3) oligonucleotide excision, (4) repair synthesis, and (5) DNA ligation (Xie et al., 2004). TCR and GGR differ only in the recognition step, which requires additional factors for GGR, but converge thereafter.

Biochemical analysis of a cell free reconstituted system revealed six essential NER factors that play a key role in the damage recognition and DNA strand incision step. Amongst them is NEF2, which is a complex consisting of Rad23 and Rad4, (Guzder et al., 1995). NEF2 mainly functions to bind DNA and to tether NER factors NEF1 and NEF3 tightly to the damage site (Guzder et al., 1995). The discovery that Rad23 can bind the proteasome through its N-terminal UbL domain immediately suggested a role for the UPP in NER. However, it was shown that the proteasome is not required for the dual incision step in NER, suggesting the proteasome most likely plays a role during post-incision steps in NER. In contrast, Rad23's UbL domain is required for full complementation of the UV sensitivity of a *rad23Δ* yeast stain ((Watkins et al., 1993).

Rad23-Rad4

The stable NEF2 (Rad23-Rad4) complex was shown to specifically bind UV-damaged DNA, and is an essential factor in the reconstituted system for dual incision (Guzder et al., 1995; Jansen et al., 1998). The human homolog HR23A-XPC performs the same function as Rad23-Rad4 in yeast. Whereas Rad4 is

absolutely essential for NER, Rad23 is not. The loss of Rad4 leads to severe UV sensitivity, whereas loss of Rad23 moderately increases UV sensitivity. This is likely to be caused by the reduced stability of Rad4, which is rapidly degraded in the absence of Rad23 (Ortolan et al., 2004). It was reported that expression of Rad4 in the temperature sensitive proteasome mutants *rpt1-1*(*cim5-1*) lead to its stabilization (Lommel et al., 2002). PolyUb conjugates to Rad4 are readily detectable by immunoblotting (Lommel et al., 2002). Interestingly, when Rad23 was co-expressed with Rad4 in *rpt1-1* proteasome mutant, the polyUb-Rad4 conjugates were not present, suggesting that Rad23 inhibited Rad4 ubiquitylation (Lommel et al., 2002). Indeed, it was later reported that Rad23 can prevent polyUb chain assembly on Rad4 and other substrates by binding to short Ub chains and blocking their assembly into longer polyUb chains (L. Chen et al., 2001; Xie et al., 2004; Kang et al., 2006). Consistent with this discovery, Pickart and colleagues reported that Rad23 can prevent the disassembly of pre-formed polyUb chains (Raasi et al., 2003). These findings suggest that Rad23 plays a regulatory role in polyUb chain dynamics. How these activities of Rad23 contribute to DNA repair and substrates shuttling remains to be determined (Wade et al., 2010).

1.7.4 Rad23 and its Role in the UPP

An efficient way of targeting substrates to the proteasome is by assembly of a polyUb chain. Although the polyUb chain might by itself permit substrate interaction with the proteasome, it is evident that additional factors can promote the targeting of many substrates to the proteasome. For instance, shuttle factors

that bind the proteasome *via* their N-terminal UbL domain and bind polyUb chains through UBA domains define one such class of trafficking proteins. Shuttle factors are not degraded after they bind the proteasome, consistent with my view that they deliver substrates. Instead they dissociate from proteasome to repeat the cycle of substrate delivery. Yeast encodes three shuttle factors, Rad23, Ddi1, and Dsk2 (Fig. 3).

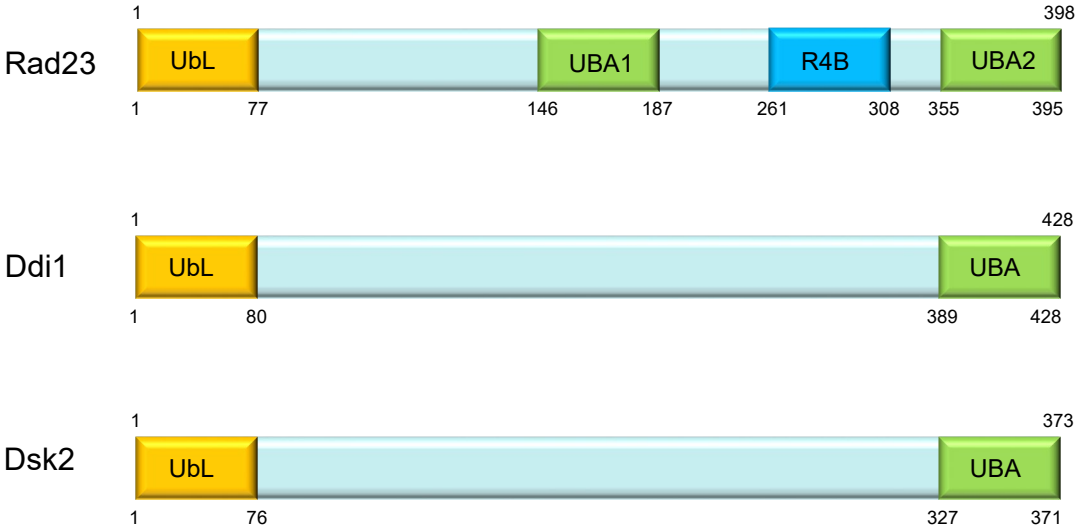

Figure 3. Schematic of domains in Rad23, Ddi1, and Dsk2 that are of significance in the UPP. All shuttle factors have one N-terminal UbL domain. Ddi1 and Dsk2 have each one C-terminal UBA domain, whereas Rad23 has two UBA domains in addition to its Rad4-Binding Domain (R4BD).

An initial connection between Rad23 and the UPP was established when the *RAD23* gene was isolated as a dosage suppressor of the toxicity caused by overexpressing the yeast E2 Ubc2 and the E3 Ubr1 (Madura et al., 1994). Rad23 was the first UbL-containing protein discovered (Watkins et al., 1993). It is a 398 amino acid protein with a predicted size of 42kDa that has no known enzymatic activity (Dantuma et al., 2009). It has three major domains including (1) a Rad4-Binding Domain (R4BD), (2) a UbL domain, and (3) two UBA domains (Dantuma et al., 2009). The R4BD binds and stabilizes Rad4, and is important for its function in NER. Its UbL was shown to be important in proteasome binding, as UbL by itself when immunoprecipitated was shown to co-purify several proteasomal subunits, while a Rad23 mutant lacking the UbL was unable to bind the proteasome (Schauber et al., 1998; Trempe et al., 2016). Interestingly, replacing Rad23's UbL domain with Ub allowed Rad23 to function in NER and bind the proteasome (Lambertson et al., 2003).

The UbL domain in Rad23 cannot be processed by DUbs, unlike Ub or ULMs, because it lacks the characteristic R-G-G motif at its C-terminus (Watkins et al., 1993). Rad23's UbL spans the first 77 amino acid and contains 14 of its 15 lysine residues. These lysine residues, similar to Ub, may be essential for its functions. For instance, Kim and colleagues reported that lysine-seven (K-7) is essential for proteasome interaction (Kim et al., 2004). The preferred proteasomal binding partner of Rad23 is Rpn1, which also binds the UbL domains in Ddi1 and Dsk2 (Elsasser et al., 2002; Rosenzweig et al., 2008). Structural studies suggest that Rpn1 and Rpn2 form a docking station for UbL containing proteins (Saeki et

al., 2002; Rosenzweig et al., 2008). Because Rpn1 is part of the base (together with the ATPases, Rpn2, and Rpn10), Rad23 docking to Rpn1 allows for an efficient transfer of polyUb substrates to Rpn10, one of the major polyUb chain binding protein in the proteasome.

In addition to the R4BD and UbL domains in Rad23, it also contains two UBA domains: UBA1 in the central region of the protein, and UBA2 at the extreme C-terminal region. Both UBA domains can interact with Ub and polyUb chains, although the affinity for polyUb chains is much higher than that of monoUb (Bertolaet et al., 2001; L. Chen et al., 2001; Wilkinson et al., 2001; L. Chen et al., 2002; Rao et al., 2002; Raasi et al., 2005). Binding studies revealed that UBA1 interacts with much higher levels of polyUb substrates than UBA2 (L. Chen et al., 2002). Mutation in UBA2 did not substantially decrease interaction of Rad23 with polyUb substrates although it destabilized the protein (L. Chen et al., 2001; L. Chen et al., 2002). In contrast, a defective UBA1 domain significantly impacts the binding properties of Rad23 to polyUb proteins (L. Chen et al., 2001; L. Chen et al., 2002). This suggests that UBA1 in Rad23 is the primary binding site for polyUb substrates.

Overexpression of Rad23 can lead to polyUb substrate accumulation *in vivo*, suggesting a role for Rad23 in proteolysis (Ortolan et al., 2000; L. Chen et al., 2002). It was previously reported that the UBA domains in Rad23 are required for inhibition of polyUb chain assembly on substrates (L. Chen et al., 2001). Consistent with a negative regulatory role for Rad23 in the UPP is the observation that purified Rad23 inhibited the degradation of polyUb substrates by purified

proteasomes, which was shown to be dependent on the UBA domains (Raasi et al., 2003). Raasi and colleagues have also shown that Rad23's UBA domains preferentially bind K-48 linked polyUb chains (K-29 and K-63 were also tested) (Raasi et al., 2005). The Rad23 homolog in *S. pombe* was also shown to protect K-48 linkage polyUb chains against disassembly by DUBs in a UBA dependent manner (Hartmann-Petersen et al., 2003). All these observations reinforce the idea that UBA domains in Rad23 play a significant role in the dynamic assembly and disassembly of polyUb chains. However, the fact that artificial substrates can be stabilized in strains lacking (*rad23Δ*), or overexpressing Rad23, excludes a simple model for Rad23 function in the UPP (Lambertson et al., 1999; Ortolan et al., 2000; Rao et al., 2002).

A further complexity in the cellular function of Rad23 is that it can interact with a number of additional proteins through its UbL or UBA domains. For instance, the binding of Ub chain elongation factor Ufd2 to its UbL domain facilitates proteasomal degradation of substrates (Kim et al., 2004). In contrast, the binding of peptidyl tRNA hydrolase Pth2 can impede this process (Ishii et al., 2006). Interaction with the Png1 protein and UBA2 promotes the turnover of glycosylated proteins (Kim et al., 2006). The Viral protein r (Vpr), an accessory protein of the Human Immunodeficiency Virus (HIV) was shown to bind the UBA2 domain in Rad23 to presumably deregulate normal cellular processes (Withers-Ward et al., 1997; Withers-Ward et al., 2000). Another protein that has been reported to interact with Rad23 through its C-terminal UBA2 domain is p300/cyclic AMP-responsive element binding (CREB) protein, a transcriptional co-activator that

supports transcriptional activity of tumor suppressor p53 (Q. Zhu et al., 2001). Although all these additional binding partners have been identified, a significance of these interactions as it relates to Rad23's role in the UPP remains to be established.

1.8 Degradation of Nuclear Substrates Requires Export from Nucleus

Nuclear proteins are among the best characterized substrates of the proteasome (Lecker et al., 2006). However, the site of their turnover remains uncertain. There is a general belief that nuclear proteins, because they function inside the nucleus, are also degraded inside the nucleus (Blondel et al., 2000; Prasad et al., 2010; S. H. Park et al., 2013). This belief is further supported by the fact that many components of the UPP, including enzymes of the tagging machinery and proteasome subunits can be detected inside the nucleus (Blondel et al., 2000; Prasad et al., 2010; S. H. Park et al., 2013) (Fig. 4). It was shown that the turnover of Far1, a bifunctional nuclear protein that is required for cell cycle arrest and establishing cell polarity during yeast mating, is increased when nuclear export was blocked (Blondel et al., 2000). In addition, its turnover was completely halted when translocation to the nucleus was prevented (Blondel et al., 2000). Similarly, it was reported that the ubiquitylation and degradation of *Xenopus* p27 required nuclear localization (Chuang et al., 2001). MyoD, a transcription factor pivotal for muscle differentiation, was described to be degraded by a fully

functioning “nuclear” UPP (Floyd et al., 2001). Taken together these observations suggest that nuclear proteins are degraded inside the nucleus.

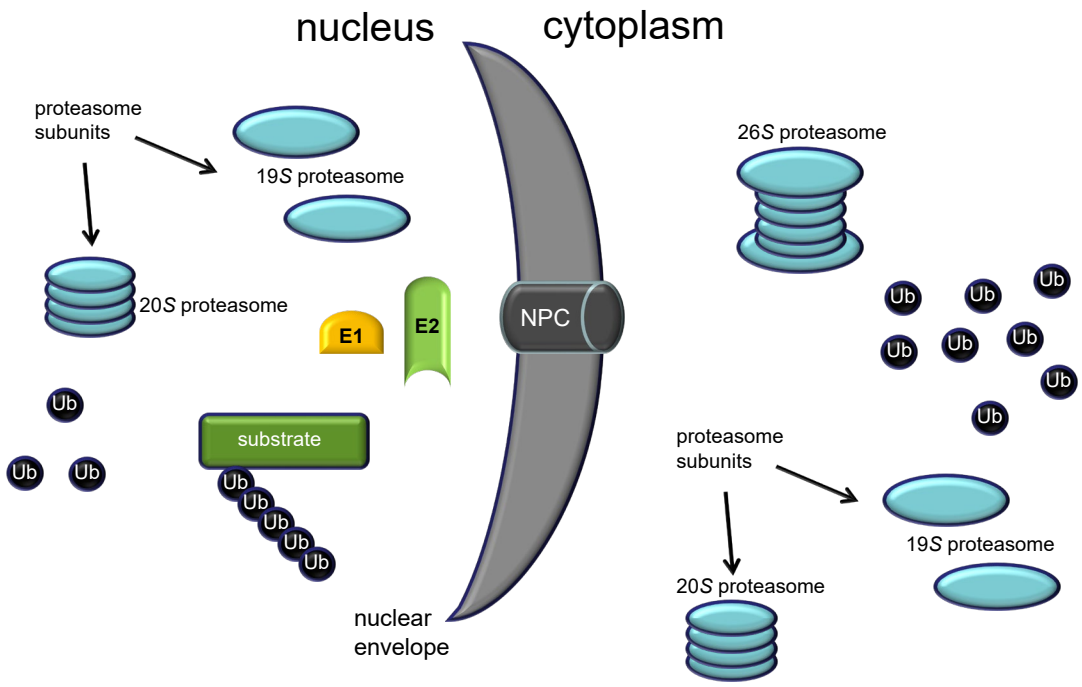

Figure 4. Model of localization of UPP components. Ub conjugation factors can be detected inside the nucleus. Subunits of the proteasome that can be detected in the nucleus were found to perform non-proteolytic functions, including transcription and DNA repair. Ub can be found in the nucleus and cytoplasm. Many proteins shown to be degraded in a Ub-proteasome dependent manner are nuclear proteins.

However, the fact that Far1 is stabilized when translocation to the nucleus is blocked can simply be explained by the fact that nuclear proteins receive their degradation signal only in the nucleus. For instance phosphorylation is a commonly used post-translational modification to trigger polyubiquitylation, and it is known that the kinase that initiates Far1 turnover is located in the nucleus. Moreover, none of the above mentioned examples convincingly demonstrated that the proteasome is fully assembled and proteolytic active inside the nucleus. However, proteasome subunits have been found to perform non-proteolytic functions in DNA repair and transcription (Aravind et al., 1998; Russell et al., 1999; Russell et al., 2001; Kodadek, 2010) (Fig. 4).

In contrast, there is compelling evidence that some nuclear proteins are degraded following their export from the nucleus. A number of discoveries in this regard were made and suggest that the cytosol is a major site for degradation of nuclear proteins.

A. Degradation of some nuclear substrates requires their export

The Madura group and others reported that the degradation of some nuclear proteins required export from the nucleus (Freedman et al., 1998; L. Chen et al., 2014a). It was first reported that the addition of Leptomycin B, a drug that inhibits Xpo1, a nuclear export factor, inhibited the degradation of p53, a tumor suppressor protein (Freedman et al., 1998). This suggests that p53 has to exit the nucleus to be degraded. Further studies have shown that the RING finger domain of the E3 Ub-ligase Mdm2 is crucial for the nuclear export of p53 (Boyd et al., 2000;

Geyer et al., 2000). The requirement of the RING finger domain, which recruits an E2, suggests that the conjugation of at least a few Ub to p53 occurs inside the nucleus, but the completion of polyUb chain assembly and degradation by the proteasome occurs in the cytosol (Lai et al., 2001).

Studies from the Madura laboratory showed that substrates that are stabilized in nuclear export mutants accumulated inside the nucleus (L. Chen et al., 2014a). This important discovery suggests that catalytically active proteasomes do not function inside the nucleus. Mutant derivatives of a yeast exportin (*xpo1-1; crm1*) are defective in nuclear export. In contrast, nuclear import is unaffected in these mutants (L. Chen – unpublished studies). Chen and Madura reported that the DNA repair protein Rad4, and the DNA polymerase I subunit Cdc17 were both stabilized in *xpo1-1* and *crm1*^{T539C}, indicating that their degradation required export from the nucleus (L. Chen et al., 2014a). If proteolysis occurred inside the nucleus, proteasome subunits should have entered the nucleus to degrade these proteins, because nuclear import is not affected in these export mutants.

B. Catalytically active proteasome are detected predominantly in the cytoplasm

Yeast and human cells were fractionated and proteasome activity in the nuclear and cytosolic fractions was measured (Dang et al., 2016). Essentially all cellular proteasome activity was detected in the cytosol (Dang et al., 2016). To verify that the nuclear and cytosolic fractions were not cross-contaminated, the level of histone deacetylase (HDAC) activity, an enzyme that functions only inside

the nucleus, was measured and its activity was present in the nuclear fraction only (Dang et al., 2016).

C. The proteasome can be targeted to the nuclear surface

Key factors that enable proteasomes to be targeted to the nuclear surface were identified (L. Chen et al., 2014b). *STS1* was isolated as a genetic suppressor of *rad23Δrpn10Δ* (Romero-Perez et al., 2007). The yeast gene *STS1* encodes for a protein of unknown function. However, it was shown that Sts1 is a very short-lived protein with a half-life of less than five min (Romero-Perez et al., 2007; L. Chen et al., 2011). The characterization of the *sts1-2* mutant revealed a proteasome localization defect, resulting in the stabilization of nuclear proteins. Sts1 contains an nuclear localization sequence (NLS), which binds Srp1, a member of the importin-α family of soluble nuclear import factors (Tabb et al., 2000). In fact, Tabb and colleagues demonstrated that Srp1 could bind both Sts1 and the proteasome subunit Rpn11 (Tabb et al., 2000).

Collectively, these results predicted a mechanism for targeting proteasomes to the nuclear pore (Tabb et al., 2000; L. Chen et al., 2014b). Recent studies indicate that Srp1 interaction with Sts1 is distinct from its well-characterized role in NLS-mediated nuclear import (L. Chen et al., 2014b). The use of genetic mutants of *SRP1* was instructive. It was reported that *srp1-49* exhibited a defect in proteasome localization, which resulted in the stabilization of nuclear substrates (L. Chen et al., 2014b). However, nuclear import of NLS-bearing proteins, such as the substrates themselves, was unaffected in *srp1-49*. In contrast, in *srp1-31* the

proteasome was properly targeted to the nucleus; even though import of NLS-proteins was blocked (L. Chen et al., 2014b). Since proteasomes were correctly localized even when nuclear import was inhibited, it was proposed that proteasomes are tethered to the nuclear surface. Consistent with this suggestion, in the fission yeast, *S. pombe*, a similar observation has been described (Tatebe et al., 2000). Cut8, a distant relative to Sts1 was shown to tether the proteasome to the nuclear surface (Tatebe et al., 2000). In agreement with my findings in *sts1-2*, nuclear substrates were stabilized in *srp1-49* due to the absence of functional proteasomes at the nuclear surface (L. Chen et al., 2014b).

D. Rad23 can bind the proteasome and polyUb substrates

Rad23 functions as a shuttle factor that can translocate polyubiquitylated proteins to the proteasome (Schauber et al., 1998; L. Chen et al., 2001; L. Chen et al., 2002). Studies from the Madura group showed that Rad23 binds the proteasome *via* its Ub-like (UbL) domain (Schauber et al., 1998). However, Rad23 also interacts with polyubiquitylated proteins *via* its two ubiquitin-associated (UBA) domains (L. Chen et al., 2001; L. Chen et al., 2002). In agreement, a model substrate was stabilized in cells expressing Rad23 variants with point mutations in its UBA domains (rad23^{uba1}, rad23^{uba2}, and rad23^{uba1,uba2}) (L. Chen et al., 2002). It was also shown that high level expression of the UbL domain of Rad23 inhibited the turnover of a model substrate (L. Chen et al., 2002). This finding is consistent with the idea that UbL can bind the proteasome and interfere with the delivery of

proteolytic substrates by other shuttle factors. These results reinforced my view that Rad23 operates as a shuttle factor (Lambertson et al., 2003).

1.9 Summary

The ubiquitin proteasome pathway (UPP) is conserved from yeast to humans, and is the primary proteolytic system for the spatial and temporal elimination of intracellular proteins. The UPP is composed of enzymes that link Ub and polyUb chains to substrates that are marked for degradation. The enzymatic cascade of polyubiquitylation begins with activation of Ub's C-terminal catalyzed by E1. The next step involves the transfer of the activated Ub from the E1 to an E2. E2s in conjunction with an E3 transfers then the Ub to a substrates, followed by polyUb chain extension. The polyUb chains is the structural feature that targets the substrate to the 26*S* proteasome, a large multi-subunit protein complex that houses the catalytic active sites deep in the interior of the 20*S* subunits. The 19*S* regulatory particle, which assembles at either end of the barrel shaped 20*S* subunit, predominantly functions to recognize, unfold, and translocate substrates. The energy for these processes is provided by six ATPases that form a hexameric ring as part of the 19*S* subunit. DUbs, which are also present in the proteasome, can reverse the polyUb chain conjugation on substrates. PolyUb chains can have varying length and topologies, and they can even be mixed with other conjugation factors, such as SUMO; all of which is believed to represent a distinct regulatory signal. There are additional factors that can interact with the polyUb substrates and the proteasome. These proteins are called shuttle factors,

and are characterized by an N-terminal UbL domain and one or two UBA domains. One such shuttle factor is Rad23. It was initially characterized as DNA repair molecule functioning in NER, but later found to contain a UbL domain with which it can interact with the proteasome. It has also been shown that Rad23 can bind polyUb substrates through its two UBA domains, and that it regulate their turnover.

My studies indicate that many nuclear proteins are exported to the cytosolic proteasomes that are located at the nuclear surface. However, this model does not explain how the substrates are targeted for export, and how they locate the proteasome after their exit from the nucleus. One possibility is that Rad23 and other shuttle factors provide a transport mechanism to specifically guide proteolytic substrates from the nucleus to the proteasomes located at the nuclear surface. With this body of work, I explored the role of Rad23 as a shuttle factor.

Chapter II

Material and Methods

2.1 Strains and Media

The yeast *S. cerevisiae* is the model organism used in my studies, and all strains were generated in the laboratory or obtained from other investigators. The source of these strains is cited in the tables below.

Growth: Complete medium (Yeast peptone + dextrose= YPD) and synthetic minimal medium (SM) were prepared according to standard protocols. Yeast cells were grown at 30°C, unless otherwise stated. Yeast expressing genes from the galactose-inducible *GAL1* promoter were first cultured in SM medium containing 2% raffinose for 18 hours. The cultures where then diluted into minimal (SM) or rich (YP) media containing 2 % galactose to induce gene expression for two to three hours. Genes expressed from the copper-inducible *CUP1* promoter were grown in SM medium supplemented with 100 μM $CuSO_4$ for 18 hours, and then diluted when needed. Yeast cultures were harvested in exponential growth phase (unless stated otherwise) and prepared immediately for experimental manipulation, or stored at -80 °C until analysis.

Yeast transformations using plasmids in Table 2 were performed using standard techniques to yield strains described in Table1.

Table 1. *Saccharomyces cerevisiae* strains used in this study

Strain	Genotype	Source
NA10	*MAT***a** *leu2-3,112 trp1-1 ura3-1 his3-11,15 ade2-1 STS1*	F. Wyers
NA25	*MAT***a** *leu2-3,112 trp1-1 ura3-1 his3-11,15 ade2-1 sts1-2*	F. Wyers
FSY86	*MAT***a** *leu2-3,112 trp1-1 ura3-1 his3-11,15 ade2-1 RNA1*	M. Roshbash
FSY87	*MAT***a** *leu2-3,112 trp1-1 ura3-1 his3-11,15 ade2-1 rna1-1*	M. Roshbash
BR4	*MAT***α** *leu2-3, 112, ura3-5 his3-11, 15 pre1-1 pre2-2*	J. Dohmen
LCY826	*MAT***a** *leu2-3,112 trp1-1 ura3-1 his3-11,15 ade2-1 RAD23*	This study
EOY32	*MAT***a** *leu2-3,112 trp1-1 ura3-1 his3-11,15 ade2-1 rad23::URA3 5-FOA treated*	This study

Table 2. Plasmids used in this study

Plasmid	Description		Source
LEP645	P_{CUP1}*-GFP-RAD23 URA3*	*CEN6*	This study
HA-GFP-Ddi1	P_{CUP1}*-HA-GFP-Ddi1 LEU2*	*2μ*	J. Gerst
LEP650	P_{CUP1}*-GFP-rad23*$^{\Delta UbL}$ *URA3*	*CEN6*	This study
LEP649	P_{CUP1}*-GFP-rad23*^{K7A} *URA3*	*CEN6*	This Study
LEP743	P_{CUP1}*-GFP-rad23*^{uba1} *URA3*	*CEN6*	This study
LEP52	P_{CUP1}*-FLAG-RAD23 LEU2*	*2μ*	This study
EOP34	P_{CUP1}*-FLAG-DDI1 LEU2*	*2μ*	This study
LEP155	P_{CUP1}*-FLAG-DSK2 LEU2*	*2μ*	This study
LEP97	P_{CUP1}*-FLAG-RPN10 LEU2*	*2μ*	This study
pYES2-GFP-Ho	P_{GAL1}*- GFP-Ho URA3*	*2μ*	D. Raveh

Matα2-GFP	P_{CUP1}-*MATα2-GFP URA3*	*CEN6*	U. Lenk
LEP793	P_{GAL1}-*Clb2-GFP URA3*	*CEN6*	This study
YCplac111	Empty vector *ARS LEU2*	*CEN4*	R. D. Gietz
EOP53	P_{CUP1}-$ddi1^{\Delta UBA}$ *LEU2*	*2μ*	This study
EOP59	P_{CUP1}-$ddi1^{UBA::UBA1(Rad23)}$ *LEU2*	*2μ*	This study
EOP18	P_{CUP1}-$rad23^{\Delta UB1A::UBA(Ddi1)}$ *TRP1*	*2μ*	This study
LEP151	P_{CUP1}-*FLAG-*$rad23^{\Delta UbL}$ *LEU2*	*2μ*	This study
LEP213	P_{CUP1}-*FLAG-*$rad23^{K7A}$ *LEU2*	*2μ*	This study
LEP740	P_{CUP1}-*FLAG-*$rad23^{uba1}$ *LEU2*	*2μ*	This study
LEP264	*pBSHU-Rpn11-GFP-HA URA3*	*integration*	C. Enenkel
LEP771	*Pup1-RFP URA3*	*integration*	This study
LEP591	Empty vector *ARS LEU2*	*2μ*	J. Brodsky
EOP83	P_{CUP1}-*myc-Ho-2HA*	*CEN4*	This study
EOP85	P_{GAL1}-*HO-2HA URA3*	*2μ*	This study

2.2 Ho-HA Plasmid Construction

The *HO* gene was amplified from plasmid DNA (KEP181) by polymerase chain reaction (PCR) using a 5' *Eco*R1 and a 3' *Kpn*1 restriction sites and the following Oligonucleotides: 5'-GCCGGAATTCATGCTTTCTGAAAACACGACTATTCTGATG-3' and 5'-ATATAGGTACC TGCAGATGCGCGCACCTGCGTTGTTACCACA-3' (Fig. 6). Plasmid LEP1004 was digested with *Eco*R1 and *Kpn*1 to remove a previously inserted Rad14 fragment (Fig. 5). The digested DNA fragments were resolved in a 0.8 % agarose gel and the bands of interest were excised and purified. PCR

products were similarly purified, following digestion with *Eco*R1 and *Kpn*1 (Fig. 6). Following the vector and insert purification, *HO* insert and vector were ligated using a 3:1 (insert to vector) ratio at 16°C overnight in 20 µL volume (Fig. 6). An aliquot of five µl of the ligation reaction were transformed into DH5α to yield *E. coli* strain EOP83 (Fig. 7). Bacterial transformants were recovered on LB agar plates containing the Ampicillin selection drug. Ligation of *HO* was confirmed by diagnostic restriction enzyme digestion, and by PCR. EOP83 was digested with *Eco*R1 and *Xba*1 to yield a fragment containing Ho-2xHA (Fig. 7), which was ligated into LEP591 (Table 2) to generate P*GAL*-Ho-HA (EOP85; Table 2) (Fig. 8).

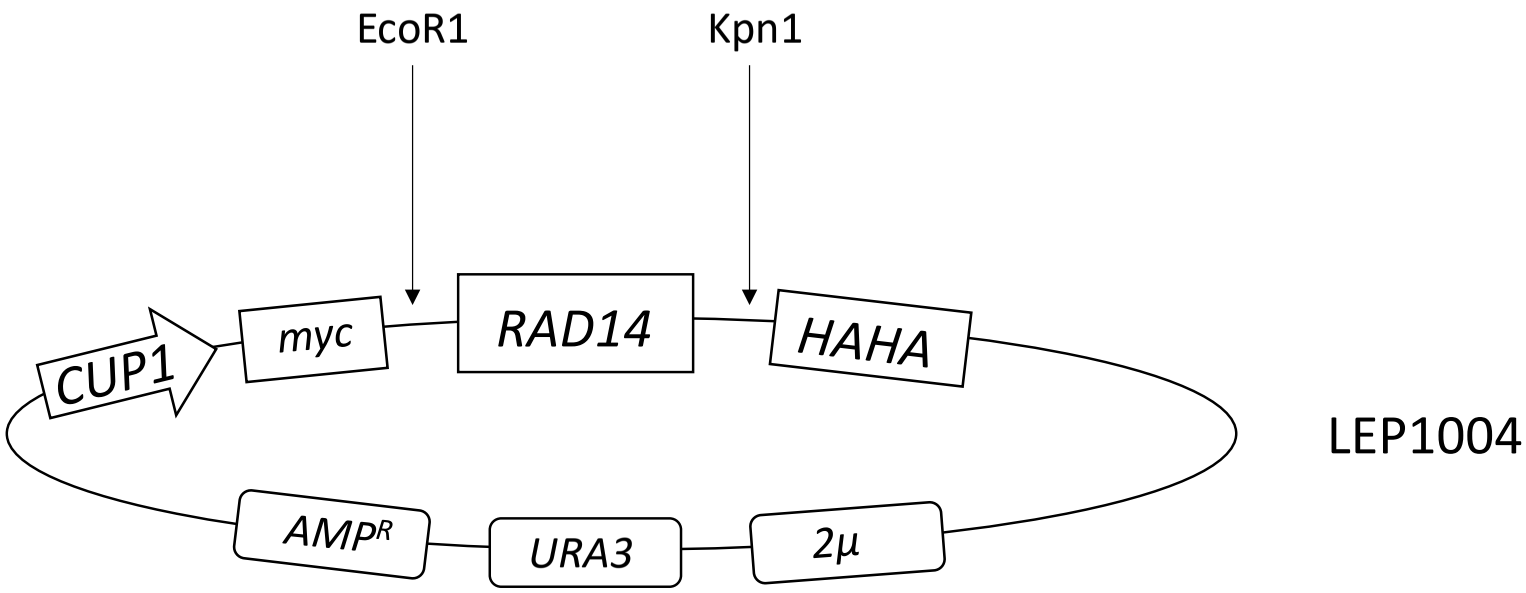

Figure 5. Previously cloned Rad14 is removed upon restriction digest using the enzymes EcoR1 and Kpn1.

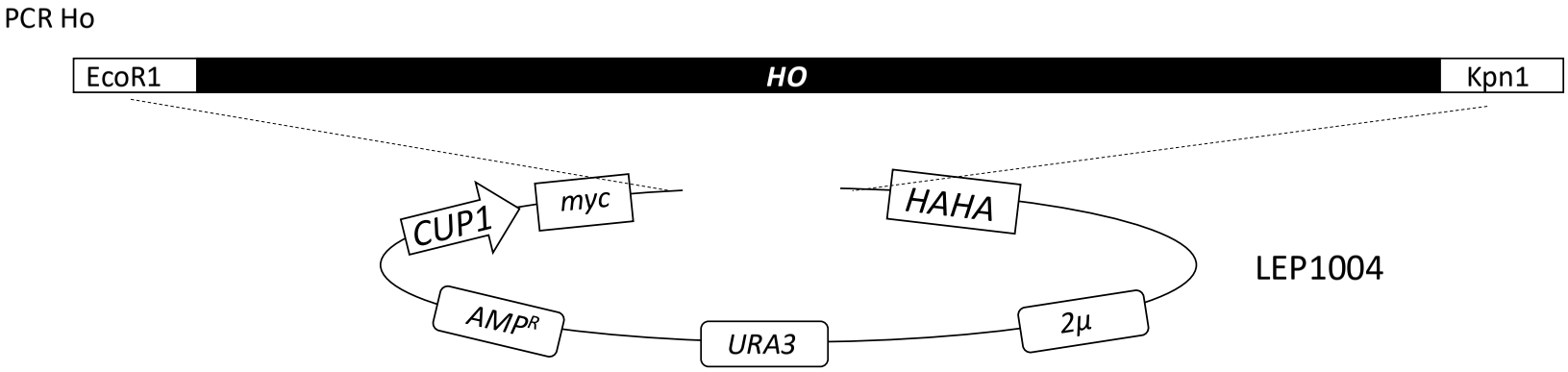

Figure 6. PCR generated Ho fragment is cloned into previously Ecor1 and Kpn1 digested vector.

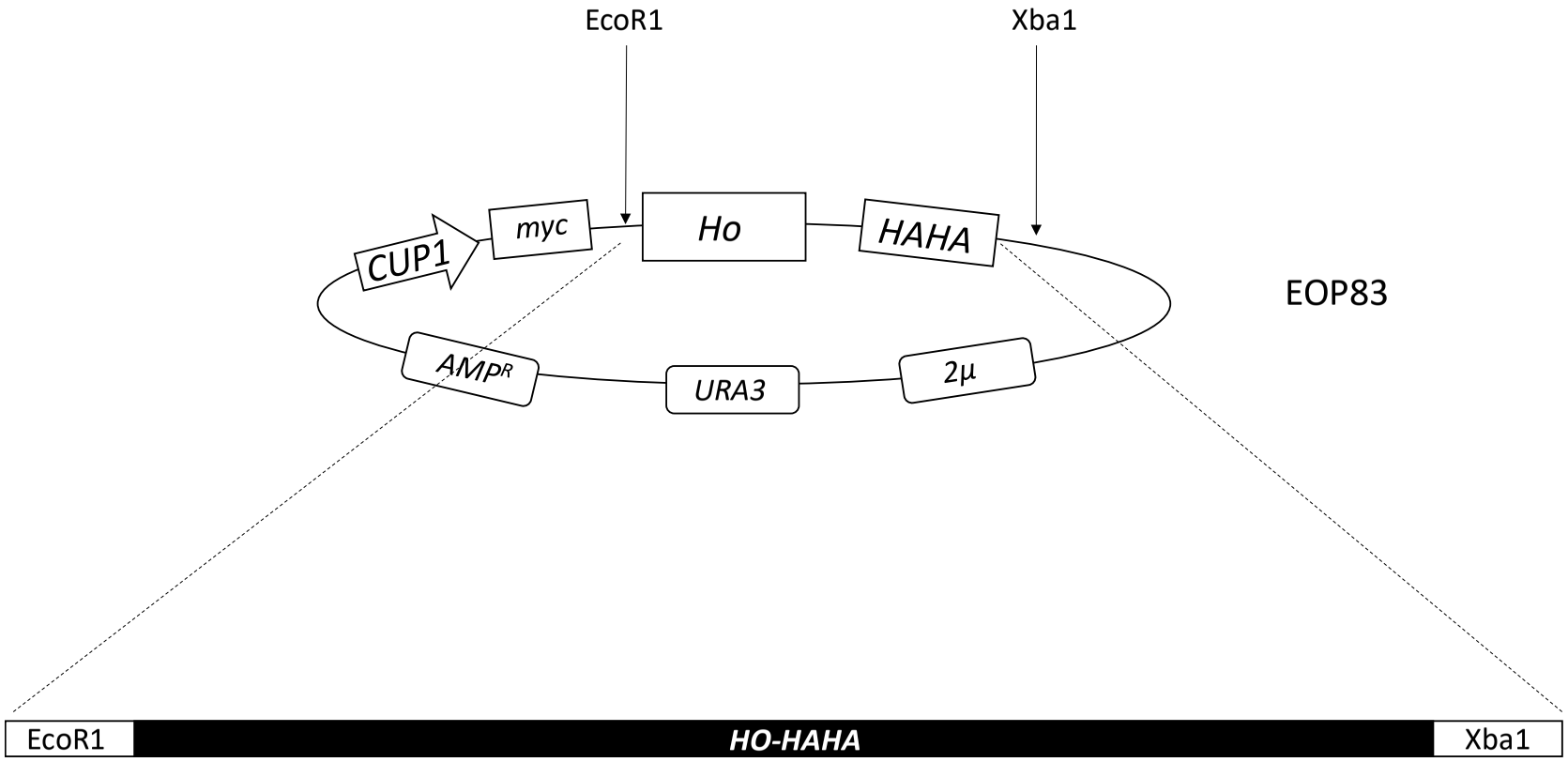

Figure 7. Newly generated gene Ho-HAHA is excised using restriction enzymes EcoR1 and Xba1.

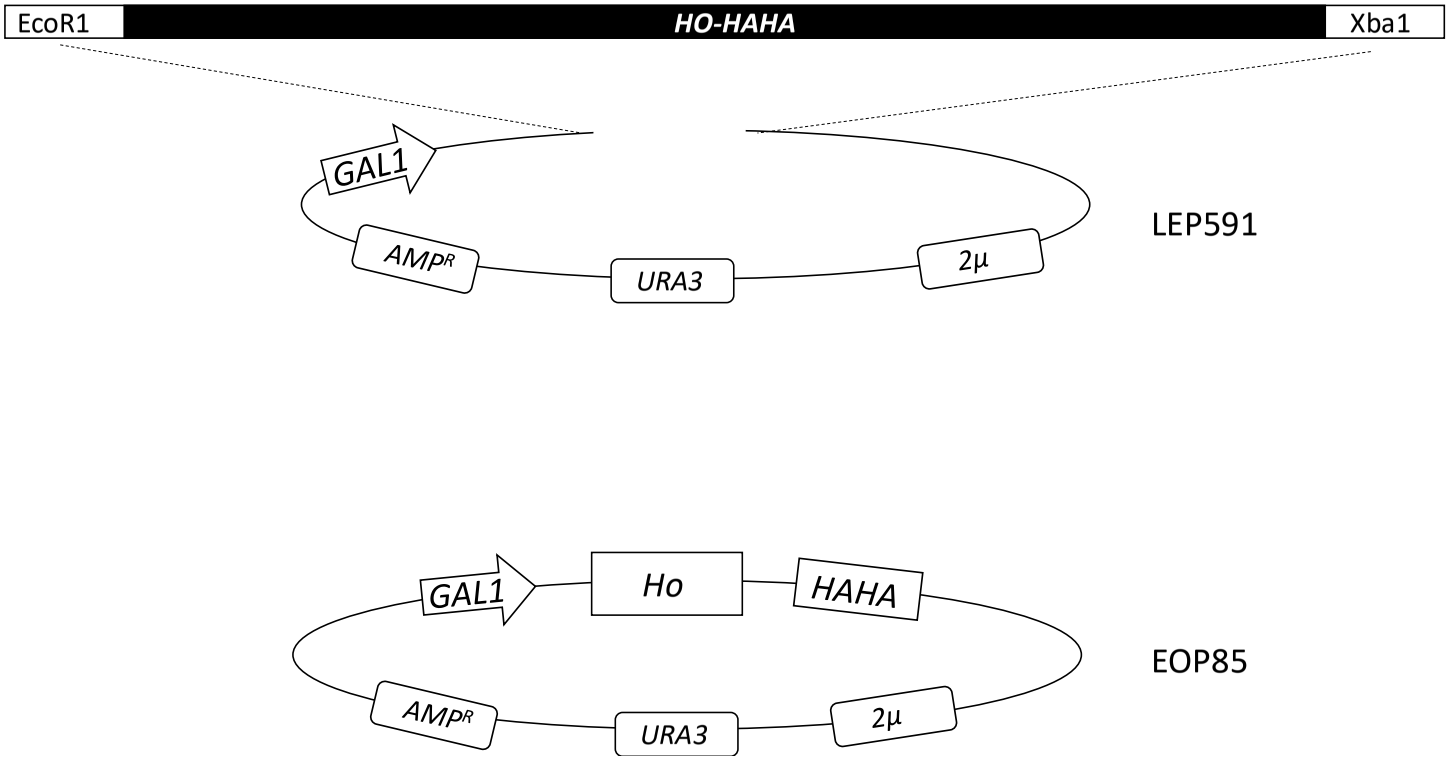

Figure 8. Excised, and purified Ho-HAHA fragment is ligated into empty vector containing *GAL1* promoter to generate EOP85.

2.3 Protein Stability Measurements

To determine the level of turnover of a protein of interest, yeast cultures were first grown in protein induction conditions as described above. If protein was produced from the *GAL1* promoter, induction was shut off by placing cells into SM or YP medium supplemented with 2% glucose and 200 µg/ml cycloheximide (CXH). If proteins of interest were expressed from the *CUP1* promoter, 200 µg/ml CXH was supplemented to the existing media. Starting volume before chase was usually 50 ml, and 10 ml aliquots were drawn at indicated time points. Time zero, is a 10 ml aliquot that was withdrawn before CXH and/or glucose was added. Aliquots were pelleted, transferred to 1.5 ml Eppendorf tubes, stored at -80°C until lysis.

Cycloheximide (Sigma)

Stock solution: 200 mg/ml in DMSO

Working concentration 200 µg/ml

2.4 Preparation and Quantification of Yeast Cell Lysate

Yeast cultures were pelleted, and suspended in pre-chilled (4°C) Buffer A supplemented with protease inhibitors. Cells were lysed twice by multidirectional mechanical disruption with glass bead (Thermo-Savant Fast Prep FP100) for 30 seconds at 6.0 intensity setting. The cells were chilled on ice for 10 minutes in between pulses. The disrupted cells were centrifuged at 10600 x *g* for five minutes.

Supernatant of each sample was transferred to pre-chilled (on ice) Eppendorf tube and centrifuged again for five minutes at 10600 x *g*. All samples and reagents were kept on ice during the preparation. Refrigerated centrifuge was pre-chilled to 4 °C.

Lysates were quantified using the Bradford method and a Beckman Coulter DU 800 spectrophotometer. One cuvettes for each sample was filled with 1 ml Bradford dye (Bio-Rad). 1 µl of sample was suspended in Bradford dye and mixed by inversion. Samples were allowed to rest at room temperature (21°C) for two minutes before analysis. DU 800 was set to fixed wavelength for protein concentration determination. If concentration of samples was not in a linear range based on the 1 mg/ml bovine serum albumin standard, samples were diluted using lysis buffer as described above. Extracts were used for further analysis, including electrophoresis, or immunoprecipitation (IP). For direct electrophoresis experiments, 50 to 100 µg total protein concentration was re- suspended in 4X sample buffer. Unused lysates were stored at -80 °C.

Buffer A:

50 mM HEPES, pH = 7.5, 150 mM NaCl, 5 mM EDTA, 1 % Triton X-100

Supplemented with protease inhibitor cocktail:

- Pefabloc: 1mM/ml working concentration
- Aprotinin: 2µl/ml working concentration
- Leupeptin: 5µl/ml working concentration
- Pepstatin: 1µg/ml working concentration
- Antipain: 50µg/ml working concentration

Acid washed glass beads (Sigma)

Protein assay dye reagent concentrate (Bio-Rad)

Thermo-Savant Fast Prep FP100

DU 800 Spectrophotometer (Beckman Coulter)

2.5 Immunoprecipitation

All affinity matrices used in this study were well suspended before aliquots were withdrawn. For isolating Flag-tagged proteins, yeast protein lysates was added to 20 µL of anti-FLAG affinity beads. Anti-HA and Glutathione Sepharose (GST) beads were first washed three times with Buffer A before yeast protein lysate was added. I used 20 µl aliquots for HA-IP and 25 µl of suspension for GST pull-down. Low retention Eppendorf tubes were used for all affinity protein purification. One to two milligrams of total protein lysate was added to the affinity beads, and incubated at 4°C with constant rocking. FLAG and HA purification were incubated for two hours, whereas GST pull-downs were incubated for a minimum of four hours. The bound proteins were pelleted by brief centrifugation (420 x *g*) in a refrigerated centrifuge and washed three times with pre-chilled (4 °C) Buffer A. SDS-containing loading buffer was combined with the pellets, and samples were either stored at -80 °C, or subjected to SDS-polyacrylamide gel electrophoresis.

Anti-Flag M2 agarose beads (Sigma)

Glutathione Sepharose beads (GE Healthcare Life Science)

Anti-HA affinity agarose matrix (Roche Applied Science)

1.5 ml low retention microcentrifuge tubes (Fisherbrand)

Gel Electrophoresis Sample Buffer (4X):

250 mM Tris-HCL, pH 6.8, 8 % SDS, 40 % glycerol, 4 % β-mercaptoethanol (BME)

2.6 SDS-PAGE and Electrotransfer

Protein samples were denatured by boiling for 10 minutes in SDS-containing loading buffer. Proteins were separated in 12% PAGE using either Hoefer SE400 or the Bio-Rad mini gel system. A 9 % - 12 % acrylamide gradient was used to separate high molecular weight proteins. For protein interaction experiments, 90% of the sample was used to detect binding, and 10% was examined to determine protein loading. Resolved proteins were transferred to nitrocellulose using a semi-dry Hoefer SemiPhor transfer system. Gels and membranes were briefly incubated in transfer buffer containing 20% methanol, and transferred for two hours (at 200mA). To efficiently transfer high molecular weight proteins, the transfer buffer contained 10% methanol, and the duration of transfer was increased to three hours (at 200mA).

10X lower buffer:

2 M Tris-HCl, pH = 8.9

10X upper buffer:

1 M Tris-HCl, pH = 8.25, 1 M Tricine, 1 % SDS

Gel Buffer:

3 M Tris-HCl, pH = 8.45, 0.3 % SDS

10X TBE

89 mM Tris-HCL, 89mM boric acids, 2 mM EDTA

1X Transfer buffer

1X TBE, 20 % methanol

1X Transfer buffer 10%

1X TBE, 10% methanol

Nitrocellulose membrane 0.45μM (Bio-Rad)

Hoefer SE400 electrophoresis unit (Amershan Pharmacia)

Hoefer SemiPhor semi-dry transfer cell (Amershan Pharmacia)

PowerPac Basic (Bio-Rad)

2.7 Immunoblotting

Following protein transfer membranes were briefly washed with ddH_2O and stained with Ponceau S. If membranes were to be probed with anti-Ub antibodies they were boiled for 10 minutes between two glass plates that were submerged in ddH_2O. Membranes were then quickly transferred into a suspension of 5 % non-fat dry milk, prepared in 1X TTBS, and blocked for one hour at 21°C. If the blots were not probed for Ub, the membranes were boiled for one minute in ddH_2O, and then blocked as described above. After blocking, the membrane was washed three

times with TTBS and incubated with primary antibodies for 18 hours at either 21°C, or 4°C. The membranes were then washed three times for 10 minutes with TTBS. Secondary antibodies were diluted 1:5000 in 1X TTBS, and applied to the membrane for one hour at 21°C. Membranes were washed three times with TTBS for 10 min and then examined by enhanced chemiluminescence (ECL). Exposure times varied from 30 seconds to two minutes.

10X TTBS

25 mM Tris-HCl, pH= 7.4, 137 mM NaCl, 2.7 mM KCl, 0.5 %Tween

Ponceau solution

1 % Ponceau S, 5 % Trichloroacetic acid (TCA)

Blocking Buffer

5 % nonfat dry milk in 1X TTBS

Stripping buffer

55 mM Tris-HCl (Trizma), 0.03 % SDS, 0.1M BME

ECL (Perker Elmer Life Science)

GelLogic 1500 Imaging system

Imaging software (Eastman Kodak Co.)

Table 3: Antibodies used in this study

Antibody	Dilutions	Secondary	Source	Catalog nr.
GST-Rad23	1:5000-10,000	anti-rabbit	our lab	n./a.
GST-Ubc2	1:2000	anti-rabbit	our lab	n./a.
Ubiquitin	1:100-500	anti-rabbit	Sigma	U5379
FLAG-HRP	1:1000	n./a.	Sigma	A8592
Myc	1:5000	anti-mouse	Sigma	630914
HA-HRP	1:1000	anti-mouse	Roche	12 013 819 001
Anti-GFP	1:2000	anti-rabbit	Sigma	C1544
Rpn12	1:10,000-20,000	anti-rabbit	D. Skowyra (St. Louis University)	n./a.
Rpn10	1:10,000-20,000	anti-rabbit	D. Skowyra (St. Louis University)	n./a.

2.8 Microscopy

For microcopy, a small volume of cultures was grown as described above. If cells were imaged live, cells were pelleted, re-suspended in residual liquid and spotted on microcopy slides. When experimental design required staining of the nucleus, Hoechst 33342 was added and cells were incubated for 30 minutes with constant rocking at 21°C. Cells were washed three times with ddH_2O before re-suspended in residual liquid and spotted on microscope slides. Yeast cells were imaged using the Zeiss Imager M1 microscope.

Hoechst 33342 (Sigma)

Poly-Prep slides (Sigma)

Zeiss Imager M1 microscope

Chapter III

The cellular location of Rad23

plays a key role in its interaction with nuclear substrates.

3.1 Experimental Results

Recent studies revealed compelling evidence that many nuclear substrates have to be exported to be degraded by the proteasome. The Madura group showed that (1) nuclear substrate are stabilized when export is blocked, (2) catalytically active proteasomes are located primarily in the cytosol, (3) a mechanism for targeting the proteasome to the nuclear surface was identified, and (4) shuttle factors, such as Rad23, can bind polyUb substrates and deliver them to the proteasome. This mechanism is envisioned to promote the delivery of nuclear substrates to cytosolic proteasomes. I hypothesized that Rad23 would play a key role in this process, which required it to repeatedly enter and exit the nucleus bearing a cargo of polyUb substrates (Fig. 7). An important aspect of this hypothesis is that Rad23 is not degraded by the proteasome, but like ubiquitin is recycled.

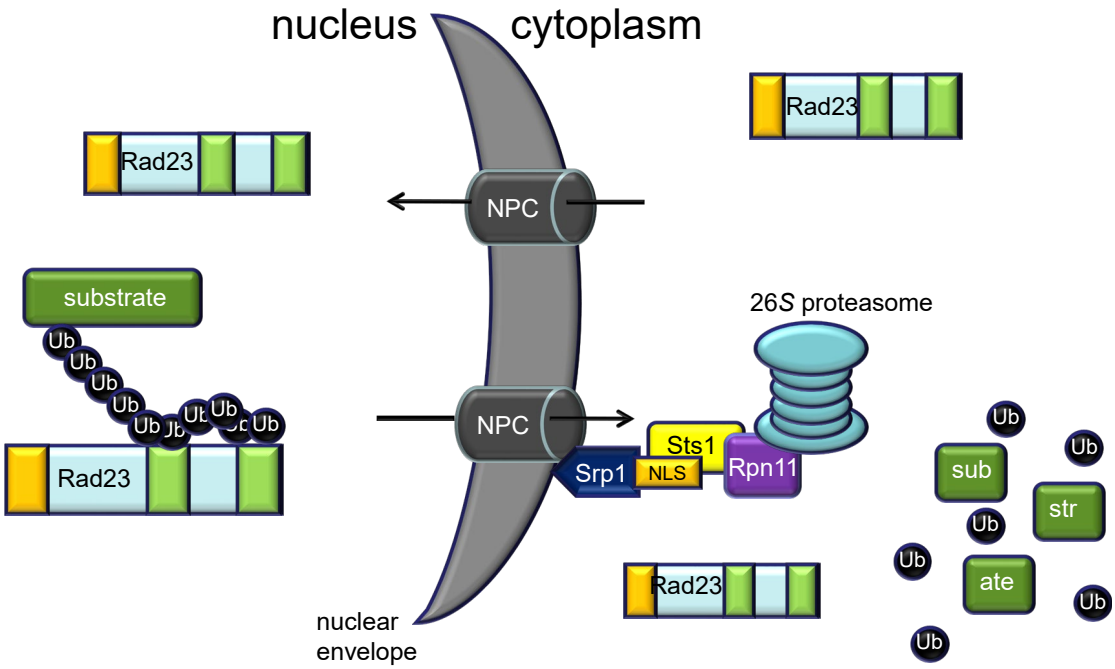

Figure 9. Model of transport mechanism of nuclear substrates. Rad23 enters the nucleus through the nuclear core complex (NPC). Inside its binds polyUb substrates and delivers them to the proteasome that is tethered to the nuclear surface for degradation.

3.1.1 Rad23 binds high levels of polyUb substrates in the nucleus

The proteasome localization defect of *sts1-2* was confirmed by examining localization of Rpn11-GFP (a 19*S* subunit) and Pup1-RFP (a 20*S* subunit). The 19*S* and 20*S* subunits were both localized to the nucleus at the non-permissive temperature (37°C) in wildtype cells, as confirmed by detecting the nuclei with DAPI (Fig. 10). The co-localization of these proteasome subunits produced an orange color when merged (Fig. 10). In contrast, Rpn11-GFP and Pup1-RFP showed diffuse signal in the cytoplasm in *sts1-2* at 37°C, and no co-localization with DAPI was observed at the non-permissive temperature (Fig. 10).

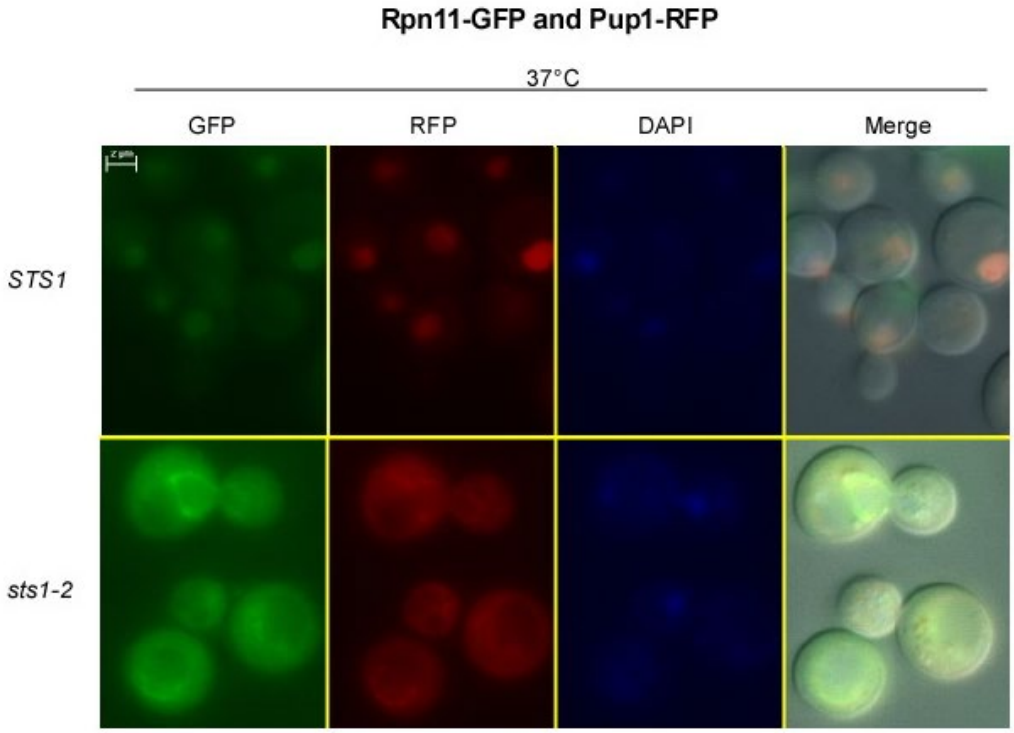

Figure 10. Proteasome is mislocalized in *sts1-2*. Rpn11-GFP and Pup1-RFP were co-expressed in either *STS1* or *sts1-2*. Cells were grown in 10ml of synthetic complete (SM) medium for 16 hours at 21°C. Cultures were then diluted into fresh SM and incubated at either 21°C or 37°C for 5 hours. One ml aliquots of exponentially growing culture were withdrawn, pelleted and re-suspended into 1 ml of sterile water containing 1 µg/ml Hoechst 33342. The cells were incubated for 30 minutes at 21°C, and then washed with water three times. Cell pellets were suspended in 50µl water. Aliquots (2.5µl) were spotted on Poly-Prep slides, and live cells were imaged.

I investigated the localization of Rad23 in the *sts1-2* mutant. I expressed GFP-Rad23 in either wildtype or *sts1-2* and examined cultures grown for five hours at either permissive (21°C) or non-permissive (37°C) temperatures. At 21°C GFP-Rad23 was detected in the nucleus and cytoplasm in both wildtype and *sts1-2* (Fig. 11). A similar localization was observed at 37°C in the wildtype strain (Fig. 11). In contrast, GFP-Rad23 was strongly enriched in the nucleus in *sts1-2* at 37°C (Fig. 11). The location of the nucleus was confirmed by imaging cells treated with Hoechst 33342 (Fig. 11).

I examined Rad23 protein levels to ensure that its mislocalization in *sts1-2* at 37°C was not caused by altered protein levels. After five hours of incubation at either 21°C or 37°C, cycloheximide was added to yeast cultures to block protein synthesis. Cells were harvested at the time points indicated (Fig. 12). GFP-Rad23 levels were unaffected in wildtype and *sts1-2* (Fig. 12). In addition, temperature did not alter GFP-Rad23 levels (Fig. 12).

The degradation of several nuclear substrates requires export. The translocation of some of these nuclear proteins is mediated by a conserved export factor that in yeast is termed Xpo1. However, since polyUb substrates bind shuttle factors, I questioned the role of Rad23 in the export of proteasome substrates. Since proteasomes are mislocalized in *sts1-2*, and results in the stabilization of nuclear substrates, I examined the localization of Rad23 (L. Chen et al., 2014b). I speculated that if Rad23 was trapped inside the nucleus it would be bound to stabilized nuclear substrates. To test this idea I examined Rad23 interaction with polyUb substrates in *sts1-2*. FLAG-Rad23 was purified from cultures grown at

21°C or 37°C, and its interaction with polyUb proteins was tested by immunoblotting (Fig. 13). Overall levels of polyUb substrates that were co-purified with FLAG-Rad23 were similar in *STS1* and *sts1-2* at 21°C (Fig. 13a, lane 2 and 3). Although the levels of polyUb substrates detected in *STS1* at 37°C were higher than in *sts1-2* (Figure 13a, compare lane 2 and 4), higher levels of polyUb proteins were co-purified with FLAG-Rad23 from *sts1-2* at 37°C (Figure 13a, compare lanes 3 and 5). Immunoblotting showed that equivalent levels of Rpn10 were co-purified with FLAG-Rad23 in *STS1* and *sts1-2* at 21°C and 37°C (Figure 13a). Densitometry showed that ~ 3-4 fold higher levels of polyUb proteins in association with FLAG-Rad23 in *sts1-2* at 37°C (Fig. 13b).

In *sts1-2*, the proteasome is mislocalized and substrates are stabilized inside the nucleus. I determined that the accumulation of Rad23 in the nucleus in *sts1-2* is not a result of altered protein levels. In addition, I showed that when Rad23 is trapped inside the nucleus it forms a robust interaction with polyUb substrates.

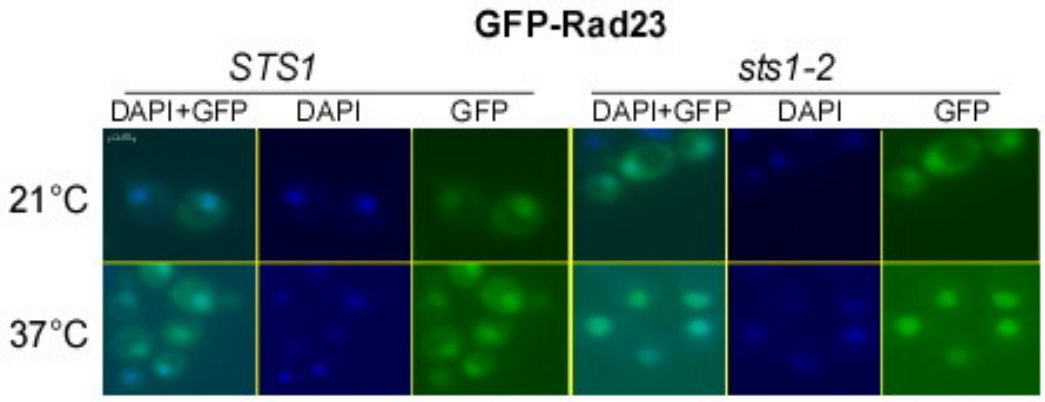

Figure 11. Rad23 is enriched in the nucleus in *sts1-2*. GFP-Rad23 was expressed in *STS1* and *sts1-2*. Cells were grown overnight in 10 ml of SM for 16 hours at 21°C overnight. Cultures were then diluted into fresh SM and incubated for 5 hours at either 21°C or 37°C. One ml aliquots were withdrawn from of exponentially growing culture, pelleted and re-suspended into 1 ml of sterile water containing 1 µg/ml Hoechst 33342. Cells were incubated for 30 minutes at 21°C. Cells were pelted, washed 3 times with dH_2O, and re-suspended in 50 µl dH_2O. For imaging, 2.5 µl aliquots were spotted on Poly-Prep slides, and cells were imaged live.

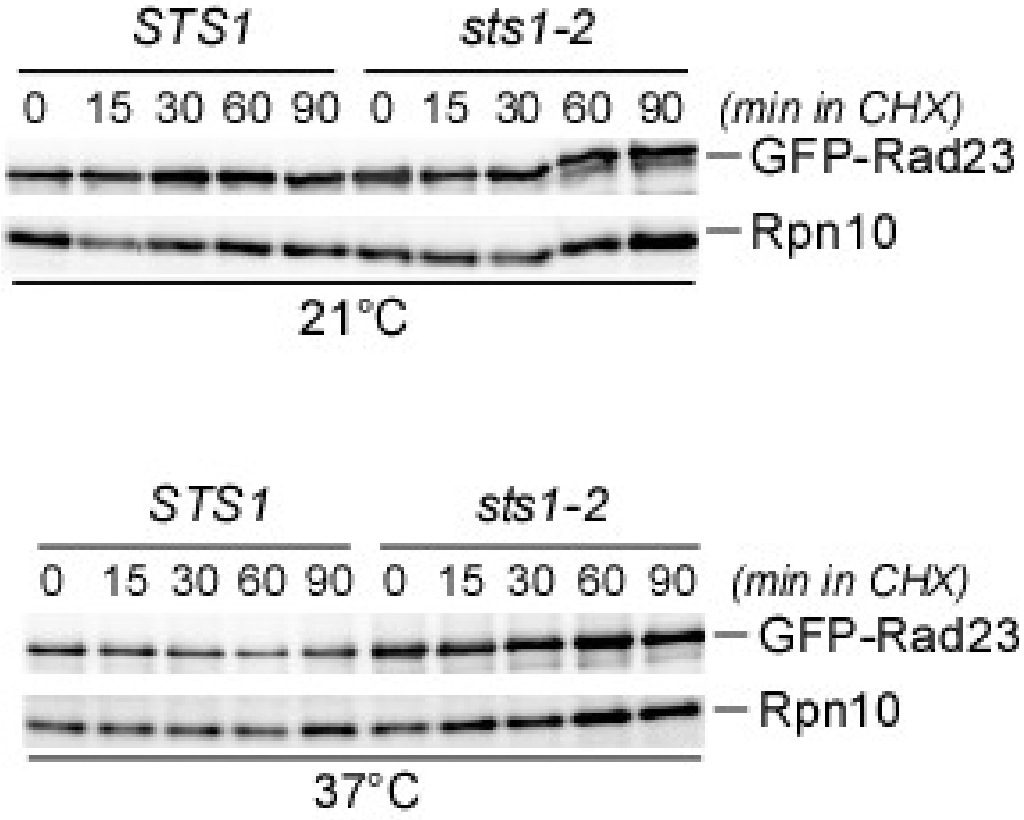

Figure 12. Rad23 protein levels are not affected in *sts1-2*. GFP-Rad23 was expressed in *STS1* and *sts1-2*. Cells were grown in 50 ml of SM for 16 hours at 21°C. Cultures were then diluted into fresh non-selective media (YPD), and incubated for 5 hours at either 21°C or 37°C. Cycloheximide (200µg/ml) cycloheximide was then added and 10 ml aliquots were withdrawn at 0, 15, 30, 60, and 90 minutes. Yeast lysates were prepared and equal amount of total protein was separated in a 12 % polyacrylamide SDS-Tricine gel. Gels were transferred to nitrocellulose membrane, and probed with antibodies against GFP, and Rpn10.

Figure 13

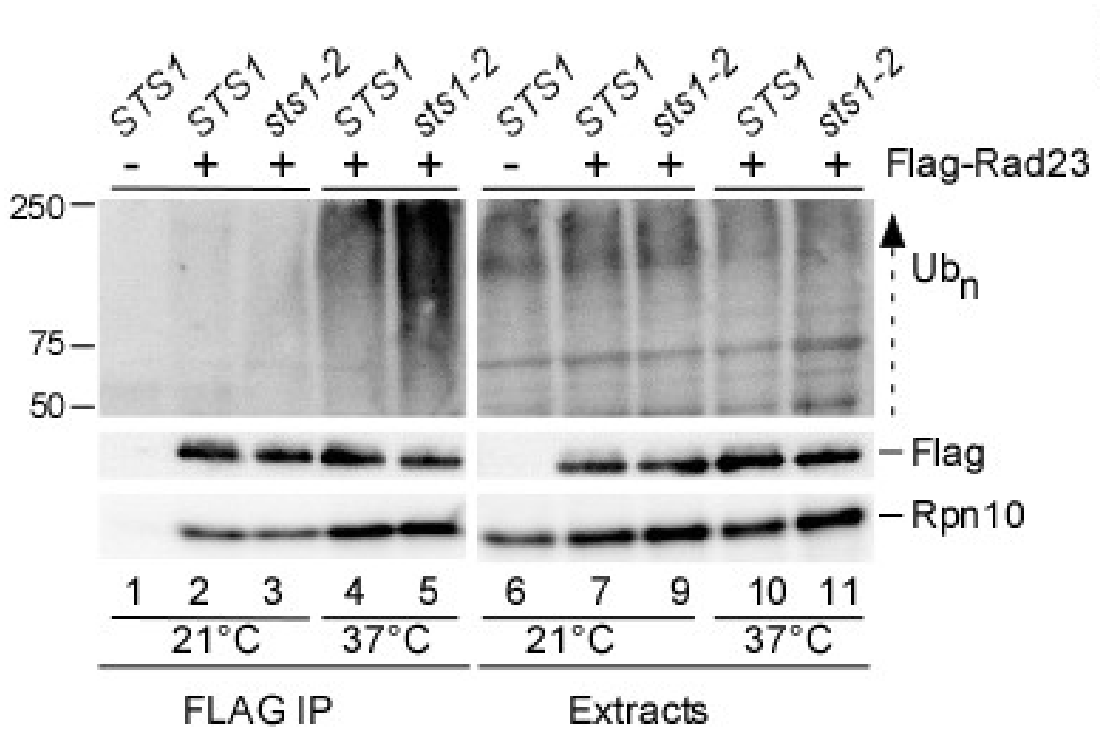
STS1
STS1
sts1-2
STS1
sts1-2
STS1
STS1
sts1-2
STS1
sts1-2
- + + + + - + + + +
Flag-Rad23
250
75
50
Ubn
Flag
Rpn10
1 2 3 4 5 6 7 9 10 11
21°C
37°C
21°C
37°C
FLAG IP
Extracts

(b)

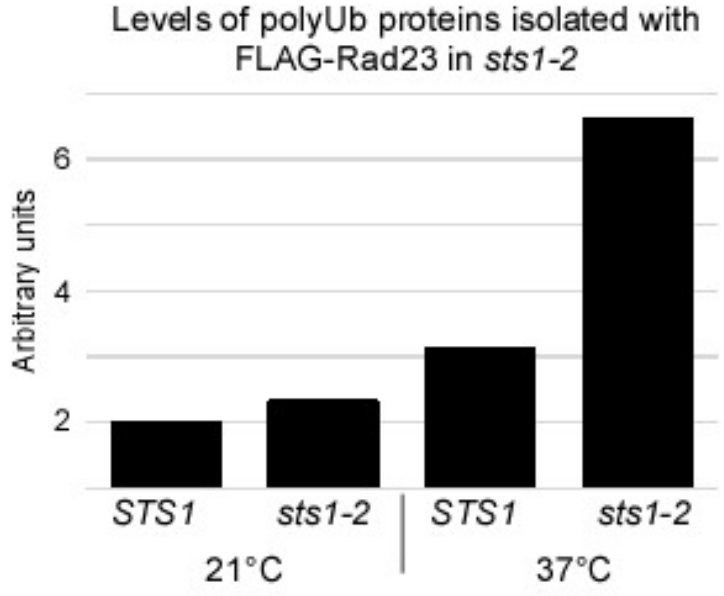
Levels of polyUb proteins isolated with FLAG-Rad23 in sts1-2
Arbitrary units
6
4
2
STS1
sts1-2
STS1
sts1-2
21°C
37°C

Figure 13. Rad23 interaction with polyUb substrates is higher in the nucleus. (a) FLAG-Rad23 was expressed in *STS1* and *sts1-2*. Cells were grown in 50 ml of SM for 16 hours 21°C. Cultures were then diluted into fresh non-selective media (YPD and incubated for 5 hours at either 21°C or 37°C. Cells were pelleted and yeast lysates were prepared. Equal amount of protein lysate was applied to anti-FLAG matrix and incubated for 2 hours at 4 °C. Purified proteins were separated in a 12 % polyacrylamide SDS-Tricine gel. Gels were transferred to nitrocellulose membrane and probed with antibody against FLAG, Ub, and Rpn10. (b) Levels of polyUb proteins co-purified with Rad23 (panel a, lanes 2-5) were quantified. Data is representative of four independent experiments.

3.1.2 Rad23 binds low levels of polyUb substrates in the cytosol

Additional studies were performed to confirm the role of the nucleocytoplasmic trafficking pathway in the export of substrates and the shuttle factor Rad23. The Madura group demonstrated that Cdc17 and Rad4 were stabilized when they were not exported in the *xpo1-1* and *crm1* export mutants. They also reported that when the proteasome is unavailable at the nuclear surface, as observed in *sts1-2* and *srp1-49*, nuclear substrates are stabilized. In addition, preliminary studies showed that mutations in a key nucleocytoplasmic trafficking factor RanGAP, (called Rna1 in yeast), stabilized DNA repair factor Rad4 (data not shown – L. Chen – unpublished studies). Rna1 facilitates nucleotide exchange on the Ran protein, which oscillates between the nucleus and cytoplasm, based on its interaction with GTP or GDP. This mechanism controls the nuclear import and export of various proteins. Intriguingly nuclear substrates are stabilized in *rna1-1* mutant, although proteasomes are properly localized (data not shown – L. Chen – unpublished studies). Because Rna1 plays a critical role in nucleocytoplasmic trafficking, I examined Rad23 localization in *rna1-1*. GFP-Rad23 was expressed in *RNA1* and *rna1-1*, and cultures were examined after growth for one hour at 21°C and 37°C (Fig. 14). GFP-Rad23 was present in both nucleus and cytoplasm at 21°C in wildtype and *rna1-1*, as well as at 37°C in the wildtype strain (Fig. 14). However, in *rna1-1* GFP-Rad23 was enriched in the cytoplasm at 37°C (Fig. 14). Thus, GFP-Rad23 in enriched in the nucleus in *sts1-2* (Fig. 11), but is cytosolic in *rna1-1* (Fig. 14). Treatment with Hoechst 33342 confirmed the location of the nucleus (Fig. 14).

I investigated if the mislocalization of Rad23 to the cytosol was caused by altered protein levels. GFP-Rad23 was expressed in *RNA1* and *rna1-1*, and yeast cells were treated with cycloheximide after one hour incubation at 21°C and 37°C (Figure 15). I determined that GFP-Rad23 protein levels were unaffected in wildtype and *rna1-1* at 21°C and 37°C (Fig. 15).

Significantly, proteasome localization is not affected in *rna1-1* (data not shown – L. Chen – unpublished studies). However, since Rad23 accumulates in the cytoplasm in this mutant, I investigated if it could still bind polyUb nuclear proteins. I examined Rad23 interaction with polyUb substrates in wildtype and *rna1-1*. FLAG-Rad23 was purified from cultures grown at 21°C or 37°C, and bound proteins were analyzed by immunoblotting (Fig. 16). While the levels of polyUb substrates that were co-purified with FLAG-Rad23 were similar in *RNA1* and *rna1-1* at 21°C (Fig. 16a, lane 2 and 3), the amount of polyUb substrates bound to FLAG-Rad23 was strongly reduced in *rna1-1* at 37°C (Figure 16a, compare lane 5 and 6). Higher levels of polyUb substrates were observed in *RNA1* at 37°C, which I believe is caused by heat stress (Figure 16a, lane 5). I confirmed that equivalent levels of Rpn10 were co-purified with FLAG-Rad23 in *RNA1* and *rna1-1* at 21°C and 37°C. The level of polyUb proteins isolated with FLAG-Rad23 was quantified by densitometry (Figure 16b).

The *rna1-1* mutant exhibits a severe defect in both nuclear import and export at the non-permissive temperature. Although proteasomes are efficiently targeted to the nuclear surface in rna1-1, nuclear substrates are stabilized (data not shown – L. Chen, unpublished studies). I determined that Rad23 is enriched in

the cytoplasm in rna1-1, which could be the result of the deficient nuclear transport system. Thus the failure to reimport Rad23 leads to its cytosolic accumulation. Moreover, Rad23 interaction with polyUb substrates is strongly reduced in *rna1-1*, leading to the conclusion that it primarily binds nuclear substrates of the proteasome. The stabilization of these nuclear substrates can be attributed to the lack of availability of the Rad23 shuttle factor.

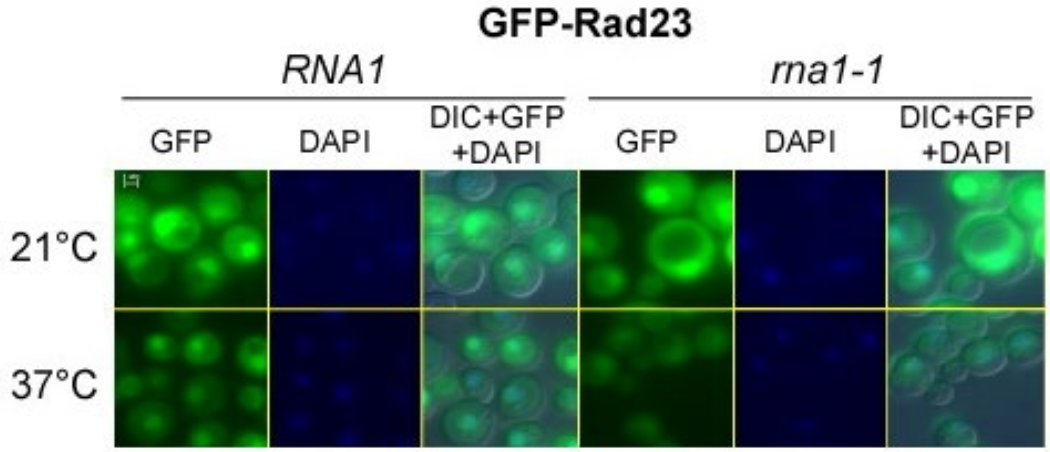

Figure 14. Rad23 is enriched in the cytoplasm in *rna1-1*. GFP-Rad23 was expressed in *RNA1* and *rna1-1*. Cells were grown in 10ml of SM for 16 hours at 21°C. Cultures were diluted into fresh SM and incubated for 2 hours at 21°C. Cultures were then split and incubated for 1 hour at 21°C or 37°C. One ml aliquots were withdrawn from exponentially growing culture, pelleted and re-suspended into 1 ml of sterile dH_2O containing 1 µg/ml Hoechst 33342. Cells are incubated for 30 minutes at 21°C. Cells were pelted, washed 3 times with dH_2O, and re-suspended in 50 µl dH_2O. For imaging, 2.5µl aliquots from each sample was withdrawn and spotted on Poly-Prep slide, and cells were imaged live.

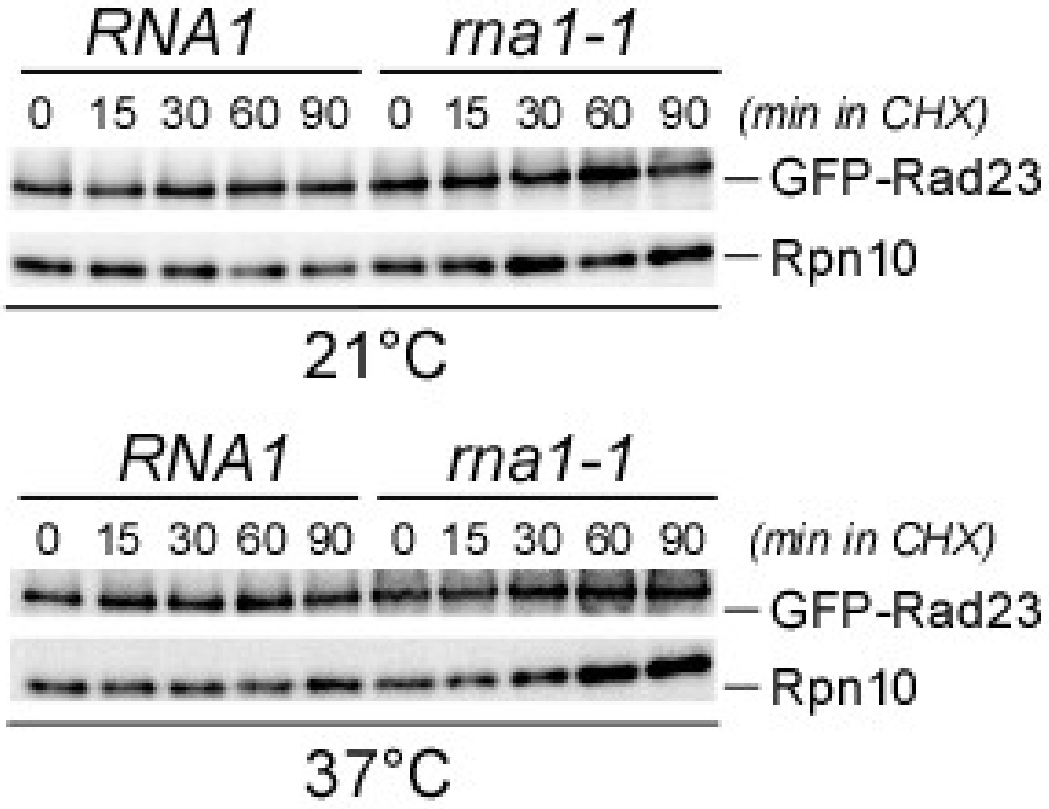

Figure 15. Rad23 protein levels are not affected in *rna1-1*. GFP-Rad23 was expressed in either *RNA1* or *rna1-1*. Cells were grown overnight in 50 ml of SM media at room temperature (21°C). Next day, cultures were diluted into fresh YPD media and incubated at either 21°C or 37°C for 1 hr. After incubation period, 200µg/ml cycloheximide was added to cultures and 10 ml aliquots were drawn at 0, 15, 30, 60, and 90 minutes interval. Yeast lysates were prepared and equal amount of total protein was separated in a 12 % polyacrylamide SDS-Tricine gel. Gels were transferred to nitrocellulose membrane, and probed with antibodies against GFP, and Rpn10.

Figure 16

(a)

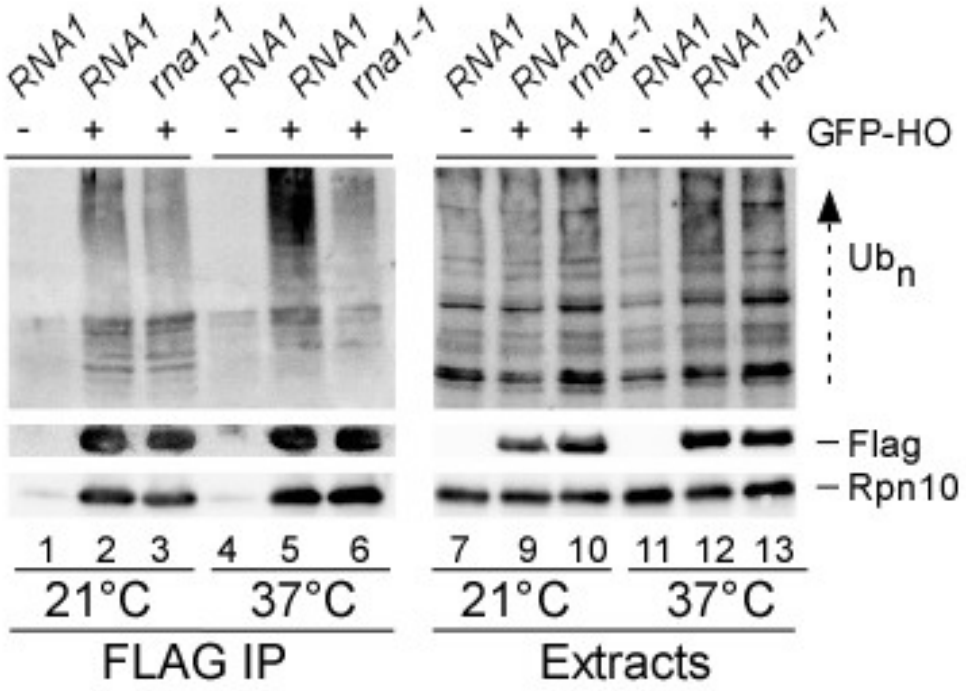
RNA1
RNA1
rna1-1
RNA1
RNA1
rna1-1
RNA1
RNA1
rna1-1
RNA1
RNA1
rna1-1
- + + - + + - + + - + + GFP-HO
Ub$_n$
Flag
Rpn10
1 2 3 4 5 6 7 9 10 11 12 13
21°C 37°C 21°C 37°C
FLAG IP
Extracts

(b)

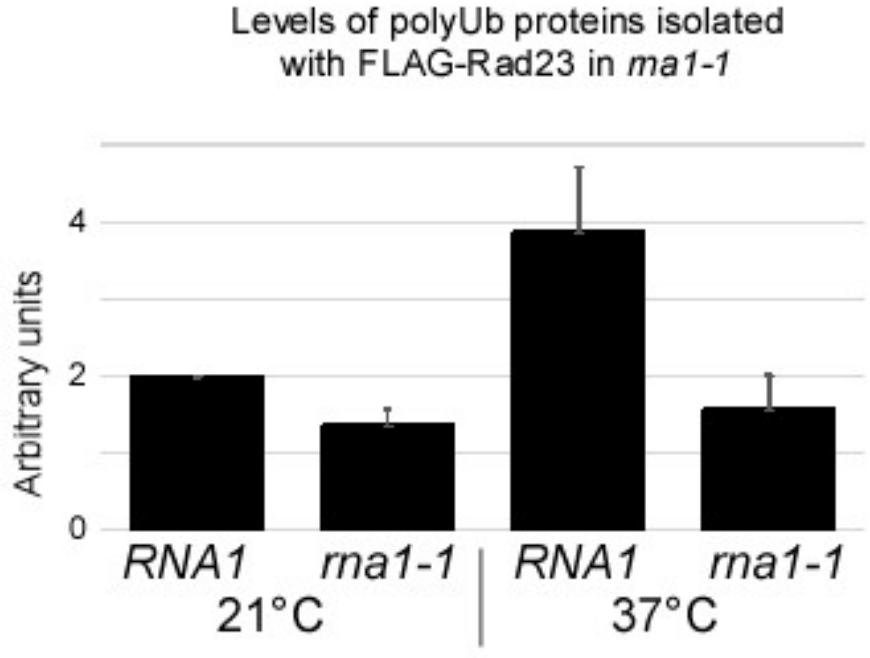
Levels of polyUb proteins isolated with FLAG-Rad23 in ma1-1
Arbitrary units
0
2
4
RNA1
rna1-1
RNA1
rna1-1
21°C
37°C

Figure 16. Rad23 interaction with polyUb substrates is lower in the cytosol. (a) FLAG-Rad23 was expressed in *RNA1* and *rna1-1*. Cells were grown in 50 ml of SM for 16 hours at 21°C. Cultures were then diluted into fresh non-selective media (YPD) and incubated for 2 hours at 21°C. Cultures were split incubated for 1 hours at 21°C and 37°C. Following the incubation, cells were pelleted and yeast lysates were prepared. Equal amount of protein lysate was applied to anti-FLAG matrix and incubated for 2 hours at 4 °C. Purified proteins were separated in a 12 % polyacrylamide SDS-Tricine gel. Gels were transferred to nitrocellulose membrane and probed with antibody against FLAG, Ub and Rpn10. (b) The levels of polyUb proteins bound to FLAG-Rad23 (panel a; lanes 2, 3, 5, 6) were quantified (N = 5).

3.1.3 Rad23 with defective UbL and UBA domains displays the same subcellular localization as the wildtype Rad23 protein

It was previously reported that Rad23 binds the proteasome through its UbL domain (Schauber et al., 1998). It was also shown that Rad23 could bind polyUb substrate *via* its two UBA domains (L. Chen et al., 2001; L. Chen et al., 2002). Therefore, I investigated if the UbL and UBA domains contributed to Rad23 trafficking into and out of the nucleus. I expressed GFP-tagged mutant derivatives of Rad23 in *STS1*, *sts1-2*, *RNA1*, and *rna1-1*. The rad23$^{\Delta UbL}$ and rad23^{K7A} are unable to interact with the proteasome, while rad23^{uba1} is unable to bind polyUb substrates. I found that rad23$^{\Delta UbL}$ and rad23^{K7A} was present in both the nucleus and cytosol at non-permissive temperature in wildtype and specific mutants strains (Fig. 17a, 17b). rad23^{uba1} also showed no alteration in localization at 21°C, despite its defect in binding polyUb substrates. All three mutants, rad23$^{\Delta UbL}$ and rad23^{K7A}, rad23^{uba1}, were completely localized to the nucleus in *sts1-2*, and to the cytosol in *rna1-1* at the non-permissive temperature, as I observed with wildtype Rad23 (Fig. 11, 14). These results suggest that the localization of Rad23 is independent of its ability to bind polyUb substrates, or the proteasome.

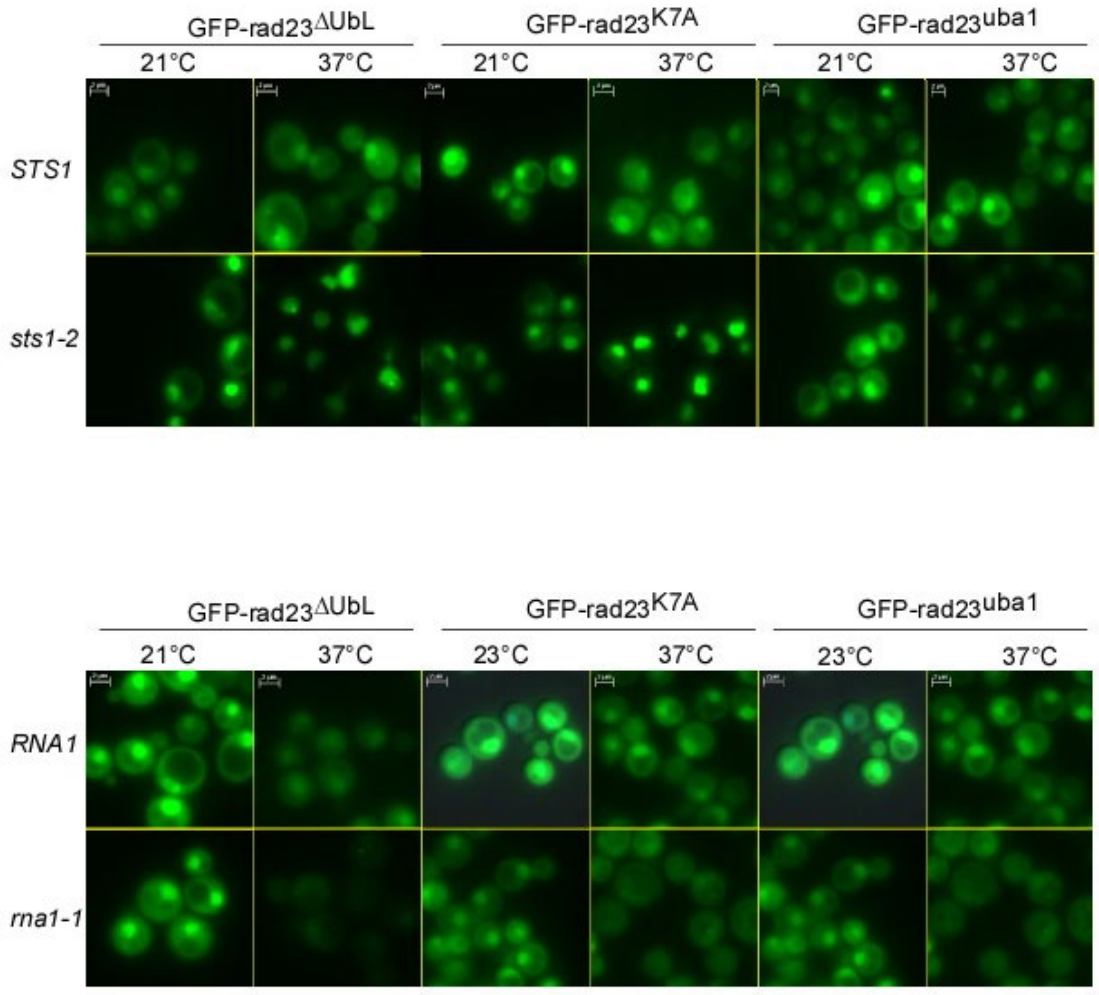

Figure 17. Mutant Rad23 is enriched in the nucleus in *sts1-2* and in the cytosol in *rna1-1*. GFP-tagged derivatives Rad23: rad23$^{\Delta UbL}$, rad23^{K7A}, and rad23^{uba1}.were expressed in (a) *STS1* and *sts1-2*, and in (b) in *RNA1* and *rna1-1*. Cells were grown in 10 ml SM for 16 hours at 21°C. Cells were diluted to fresh SM and incubated (a) for 5 hours at 21°C and 37°C, and (b) for 2 hours at 21°C before cultures were split and grown for 1 hour at 21°C and 37°C. For (a) and (b) one ml aliquots were withdrawn, pelleted and re-suspended in residual liquid. A 2.5 µl aliquot was spotted on Poly-prep slides for live cell imaging.

3.1.4 Ddi1 shows same pattern of localization and polyUb substrate binding as Rad23 in *sts1-2* and *rna1-1*

Substrate specificity in the UPP is in part mediated by selectively targeting substrates for ubiquitylation. However, shuttle factors are not intrinsic subunits of the proteasome, but are thought to play a critical role in trafficking substrates to the proteasome (Wade et al., 2010). There are three known shuttle factors in yeast: Rad23, Ddi1, and Dsk2. These proteins are thought to have overlapping functions in targeting substrates to the proteasome, although the evidence in support of this conjecture is limited (C. Liu et al., 2009).

Each yeast shuttle factors was initially characterized in other cellular processes. For instance, Rad23 was shown to function in DNA repair. Rad23 was also the first protein reported to contain an N-terminal UbL domain, although the significance of this feature was unknown at that time (Watkins et al., 1993). Biggins and colleagues reported Dsk2 as the second protein to contain an N-terminal UbL domain (Biggins et al., 1996). It has a well-characterized role in spindle pole duplication and transition through G2/M phase in the cell cycle, although a specific role in the UPP was not investigated (Biggins et al., 1996).

The shuttle factor Ddi1 was found be expressed from a bidirectional promoter expressing also *MAG1*, a 3-methyladenine DNA glycosylase involved in base excision repair (BER) (Y. Liu et al., 1997a; Y. Liu et al., 1997b). Therefore it was suggested that Ddi1 functions in one of the DNA-damage checkpoint pathways (Zhu et al., 1998; Y. Zhu et al., 2001; Fu et al., 2008). It was recently reported that Ddi1 plays a key role in the DNA replication stress response pathway

(Svoboda et al., 2019). Ddi1 was also identified as a SNARE-interacting protein, and its overexpression in *sec9* mutant yeast inhibited protein secretion; thus Ddi1 is suggested to functions as negative regulator of exocytosis (Lustgarten et al., 1999; Marash et al., 2003). Structural studies revealed that Ddi1 harbors a central retroviral protease-like (RVP) domain, which in yeast is required for protein secretion (Krylov et al., 2001; White et al., 2011). Similar to Dsk2, Ddi1 contains an N-terminal UbL domain and only one C-terminal UBA domain. It is predicted that Ddi1 will function as a polyUb shuttle factor, with Rad23 and Dsk2. In agreement, Bertolaet and colleagues reported that Ddi1 could bind polyUb substrates (Bertolaet et al., 2001).

I investigated Ddi1 localization, stability, and interaction with polyUb substrates. I also investigated if these interactions would resemble the properties of Rad23 in *sts1-2* and *rna1-1*. I expressed GFP-Ddi1 in *STS1*, *sts1-2*, *RNA1*, and *rna1-1*, and exposed cultures to either 21°C, or 37°C for either 5 hours (*STS1, sts1-2*) or 1 hour (*RNA1, rna1-1*) (Fig 18, 20). Similar to Rad23, I discovered that GFP-Ddi1 was present in both the nucleus and cytoplasm in *STS1* and *sts1-2* at 21°C, and *STS1* at 37°C. However, it was completely localized to nucleus in *sts1-2* at 37°C (Fig 18). The same was observed for Ddi1 in the *rna1-1* mutant. While Ddi1 was localized to the nucleus and cytoplasm in wildtype and *rna1-1* at the permissive temperature, it was completely cytosolic in *rna1-1* at non-permissive temperature (Fig.20). In addition, I found that Ddi1 is stable in *STS1* and *sts1-2* at both 21°C and 37°C (Fig. 19), and in *RNA1* and *rna1-1* (Fig. 21). To characterize Ddi1 interaction with polyUb substrates in these two genetic mutants, FLAG-Ddi1

was expressed in *STS1*, *sts1-2*, *RNA1* and *rna1-1*, and cultures were grown for five hours (*sts1-2*), or one hour (*rna1-1*) at 21°C and 37°C. I discovered that Ddi1 exhibited increased binding to polyUb substrates in *sts1-2* at the non-permissive temperature (data not shown – L. Chen, unpublished studies). In contrast, its binding to polyUb substrates was reduced in *rna1-1* at non-permissive temperature (Fig. 22).

The discovery that Ddi1 exhibits the same localization and polyUb substrate binding properties as seen with Rad23 suggests that these shuttle factors are functionally similar.

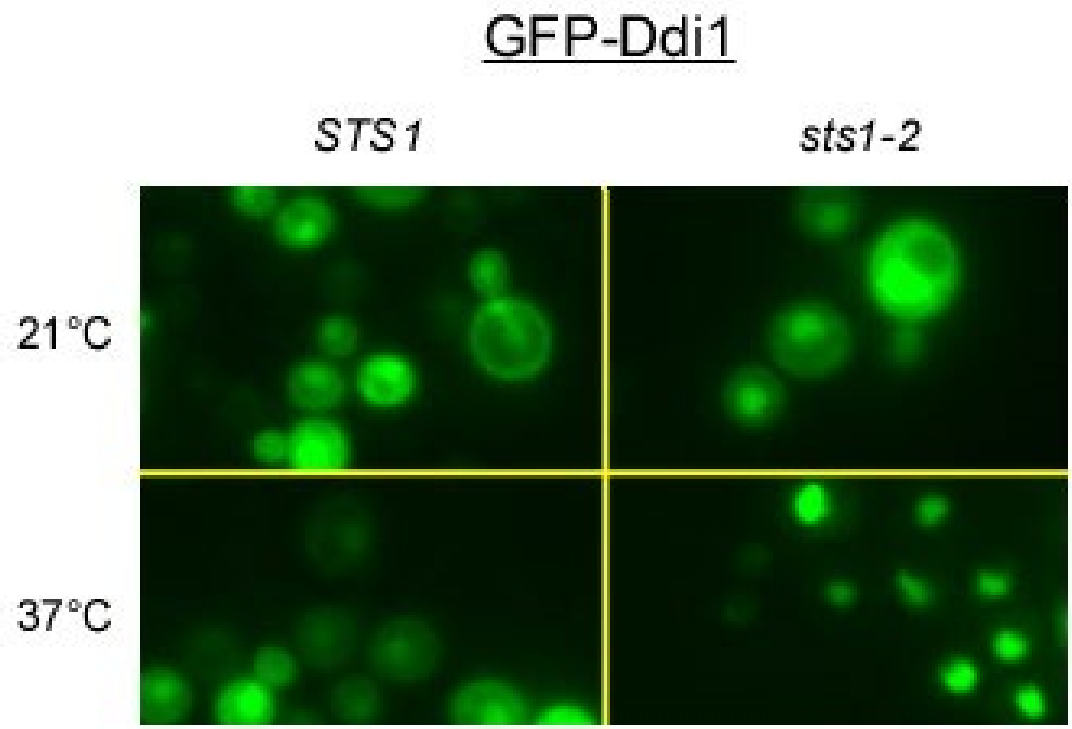

Figure 18. Ddi1 is enriched in the nucleus in *sts1-2*. GFP-Ddi1 was expressed in *STS1* and *sts1-2*. Cells were grown in 10 ml of SM for 16 hours at 21°C. Cultures were diluted into fresh SM and incubated at for 5 hours at 21°C and 37°C. One ml aliquots were withdrawn from exponentially growing culture and pelleted. For imaging, 2.5 µl aliquots from each sample was withdrawn, spotted on Poly-Prep slides, and cells were imaged live.

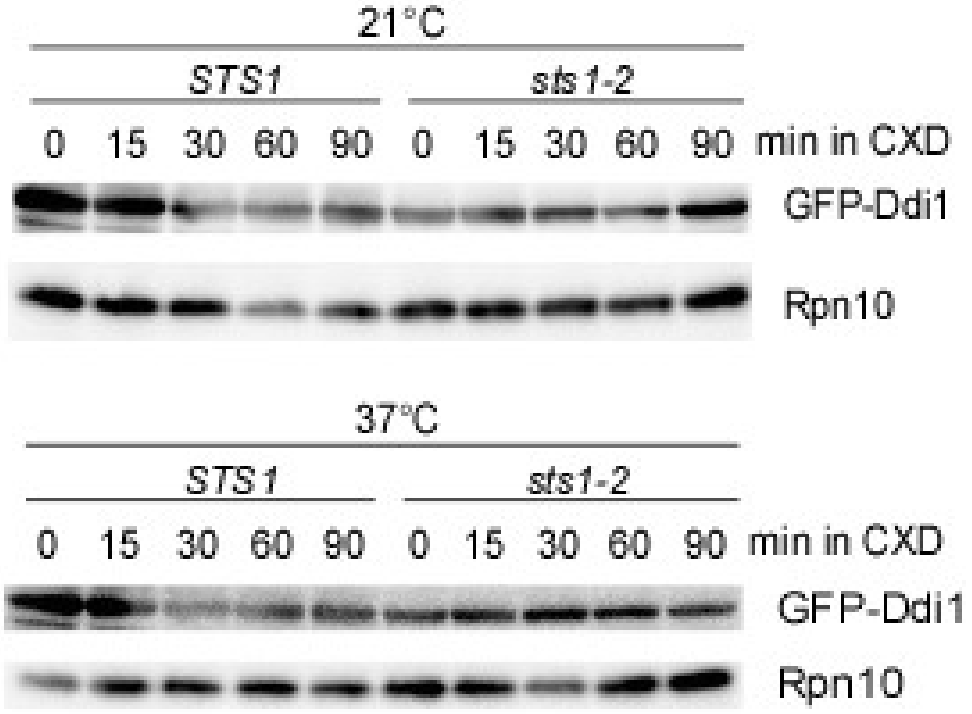

Figure 19. Ddi1 protein levels are not affected in *sts1-2*. GFP-Ddi1 was expressed in *STS1* and *sts1-2*. Cells were grown in 50 ml of SM for 16 hours at 21°C. Cultures were then diluted into fresh YPD media and incubated for 5 hours at 21°C and 37°C. After incubation period, 200µg/ml cycloheximide was added to cultures and 10 ml aliquots were withdrawn at 0, 15, 30, 60, and 90 minutes. Yeast lysates were prepared and equal amount of total protein was separated in a 12 % polyacrylamide SDS-Tricine gel. Gels were transferred to nitrocellulose membrane, and probed with antibodies against GFP, and Rpn10.

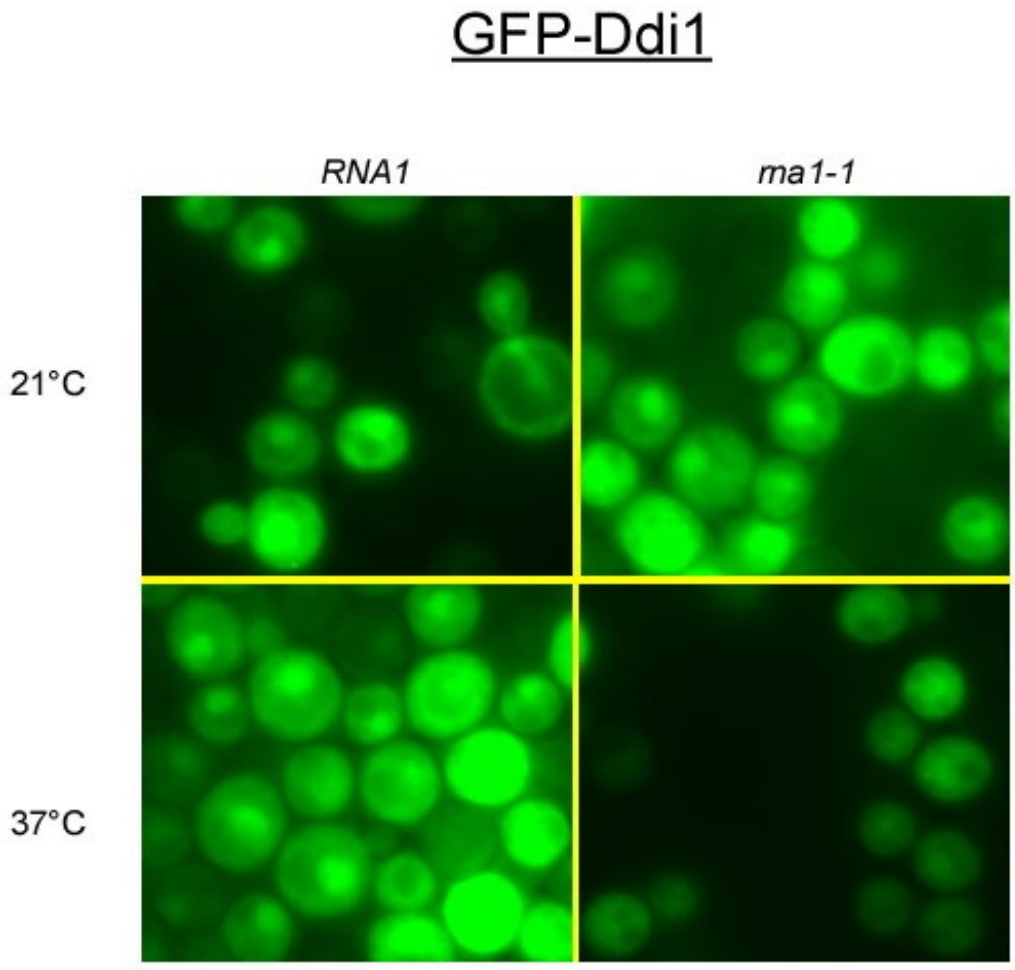

Figure 20. Ddi1 is enriched in the cytoplasm in *rna1-1*. GFP-Ddi1 was expressed in *RNA1* and *rna1-1*. Cells were grown in 10ml of SM for 16 hours 21°C. Cultures were then diluted into fresh SM and incubated for 2 hours at 21°C. Following this incubation, cultures were split and incubated for 1 hour at 21°C and 37°C. One ml aliquots were withdrawn from exponentially growing cultures, pelleted, and suspended in residual liquid. For imaging, 2.5µl aliquots from each sample was withdrawn, spotted onto Poly-Prep slides, and cells were imaged live.

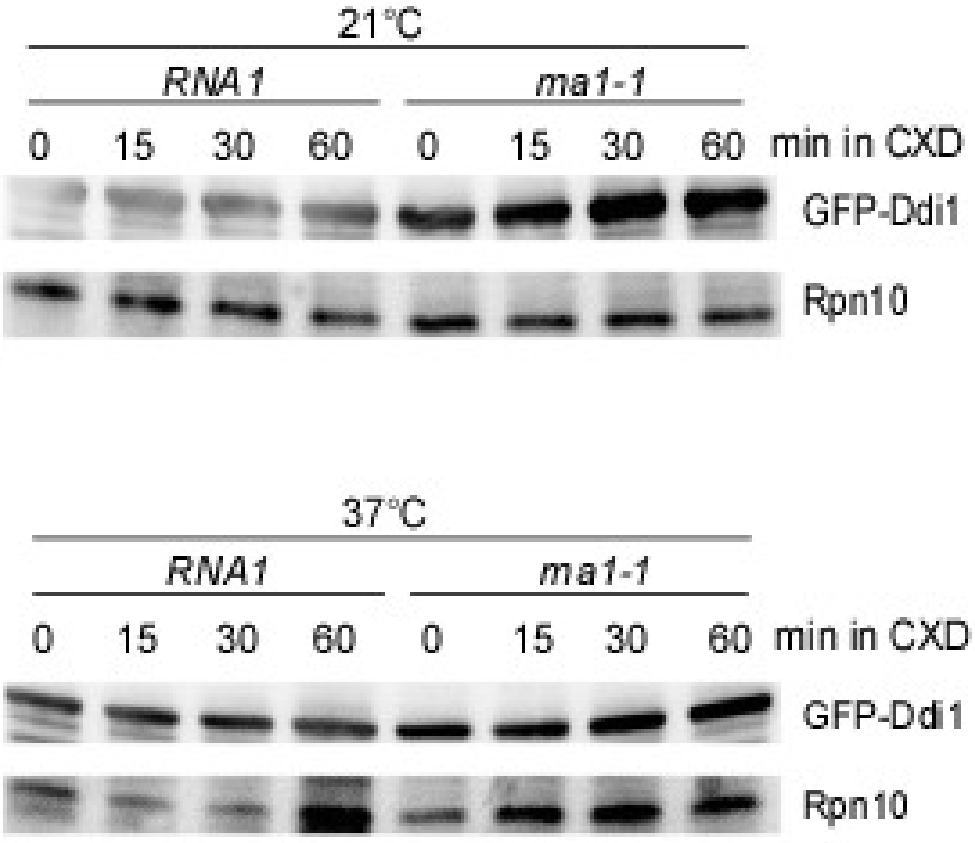

Figure 21. Ddi1 protein levels are not affected in *rna1-1*. GFP-Ddi1 was expressed in *RNA1* and *rna1-1*. Cells were grown in 50 ml of SM for 16 hours at 21°C. Cultures were then diluted into fresh YPD media and incubated for 2 hours at either 21°C. Following this incubation, cultures were split and incubated for 1 hour at 21°C or 37°C. After this incubation, 200µg/ml cycloheximide was added to cultures and 10 ml aliquots were withdrawn at 0, 15, 30, 60, and 90 minutes. Yeast lysates were prepared and equal amount of total protein was separated in a 12 % polyacrylamide SDS-Tricine gel. Gels were transferred to nitrocellulose membrane, and probed with antibodies against GFP, and Rpn10.

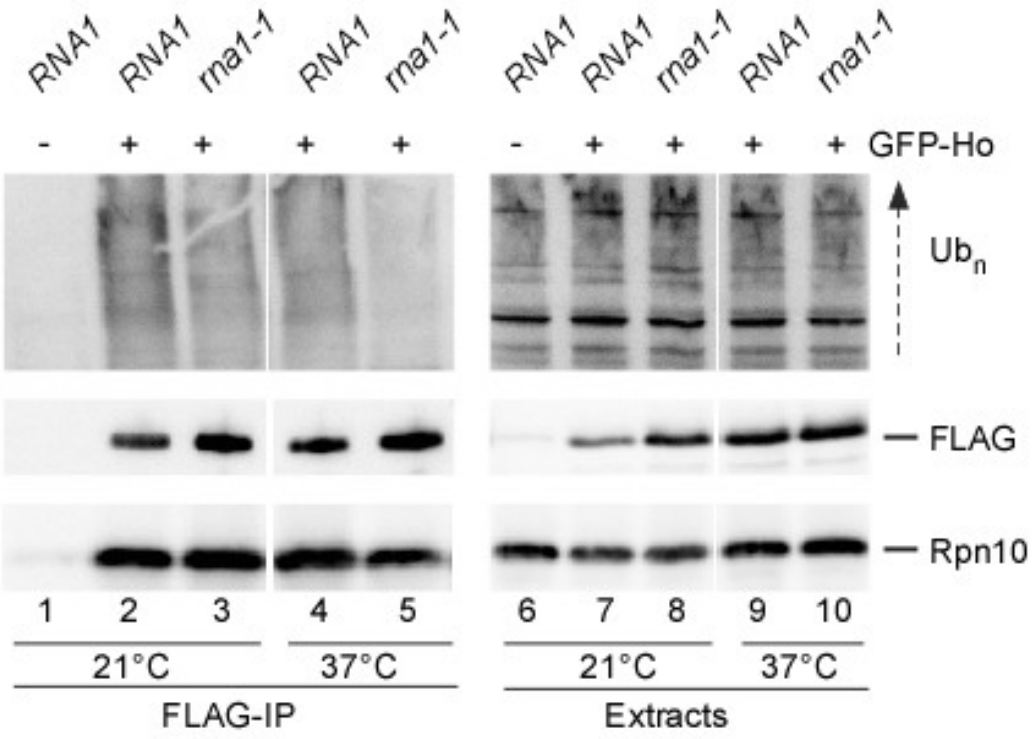

Figure 22. Ddi1 interaction with polyUb substrates is decreased in the cytosol. FLAG-Ddi1 was expressed in *RNA1* and *rna1-1*. Cells were grown in 50 ml of SM for 16 hours at 21°C. Cultures were diluted into fresh YPD media and incubated for 2 hours at either 21°C. Cultures were then split and incubated for 1 hour at 21°C, and 37°C. Cells were pelleted and yeast lysates were prepared. Equal amount of protein lysate was applied to anti-FLAG matrix and incubated for 2 hours at 4 °C. Purified proteins were separated in a 12 % polyacrylamide SDS-Tricine gel. Gels were transferred to nitrocellulose membrane and probed with antibody against FLAG, Ub and Rpn10.

3.1.5 The degradation of some nuclear substrates involves the nucleocytoplasmic transport system

The Madura lab previously reported that some nuclear proteins, including Rad4 and Cdc17 are degraded only after export from the nucleus (L. Chen et al., 2014a). Raveh and co-workers found that Ho-endonuclease (Ho) was similarly degraded by the proteasome in an export-dependent mechanism, with a specific role for the Ddi1 shuttle factor (Kaplun et al., 2005). However, the shuttle factors that promote turnover of most nuclear substrates of the proteasome have not been described. Only a few physiological targets of Rad23 have been identified; thus I expanded my efforts to identify other substrates whose proteasome-mediated degradation required nuclear export.

The Matα2 protein is a well-studied proteasome substrate (P. Chen et al., 1993), and its turnover requires nuclear export (data not shown – L. Chen, unpublished studies). Matα2-GFP was expressed in *STS1* and *sts1-2* mutants and I found that Matα2-GFP levels increased markedly in *sts1-2* at 37°C (Fig. 23). I also examined Matα2-GFP in *RNA1* and *rna1-1* and I found that it was depleted from the nucleus in *rna1-1* within 15 minutes (Fig. 23). Matα2-GFP was detected in discrete cytosolic deposits after 90 minutes (APPENDIX II – Okeke et al., manuscript in review). Based on these results, I propose that the transport of nuclear substrates to cytoplasmic proteasomes requires a functional export mechanism.

To determine if the cytosolic aggregates contained intact Matα2-GFP cells expressing Matα2-GFP were grown at 21°C and 37°C. Yeast lysates were

prepared and equal amount of protein was characterized by immunoblotting with antibody against GFP. It was determined that Matα2-GFP levels in *rna1-1* increased significantly at 37°C when compared to 21°C suggesting that the cytosolic aggregates contain intact Matα2-GFP (APPENDIX II – Okeke et al., manuscript in review).

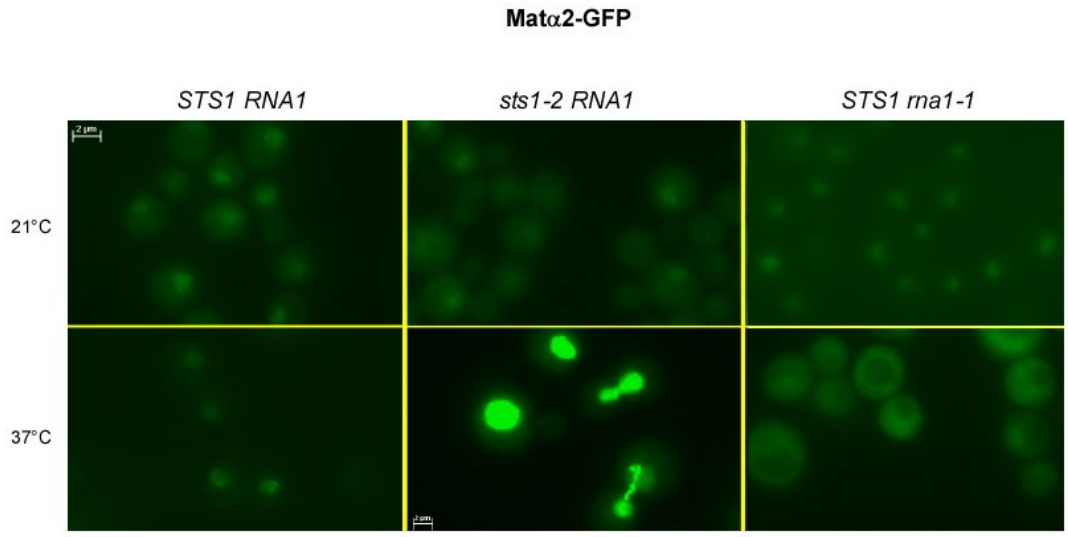

Figure 23. Matα2 accumulates in the nucleus in *sts1-2*, but localizes to the cytosol in *rna1-1*. Matα2-GFP was expressed in wildtype, *sts1-2* and *rna1-1*. Cultures were grown in 10 ml SM for 16 hours at 21°C. Cultures were then diluted into fresh SM media and split for *STS1* and *sts1-2*, and incubated at for 5 hours at 21°C, and 37°C. Cultures for *RNA1* and *rna1-1* were incubated for 2 hours at 21°C, before their were split and further incubated for 15 minutes at 21°C, and 37°C. One ml aliquots were withdrawn, pelleted, and suspended in residual liquid. For imaging, 2.5 µl aliquots were spotted Poly-prep slides, and cells were imaged live.

Clb2 is a well-studied nuclear substrate of the proteasome. It is a cell cycle protein that is involved in cell cycle progression. Clb2 stimulates Cdc28 to promote transition through G2/M phase of the cell cycle. It is only expressed during G2 and M phase, and is then rapidly degraded by the UPP. Since Clb2 is a nuclear substrate of the proteasome, I was interested in studying its turnover, and the possible requirement for nuclear export.

I expressed GFP-Clb2 in *STS1* and *sts1-2* yeast cells, and incubated cultures at 21°C and 37°C. Following two hour incubation, exponential-phase cells were arrested in G2/M phase with 15 µg/ml Nocodazole. This allowed Clb2 protein levels to increase. Incubation was continued for three hours at either permissive or non-permissive temperatures. After five hour incubation aliquots were withdrawn and examined microscopically (Fig 24a). The remainder of the cultures was released from cell cycle arrest and incubated for an additional hour at 21°C and 37°C before imaging (Fig. 24b). As expected, Clb2 accumulated inside the nucleus during G2/M phase arrest at 21°C and 37°C in wildtype and *sts1-2* (Fig. 24a). Cells were stained with Hoechst 33342 to confirm nuclear co-localization of Clb2 (Fig. 24a). After the cells were released from G2/M phase, GFP-Clb2 was barely detectable in *STS1* at 21°C and 37°C, and *sts1-2* at 21°C. In contrast, GFP-Clb2 levels remained elevated in *sts1-2* at 37°C (Fig. 24b), as observed Matα2-GFP in *sts1-2* (Fig. 23). Turnover and localization of GFP-Clb2 in *rna1-1* was also examined, and it was found be stabilized and aggregate in the cytosol similar to Matα2 (data not shown – L. Chen, unpublished studies).

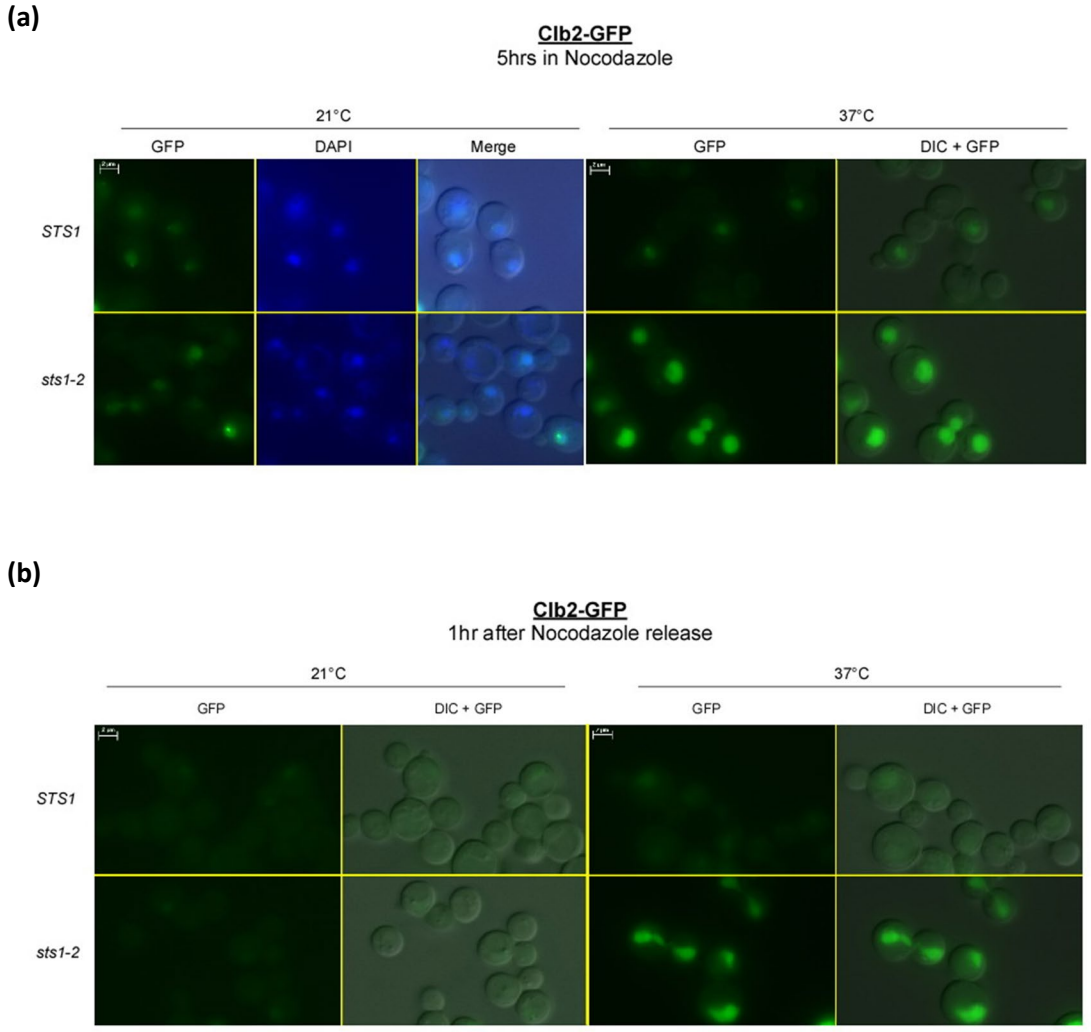

Figure 24. Clb2 is stabilized in *sts1-2*. Clb2-GFP was expressed in *STS1* and *sts1-2*. Cultures were grown in SM for 16 hours at 21°C. Cultures were diluted into fresh SM and incubated for 2 hours at 21°C, and 37°C. Exponentially growing cells were supplemented with 15 µg/ml Nocodazole and incubated for 3 hours at above listed temperatures. One ml aliquots were withdrawn, and pelleted. Cells from 21°C were re-suspended in 1 ml dH2O with 1µg/ml Hoechst 33342 and incubated for 30 min at 21°C. Before imaging Hoechst 33342 stained cells were washed 3 times with dH_20. The remainder of cultures were washed 4 times with sterile dH_2O, and re-suspended SM. Cultures from 37°C were placed in pre-warmed media. Cells were incubated for 1 hour at 21°C and 37°C before imaged. For all samples, 2.5 µl aliquots were spotted on Poly-prep slides, and cells were imaged live.

3.1.6 The localization of Rad23 affects turnover of Ho-endonuclease

My discovery that Rad23 can be confined to the nucleus (*sts1-2*) or cytosol (*rna1-1*) offered a unique opportunity to test its interaction with a physiological substrate in the nucleus versus the cytosol. I investigated if GFP-Ho localization was influenced by the sub-cellular distribution of Rad23. Proteasomes are mislocalized to the cytosol in *sts1-2* at 37°C (Fig. 10), and nuclear substrates were stabilized (L. Chen et al., 2014a). Significantly, Rad23 was enriched in the nucleus in *sts1-2* (Fig. 11), where it interacted with higher levels of polyUb proteins (Fig. 13). I detected higher levels of GFP fluorescence in the nucleus at 37°C in *sts1-2*, compared to *STS1* (Fig. 25; right panel).

It was previously shown that the stability of artificial substrates increased in *sts1-2* (Romero-Perez et al., 2007). However, the localization of these engineered substrates was not examined. I therefore examined if the elevated levels of nuclear GFP-Ho was caused by stabilization. Lysates containing GFP-Ho were prepared from *STS1* and *sts1-2* cells grown at 21°C and 37°C. Immunoblotting showed that GFP-Ho was efficiently degraded at 21°C in both *STS1* and *sts1-2* (Fig. 26a). However, GFP-Ho was stabilized in *sts1-2* at 37°C (Fig. 27a), indicating that the higher GFP signal observed in *sts1-2* is the result of protein stabilization. The relative turnover of GFP-Ho was quantified (Fig. 26b, 27b).

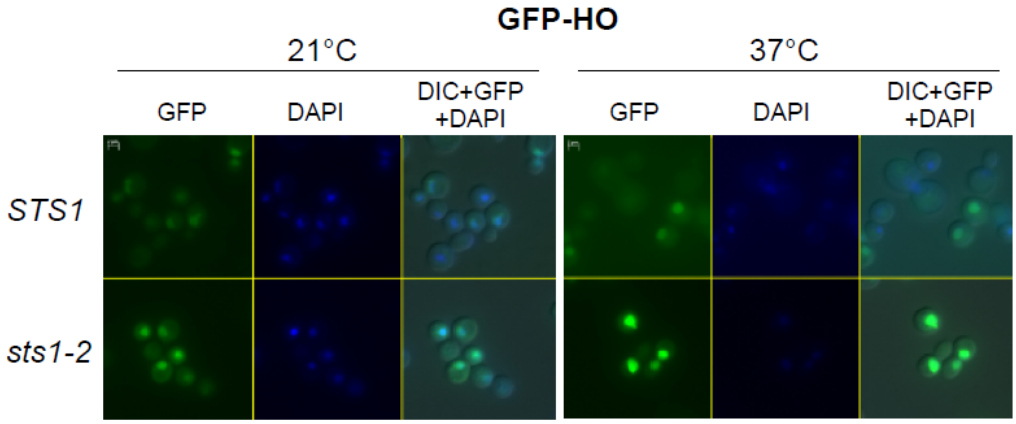

Figure 25. Ho-endonuclease accumulates inside the nucleus in *sts1-2*. GFP-Ho was expressed from the *GAL1* inducible promoter in either *STS1* or *sts1-2*. Cells were grown overnight in 10 ml of SM media containing raffinose at 21°C. Next day, cultures were diluted into fresh SM media and incubated at either 21°C or 37°C. After two hours incubation, cultures were places in media containing galactose for GFP-Ho induction. Cultures at 37°C were placed in pre-warmed media (37°C). Incubation continued at temperatures listed above for three hours. 1 ml aliquots of exponentially growing culture were drawn, pelleted and re-suspended into 1ml of sterile water containing 1 µg/ml Hoechst 33342. Cells are incubated with Hoechst solution for 30 minutes at 21°C. Aliquots were pelted and washed with water three times and re-suspended in 50 µl water. For imaging, 2.5 µl aliquots were spotted onto microscope slides. Yeast cells were imaged live.

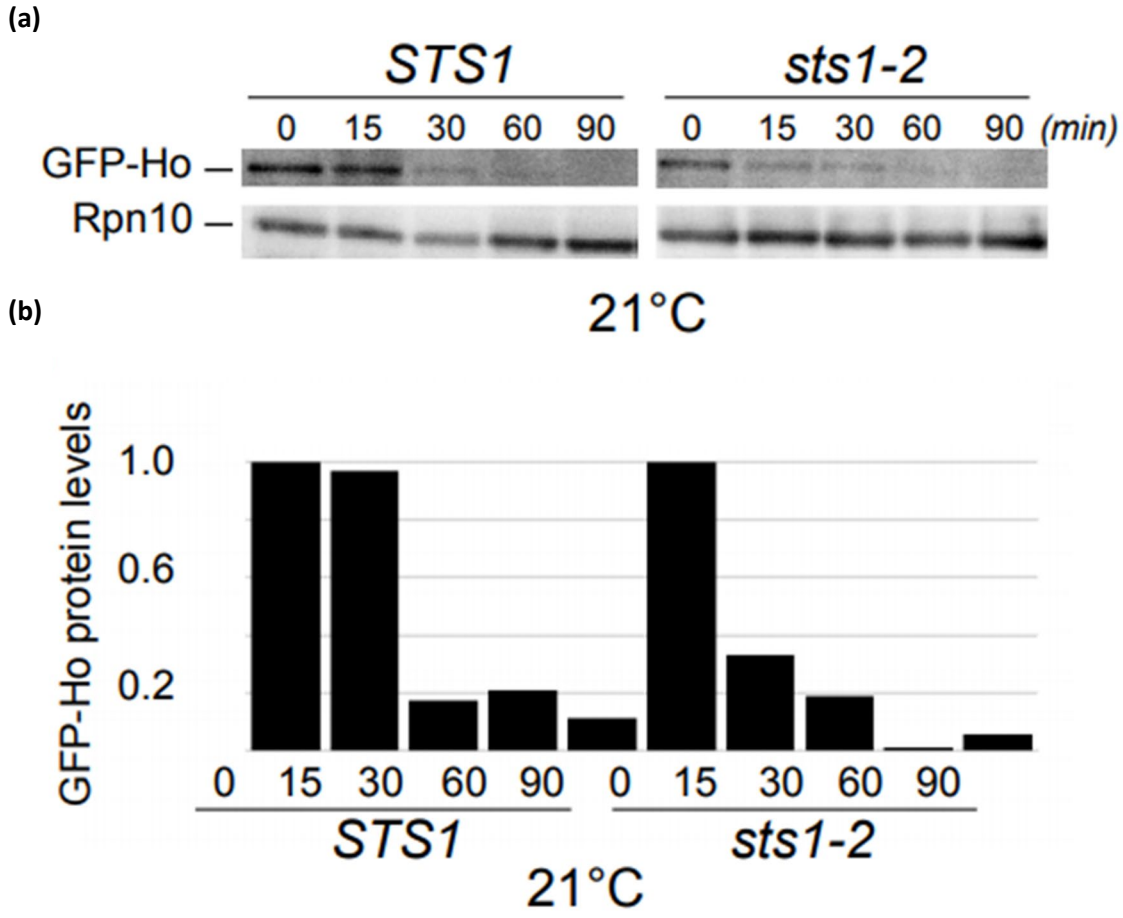

Figure 26. GFP-Ho turnover not affected in *STS1* and *sts1-2* at 21°C. (a) GFP-Ho was expressed from the *GAL1* inducible promoter in either *STS1* or *sts1-2*. Cells were grown overnight in 50 ml of SM media containing raffinose at 21°C. Next day, cultures were diluted into fresh SM media and incubated at either 21°C. After two hours incubation, cultures were places in media containing galactose for GFP-Ho induction. Incubation continued at 21°C for three hours. To discontinue expression cells places in glucose containing media with 200µg/ml cycloheximide. 10 ml aliquots were drawn at 0, 15, 30, 60, and 90 minutes interval. Yeast lysate was prepared and equal amount of total protein was resolved in a 12 % polyacrylamide SDS-Tricine gel. Gels were transferred to nitrocellulose membrane, and probed with antibodies against GFP and Rpn10. (b) quantification of results in panel (a).

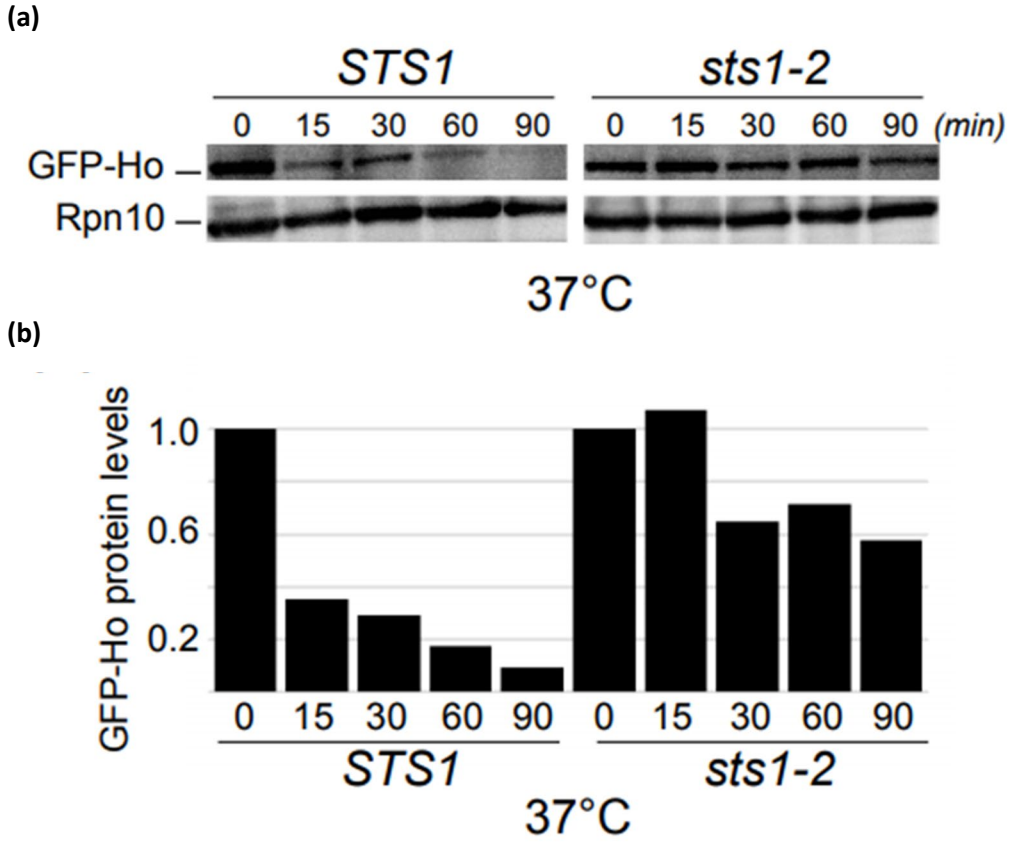

Figure 27. GFP-Ho is stabilized in *sts1-2* at 37°C. (a) GFP-Ho was expressed from the *GAL1* inducible promoter in either *STS1* or *sts1-2*. Cells were grown overnight in 50 ml of SM media containing raffinose at 21°C. Next day, cultures were diluted into fresh SM media and incubated at 37°C. After two hours incubation, cultures were places in media containing galactose for GFP-Ho induction. Incubation continued at 37°C for three hours. To discontinue expression, cells were placed in glucose containing media with 200µg/ml cycloheximide that was pre-warmed media (37°C). 10 ml aliquots were drawn at 0, 15, 30, 60, and 90 minutes interval. Yeast lysate was prepared and equal amount of total protein was resolved in a 12 % polyacrylamide SDS-Tricine gel. Gels were transferred to nitrocellulose membrane, and probed with antibodies against GFP and Rpn10. (b) quantification of results in panel (a).

Similarly, I expressed GFP-Ho in *RNA1* and *rna1-1* mutant. Cells were examined at 21°C and 37°C, and nuclear localization was observed in both wildtype and *rna1-1* at 21°C (Fig. 28; left panel) After transfer to 37°C GFP-Ho was detected in the nucleus in *RNA1*, but was not localized to the nucleus in *rna1-1* (Fig. 28; right panel). Instead, GFP-Ho was observed in multiple punctate cytosolic aggregates (Fig. 28; right panel). Interestingly, other reports also reported that nuclear proteins were detected in cytosolic aggregates in Rna1 mutants (Schlenstedt et al., 1995).

The lack of hydrolysis of RanGTP (by cytosolic Rna1) leads to a failure to dissociate an exported substrates from the export complex. This could cause cytosolic aggregation of exported complexes (Schlenstedt et al., 1995). Immunoblotting showed that GFP-Ho was efficiently degraded at 21°C in both *RNA1* and *rna1-1* mutant (Fig. 29a). The levels of Rpn10 confirmed equal loading. GFP-Ho was also degraded at 37°C in *RNA1*, but was stabilized in *rna1-1* (Fig. 30a). These results suggest that the cytosolic aggregates seen in Fig. 28 represent GFP-Ho that exited the nucleus but was not degraded. The relative turnover of GFP-HO was quantified (Fig. 29b, 30b).

In agreement with the localization and turnover of nuclear proteins Matα2 and Clb2, I determined that Ho is also stabilized, and accumulates inside the nucleus in *sts1-2* and in the cytosol in *rna1-1*. Although these studies established that the proteasome has to available at the nuclear surface to degrade nuclear substrates, it does not explain how substrates accumulate in the cytosol.

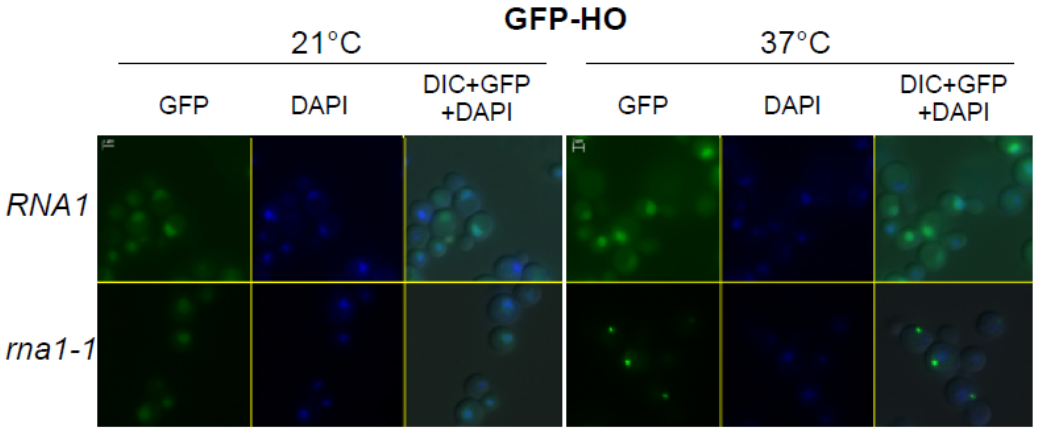

Figure 28. GFP-Ho accumulates in the cytoplasm in *rna1-1*. GFP-Ho was expressed from the *GAL1* inducible promoter in *RNA1* and *rna1-1*. Cells were grown in 10 ml of SM containing raffinose for 16 hours at 21°C. Cultures were then diluted into SM containing galactose and incubated for 2 hours at either 21°C. After two hour incubation cultures were split, and incubated for 1 hour at 21°C and 37°C. One ml aliquots were withdrawn from exponentially growing cultures, pelleted and re-suspended into 1 ml of sterile dH_20 containing 1 µg/ml Hoechst 33342. Cells are incubated for 30 minutes at 21°C. Aliquots were pelted, and washed 3 times with dH_20, and re-suspended in 50 µl dH_20. For imaging, 2.5 µl aliquots were spotted on Poly-prep, and cells were imaged live.

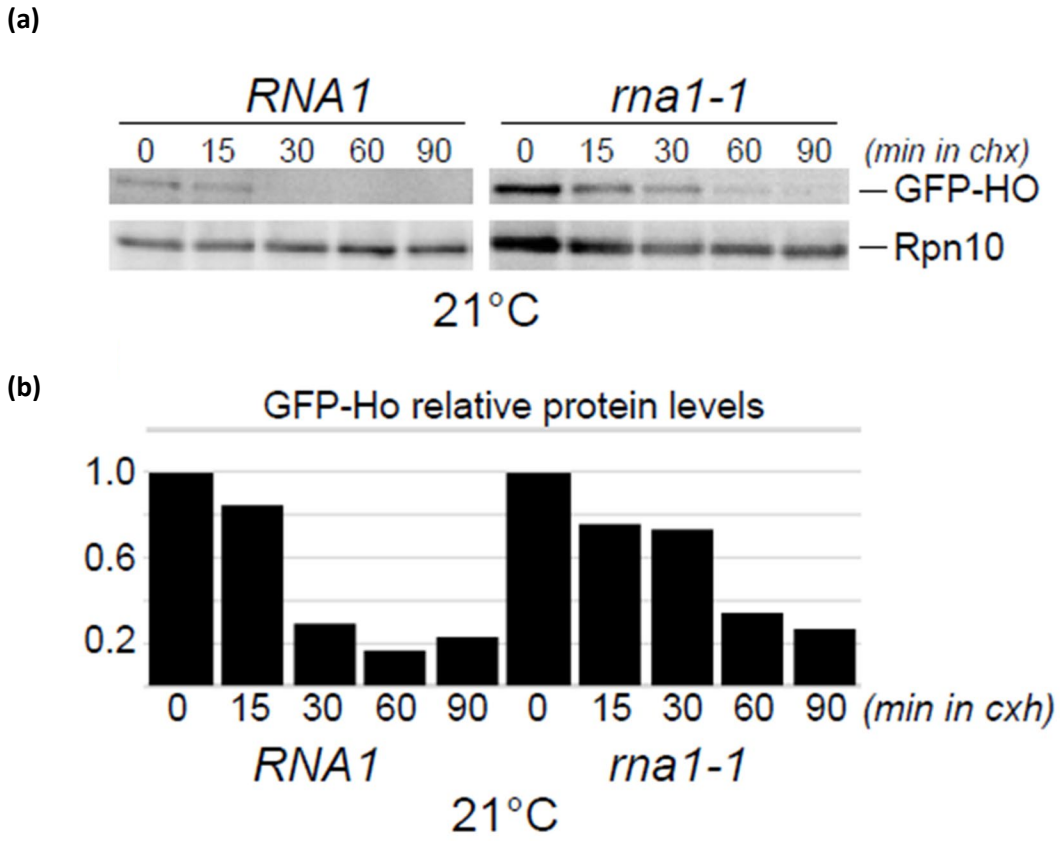

Figure 29. GFP-Ho turnover not affected in *RNA1* and *rna1-1* at 21°C. (a) GFP-Ho was expressed from the *GAL1* inducible promoter in *RNA1* and *rna1-1*. Cells were grown in 50 ml of SM containing raffinose for 16 hours at 21°C. Cultures were then diluted into fresh SM containing galactose and incubated for 2 hours at 21°C. After two hours incubation, cultures incubated for 1 hours at 21°C. To discontinue expression cells placed YPD with 200µg/ml cycloheximide. 10 ml aliquots were withdrawn at 0, 15, 30, 60, and 90 minutes. Yeast lysate was prepared and equal amount of total protein was resolved in a 12 % polyacrylamide SDS-Tricine gel. Gels were transferred to nitrocellulose membrane, and probed with antibodies against GFP and Rpn10. (b) quantification of results in panel (a)

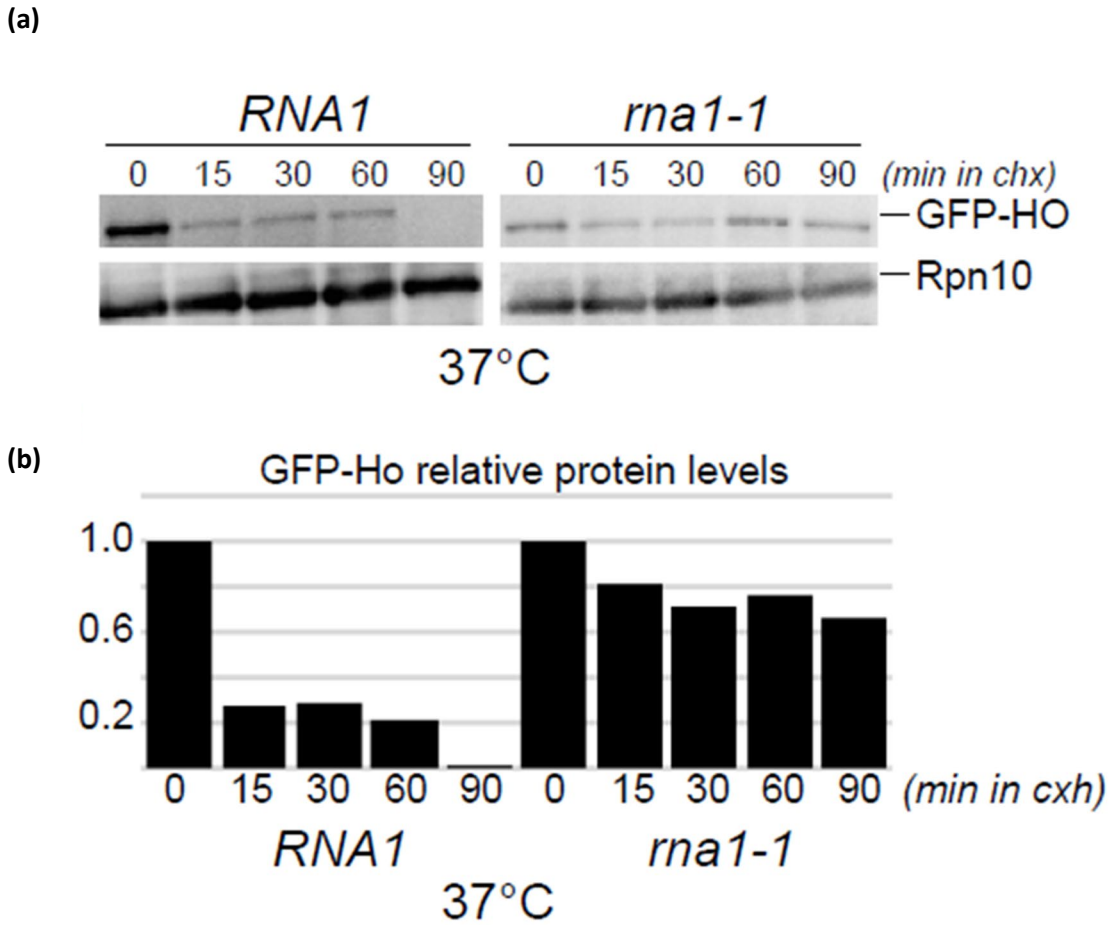

Figure 30. GFP-Ho is stabilized in *rna1-1* at 37°C. (a) GFP-Ho was expressed from the *GAL1* inducible promoter in *RNA1* and *rna1-1*. Cells were grown in 50 ml of SM containing raffinose for 16 hours at 21°C. Cultures were then diluted into fresh SM containing galactose and incubated for 2 hours at 21°C. After two hours incubation, cultures were incubated for 1 hour at 37°C. To discontinue expression, cells switched to YPD with 200µg/ml cycloheximide. 10 ml aliquots were withdrawn at 0, 15, 30, 60, and 90 minutes. Yeast lysate was prepared and equal amount of total protein was resolved in a 12 % polyacrylamide SDS-Tricine gel. Gels were transferred to nitrocellulose membrane, and probed with antibodies against GFP and Rpn10. (b) quantification of results in panel (a)

3.1.7 Rad23 is the major shuttle factor that traffics Ho-endonuclease

Substrates of the proteasome can represent either nuclear or cytosolic proteins. Therefore, examining shuttle factor interaction with bulk polyUb substrates offers only limited insight into the export-dependent transport of polyUb substrates to the cytosolic proteasome. However, studying the interaction with a specific physiological substrate can provide valuable insight into this mechanism, since mutations can be generated in the substrate. In addition, the two genetic mutants, *sts1-2* and *rna1-1*, will allow me to regulate the localization of the substrate-specific shuttle factors (Rad23; Ddi1). Moreover, these mutants would permit me to study compartment specific interaction of shuttle factors with its physiological substrates. The Ub-proteasome dependent degradation of Ho-endonuclease was reported to require interaction with Ddi1 (Kaplun et al., 2000). To test if this was a general property of shuttle factors, I investigated if Rad23 and Dsk2 could also bind Ho. I co-expressed GFP-Ho with epitope-tagged (FLAG-) derivatives of the three primary yeast shuttle-factors; Rad23, Ddi1, and Dsk2, as well as Ub-receptor Rpn10 (Fig. 31a). I detected a strong interaction between GFP-Ho and FLAG-Rad23 (Fig. 31a, lane 2), but an unexpectedly weak interaction with FLAG-Ddi1 (Fig. 31a, lane 3). Significantly, FLAG-Ddi1 was expressed at higher levels than FLAG-Rad23 (Fig. 31b; compare lanes 2 and 3).

I confirmed that GFP-Ho is conjugated to ubiquitin, because a key role for shuttle factors is to interact with polyUb chains on proteasomal substrates. I co-expressed myc-tagged Ub and Ho-HA, and yeast lysates were incubated with antibodies against HA. The purified proteins were separated by SDS/PAGE,

transferred to nitrocellulose and incubated with antibody against the myc epitope (Fig. 32a). An extensive smear representing polyubiquitylated Ho-HA was seen (lane 1), consistent with the idea that Ho is conjugated to polyUb chains. As noted earlier, Rad23 efficiently binds cellular proteins that are conjugated to Ub (see Fig. 13, 16), suggesting that it also binds Ho through its ubiquitin chains. I also confirmed Ho as substrate of the proteasome, by expressing GFP-Ho in a yeast proteasome mutant that is deficient for proteolysis (Fig. 32b). I found that GFP-Ho stabilized in this mutant (Fig. 32b).

Figure 31

(a)

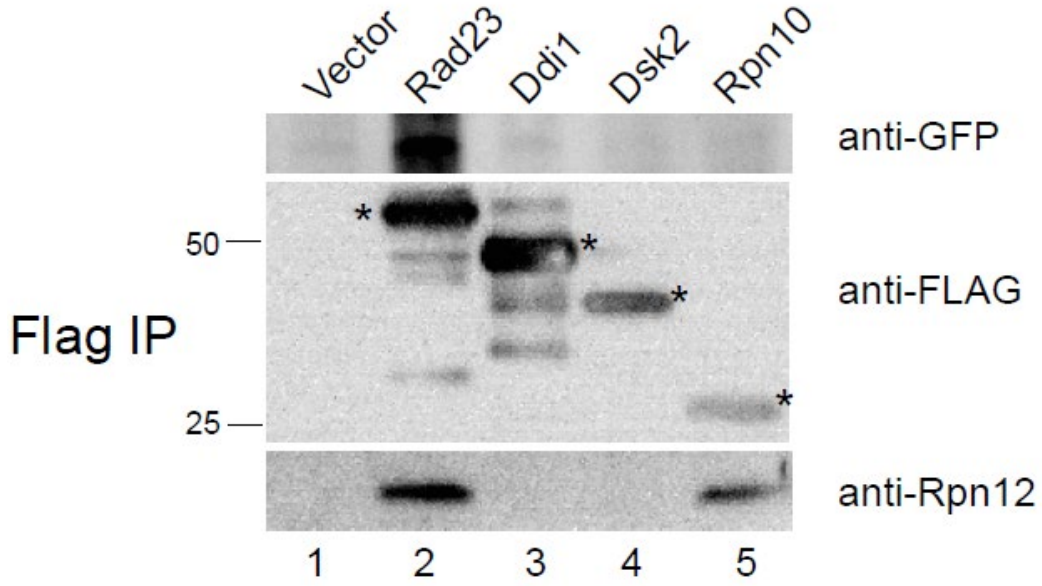
Vector
Rad23
Ddi1
Dsk2
Rpn10
anti-GFP
50
anti-FLAG
Flag IP
25
anti-Rpn12
1
2
3
4
5

(b)

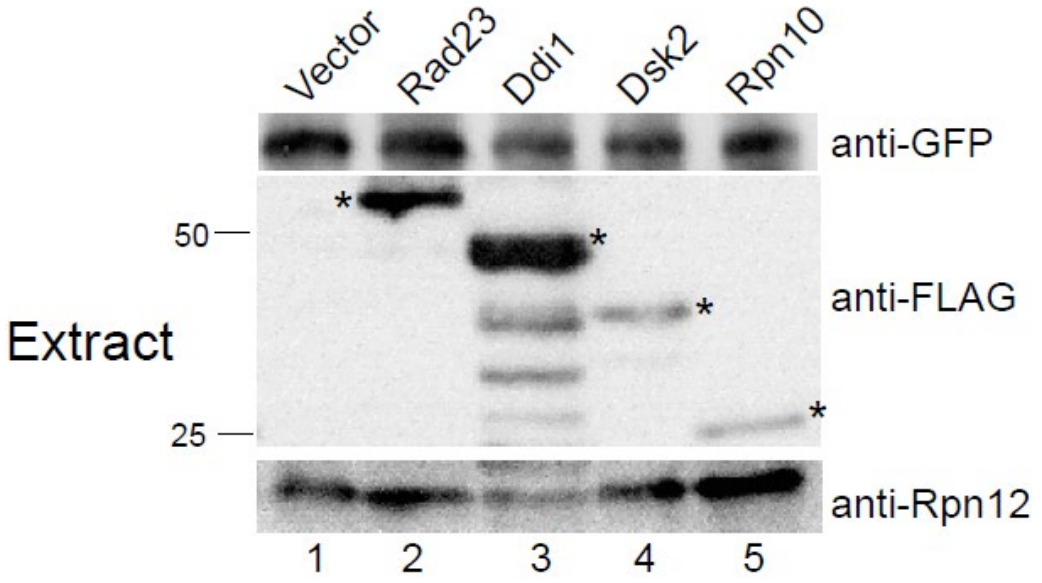
Vector
Rad23
Ddi1
Dsk2
Rpn10
anti-GFP
50
anti-FLAG
Extract
25
anti-Rpn12
1
2
3
4
5

Figure 31. Rad23 is a major shuttle factor for Ho-endonuclease. (a) Wildtype cells expressing GFP-Ho endonuclease were co-transformed with constructs expressing different FLAG-tagged polyUb chain binding proteins. The interaction between GFP-Ho and shuttle-factors FLAG-Rad23, FLAG-Ddi1, and FLAG-Dsk2, as well as a proteasome receptor FLAG-Rpn10 was investigated. GFP-Ho was expressed from galactose-inducible *GAL1* promoter, thus cultures were grown in SM with raffinose overnight, and then transferred to galactose medium three hours. Yeast lysates were prepared. FLAG-tagged proteins were first purified, and resolved in a 12% SDS-polyacrylamide gel. Gels transferred to nitrocellulose membrane and blots were examined by immunoblotting to detect GFP, FLAG, Rpn12, and ubiquitin (not shown). (b) 100µg total lysates were examined to gauge the expression level of the FLAG-tagged proteins and GFP-Ho.

Figure 32

(a)

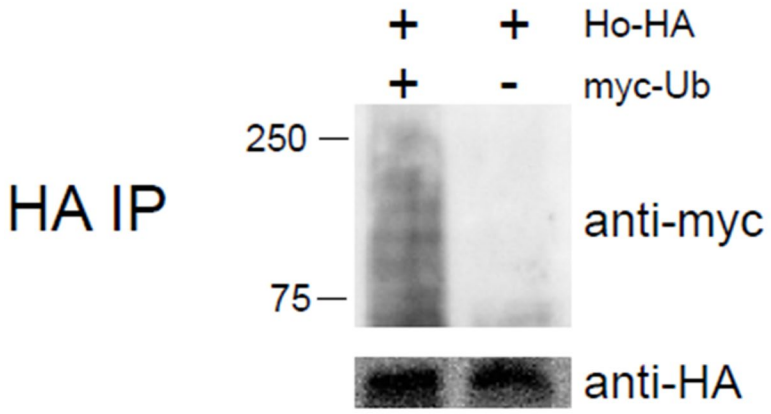
+ + Ho-HA
+ - myc-Ub
250
HA IP
anti-myc
75
anti-HA

(b)

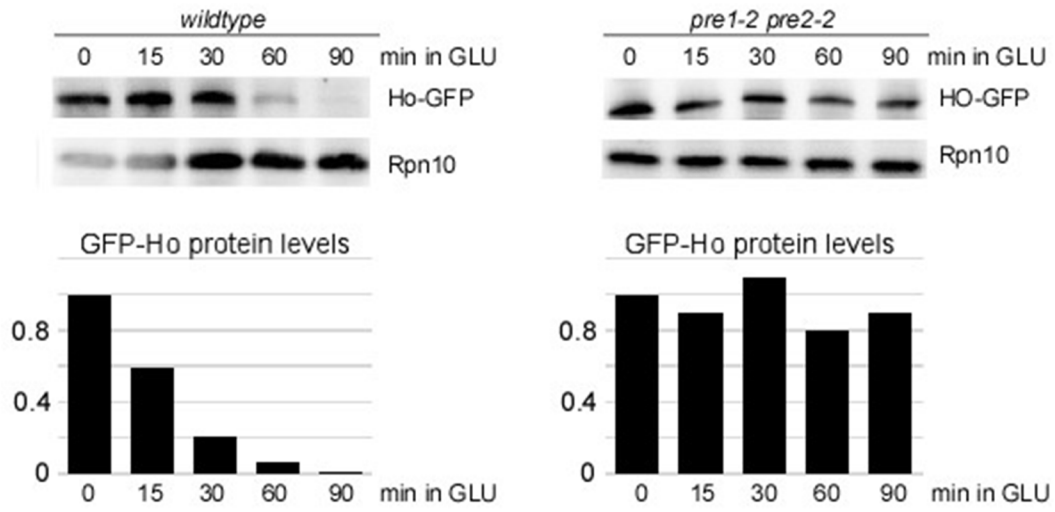
wildtype
0 15 30 60 90 min in GLU
Ho-GFP
Rpn10
pre1-2 pre2-2
0 15 30 60 90 min in GLU
HO-GFP
Rpn10
GFP-Ho protein levels
0.8
0.4
0
0 15 30 60 90 min in GLU
GFP-Ho protein levels
0.8
0.4
0
0 15 30 60 90 min in GLU

Figure 32. Ho is a substrate of the proteasome. (a) Ho-2xHA was co-expressed with myc-Ub. Ho-2xHA was expressed from galactose-inducible *GAL1* promoter, thus cultures were grown in SM with raffinose for 16 hours, and then transferred to SM with galactose for 2 hours. Yeast lysates were prepared. Equal amount of total protein was applied to an antibody matrix against HA. Purified proteins were resolved in a 12 % polyacrylamide SDS-Tricine gel, and transferred to nitrocellulose membrane. Proteins were examined by immunoblotting with antibodies against myc and HA epitopes. (b) GFP was expressed galactose-inducible *GAL1* promoter in wildtype and *pre1-1 pre2-2*. Yeast were grown in 50 ml SM with raffinose for 16 hours. Cells were diluted into YP with galactose and incubated for 2 hours. Cycloheximide (200 µg/ml) was added and 10 ml aliquots were withdrawn at 0, 15, 30, 60, and 90 minutes. Yeast lysate were prepared and 100 µg of total protein was resolved in a 12 % SDS-polyacrylamide gel, and transferred to nitrocellulose membrane. Proteins were examined by immunoblotting with antibodies against the GFP epitopes, and Rpn 10. Quantification is representative of 3 independent experiments for wildtype and *pre1-1 pre2-2*. Ho levels were normalized to that of Rpn10 levels.

A polyUb chain is present on many substrates of the proteasome. Therefore, this general structure cannot confer substrate specificity. However, the polyUb chain could affect binding to other proteins, such as the interaction between the Rad4 protein and R4BD in Rad23 (Ortolan et al., 2004). Rad23 showed a much stronger interaction with Ho than Ddi1 (Fig. 31). A possible explanation for this is that shuttle factors may exhibit some specificity towards their substrates following their conjugation to polyUb chains. Therefore, I investigated if Rad23 exhibited a preference for binding Ho by swapping their polyUb binding domains. The constructs I made include a Rad23 that had its UBA1 domain replaced with the one UBA domain of Ddi1 (rad23$^{UBA1::UBA(Ddi1)}$), and a Ddi1 construct that received Rad23's UBA1 in place of its one UBA domain (ddi1$^{UBA::UBA1(Rad23)}$). All constructs were tagged with epitope tagged (FLAG) and co-expressed with GFP-Ho. Because GFP-Ho was expressed from the galactose inducible *GAL1* promoter, cells were first grown in raffinose and then switched to galactose. FLAG-tagged proteins were purified and examined for co-purification of GFP-Ho. I confirmed that Rad23 exhibits a more robust interaction with GFP-Ho than Ddi1 (Fig. 33, compare lanes 2 and 6). As expected, I found that ddi1$^{\Delta UBA}$ does not bind GFP-Ho, indicating a requirement for the UBA domain (Fig. 33, lane 3). In contrast, Rad23 with the UBA domain from Ddi1 still showed high levels of GFP-Ho binding when compared wildtype Ddi1 (Fig. 33, compare lanes 2 and 4). Interestingly, a Ddi1 construct containing the UBA1 domain from Rad23 did not show increased binding to GFP-Ho (Fig. 33, compare lanes 2 and 6). Total extracts were examined to verify

equivalent expression of the protein constructs (Fig. 33, right panel, and lanes 8 to 14).

Interestingly, Rad23 and Ddi1 did not show altered binding to polyUb Ho when UBA domains were swapped. This suggests shuttle factors may not bind specific substrates. However, a possible explanation for increased binding of Rad23 to polyUb Ho is that Rad23 has two UBA domains instead of one UBA domain like Ddi1. This would also explain why Rad23 forms a more robust interaction with Ho than Ddi1.

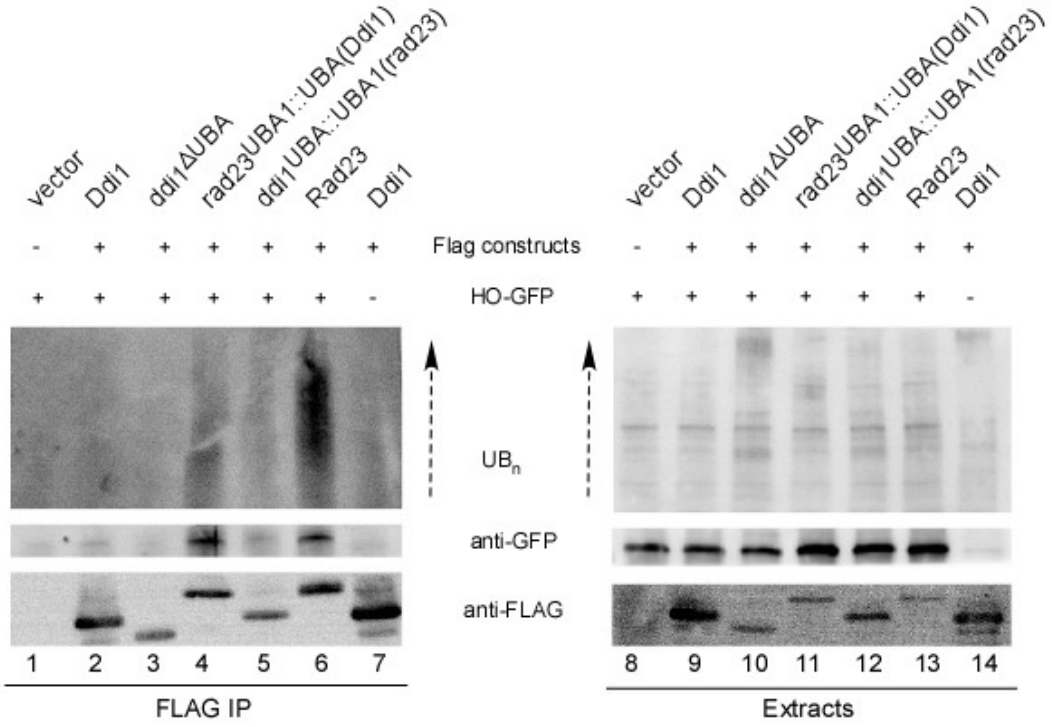

Figure 33. UBA domains do not exhibit substrate specificity. GFP-Ho was expressed from GAL1 promoter; thus cells were grown SM with raffinose for 16 hours, and then switched to SM with galactose for 2 hours. GFP-Ho was co-expressed with FLAG-tagged Rad23, ddi1$^{\Delta UBA}$, rad23$^{UBA1::UBA(Ddi1)}$, ddi1$^{UBA::UBA1(Rad23)}$, empty vector. Yeast lysates were prepared, and equal amount of protein was incubated with anti-FLAG matrix for 2 hours at 4°C. Purified proteins were washed and resolved in a 12 % polyacrylamide SDS-Tricine gel. Gels were transferred to nitrocellulose membrane, and blots were immunoblotted with antibodies against FLAG, GFP, and Ub.

To test the importance of UBA1 and UBA2 in Rad23 binding to its physiological substrate I studied the binding of mutant Rad23 proteins with GFP-Ho. I examined wildtype Rad23, as well as two Rad23 mutants that are unable to bind the proteasome (rad23$^{\Delta UbL}$ and rad23^{K7A}). I also examined Rad23 with a point mutation in UBA1 which disables binding to polyUb proteins (rad23^{uba1}). Although the UBA2 domain is still present in rad23^{uba1}, it binds polyUb substrates very poorly. FLAG-tagged constructs were co-expressed with GFP-Ho in *rad23Δ* (Fig. 34). FLAG-tagged proteins were purified, and the co-purification of GFP-Ho was examined (Fig. 34). I determined that Rad23, rad23$^{\Delta UbL}$ and rad23^{K7A} interacted strongly with GFP-Ho (Fig. 34, compare lanes 1, 2, and 3). However, this binding was lost when rad23^{uba1} was co-expressed with GFP-Ho (Fig. 34, lane 4). Extracts were characterized to verify that protein levels were unaffected (Fig. 34, lane 5 to 8).

In this study I verified the degradation of Ho by the proteasome, and that it is conjugated to a polyUb chain. In addition, I found that Rad23 binds significant higher levels or Rad23 than Ddi1. In contrast, Dsk2 showed no appreciable binding to Ho. I also discovered that the binding to polyUb Ho did not change when UBA domains of Rad23 and Ddi1 were swapped. This result suggests that shuttle factors do not exhibit specificity towards polyUb substrates. However, the stronger binding exhibited by Rad23 could be due to the presence of two UBA domains, unlike Dsk2 and Ddi1, which have only one. Indeed, the loss of a single functional UBA domain in Rad23 prevents its interaction with polyUb substrates, and as

expected, disrupts interaction with polyUb Ho. In agreement with previous studies, I confirmed that the UBA1 domain in Rad23 is the primary polyUb binding motif. My studies also suggest that Rad23 is the predominant shuttle factor that traffics polyUb substrates to the cytosolic 26*S* proteasome.

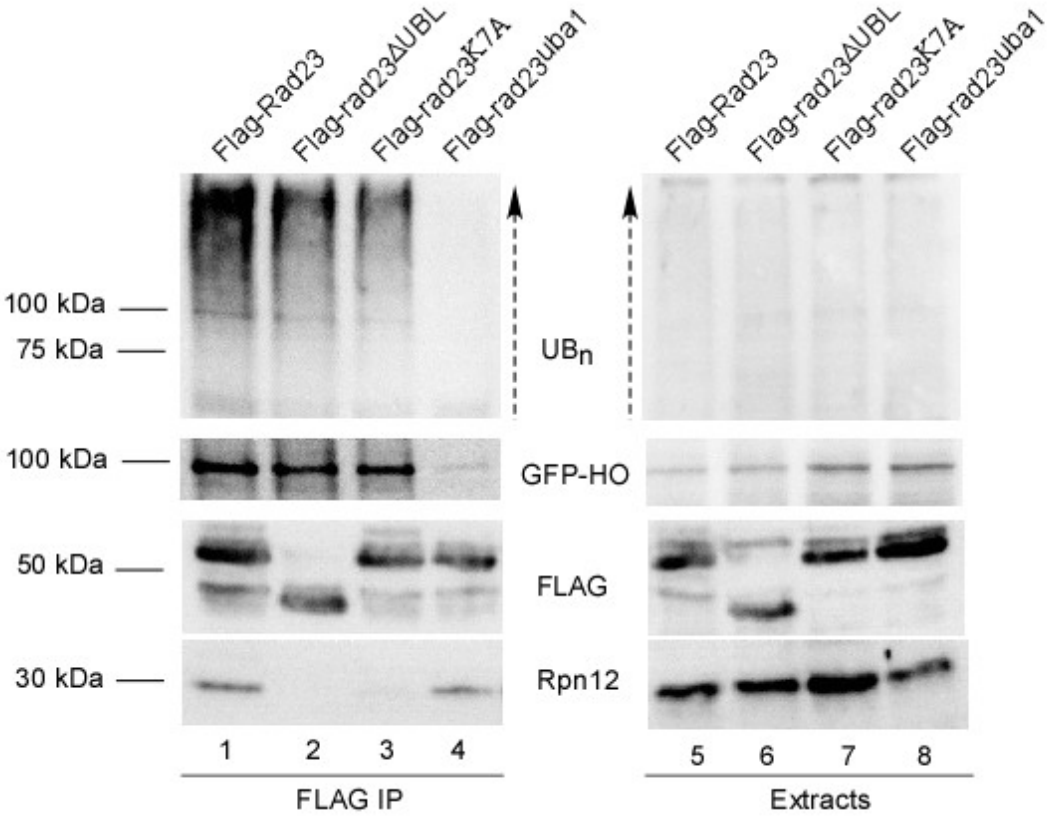

Figure 34. Rad23 binds Ho predominantly through its UBA1 domain. GFP-Ho was expressed from the galactose-inducible *GAL1* promoter. Cells were grown in 50 ml SM containing raffinose for 16 hours, and then diluted in fresh non-selective rich media (YP) with galactose for 2 hours. GFP-Ho was co-expressed with FLAG-tagged Rad23, rad23$^{\Delta UbL}$, rad23^{K7A}, and rad23^{uba1}. Yeast lysates were prepared, and equal amount of protein was incubated with anti-FLAG matrix at 4°C for 2 hours. Purified proteins were washed and resolved in a 12 % polyacrylamide SDS-Tricine gel. Gels were transferred to nitrocellulose membrane, and blots were immunoblotted with antibodies against FLAG, GFP, and Ub.

3.1.8 Rad23 interaction with Ho-endonuclease is altered by its subcellular localization

The use of *sts1-2* and *rna1-1* mutants allowed me to manipulate the localization of Rad23, and demonstrate that its binding to polyUb proteins increased when it was present in the nucleus, but decreased when it was trapped in the cytosol. Since Rad23 forms a robust interaction with Ho, I investigated their interaction in *sts1-2* and *rna1-1*. Both proteins were co-expressed and examined at 21°C and 37°C (Fig. 35). Consistent with results described in Fig. 13, FLAG-Rad23 interaction with GFP-Ho was higher in *sts1-2*, than in *STS1* at 37°C (Fig. 35a; compare lanes 4 and 5). Differential binding was also evident at 21°C (Fig. 35a, compare lanes 2 and 3). I speculate that the higher levels of nuclear Rad23 accounts for increased binding to Ho. Total protein lysates were also examined (Fig. 35b) to verify equal expression of FLAG-Rad23. The amount of GFP-Ho detected in Fig. 35a was quantified by densitometry, and adjusted to the levels of FLAG-Rad23 (Fig. 35c). In a similar analysis, FLAG-Rad23 and GFP-Ho were co-expressed in *RNA1* and *rna1-1* mutant (Fig. 36). I detected no interaction between Rad23 and Ho at 37°C in *rna1-1* (Fig. 36a, lane 5), which is consistent with reduced interaction of Rad23 and polyUb substrates observed in Fig. 16. Analysis of total protein showed comparable expression of FLAG-Rad23 (Fig. 36b). The results in Fig. 36a were quantified by densitometry (Fig. 36c).

Figure 35

(a)

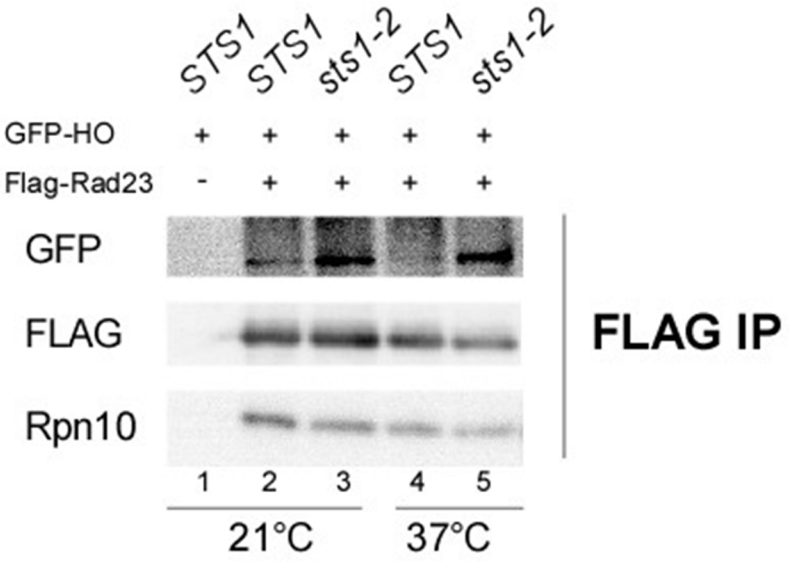

(b)

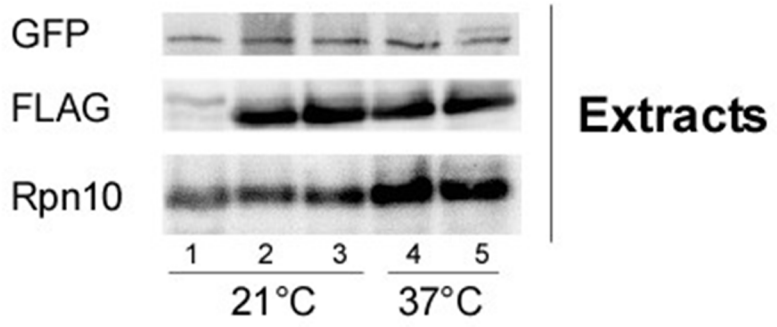

(C)

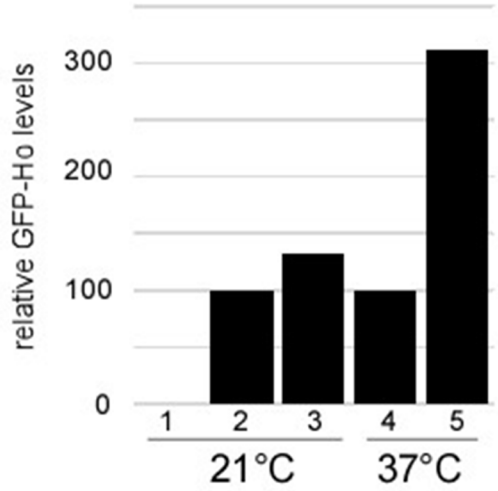

Figure 35. Rad23 interaction with GFP-Ho is increased in the nucleus. (a) Yeast co-expressing GFP-Ho from the *GAL1* promoter, and FLAG-Rad23 from the *CUP1* promoter were grown in SM with raffinose at 21°C overnight. Next day, cultures were diluted into YP raffinose and incubated at either 21°C or 37°C for 3 hours. Cultures were switched to YP galactose and incubated for an additional 2 hours at 21°C and 37°C. Cultures from 37°C were placed in pre-warmed media. Yeast lysate were prepared and equal amount of total protein was incubated with anti-FLAG agarose matrix. Purified proteins were resolved in a 12 % polyacrylamide SDS-Tricine gel. Gels were transferred to nitrocellulose membrane, and probed with antibodies against GFP, FLAG, and Rpn10. A lysate prepared from a strain expressing GFP-Ho, but lacking FLAG-Rad23, is shown (lane 1). (b) Total protein lysate was separated in a 12 % polyacrylamide SDS-Tricine gel, and analyzed as described in (a). The expression levels of GFP-Ho, FLAG-Rad23, and Rpn10 are shown. (c) The results in panel (a) were quantified by densitometry, and the relative amount GFP-Ho that was co-purified with FLAG-Rad23 is shown.

Figure 36

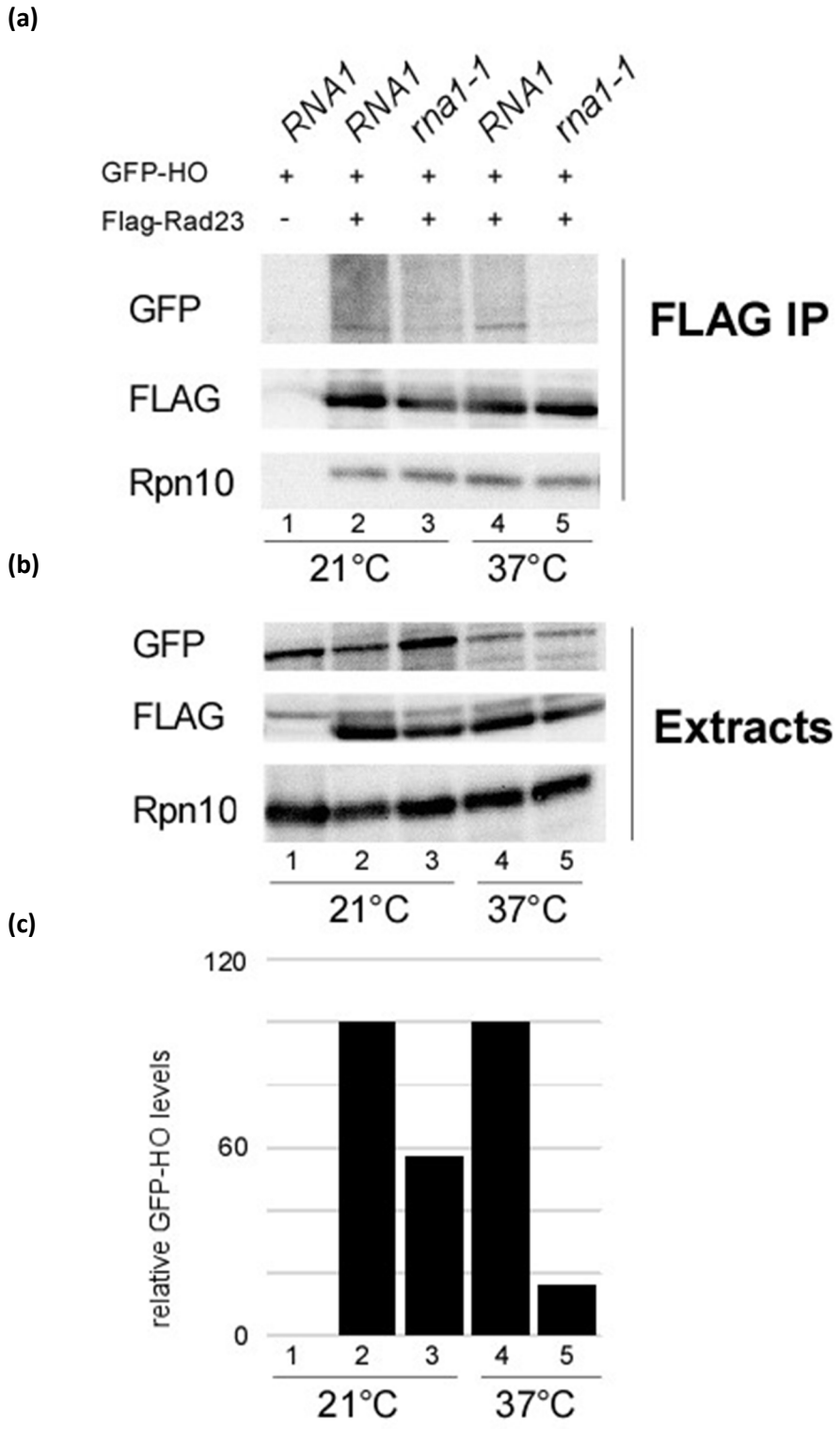
(a)
RNA1
RNA1
rna1-1
RNA1
rna1-1
GFP-HO + + + + +
Flag-Rad23 - + + + +
GFP
FLAG
Rpn10
FLAG IP
1 2 3 4 5
21°C 37°C
(b)
GFP
FLAG
Rpn10
Extracts
1 2 3 4 5
21°C 37°C
(c)
120
60
0
relative GFP-HO levels
1 2 3 4 5
21°C 37°C

Figure 36. Rad23 interaction with GFP-Ho is decreased in the cytosol. (a) Yeast co-expressing GFP-Ho from the *GAL1* promoter, and FLAG-Rad23 from the *CUP1* promoter were grown in 50 ml SM with raffinose at 21°C overnight. Next day, cultures were diluted into 100 ml YP galactose and incubated at 21°C for 2 hours. Cultures were split and incubated at 21°C and 37°C for one hour. Yeast lysate were prepared and equal amount of total protein was incubated with anti-FLAG agarose matrix. Purified proteins were resolved in a 12 % polyacrylamide SDS-Tricine gel. Gels were transferred to nitrocellulose membrane, and probed with antibodies against GFP, FLAG, and Rpn10. A lysate prepared from a strain expressing GFP-Ho, but lacking FLAG-Rad23, is shown (lane 1). (b) Total protein lysate was separated in a 12 % polyacrylamide SDS-Tricine gel, and analyzed as described in (a). The expression levels of GFP-Ho, FLAG-Rad23, and Rpn10 are shown. (c) The results in panel (a) were quantified by densitometry, and the relative amount GFP-Ho that was co-purified with FLAG-Rad23 is shown.

Examining shuttle factor interaction with bulk polyUb substrates was instructive, but studying the interaction with a specific substrate provided me with more insight into the compartment-specific interaction of Rad23 with a physiological substrate. By using *sts1-2* an *rna1-1* mutants I demonstrated that Rad23 binds high levels of Ho when it is trapped inside the nucleus, but low levels when it is trapped in the cytosol. These findings are fully consistent with my characterization of Rad23 binding to bulk polyUb proteins. This suggests that Rad23 functions to shuttle predominantly nuclear substrates to the proteasome at the nuclear surface.

3.1.9 Sub-cellular distribution of Ub is affected in *sts1-2* and *rna1-1*

To determine if the cellular stabilization of nuclear substrates was caused by the failure to translocate Ub to the nucleus, I examined the cellular distribution of GFP-Ub, and found that it was distributed throughout the cell, with no enrichment in the nucleus in *STS1* and *sts1-2* at 21°C. However, at 37°C GFP-Ub showed clear nuclear enrichment in *sts1-2*, which is similar to the nuclear accumulation of substrates, and Rad23. I also examined the localization of GF-Ub in *rna1-1*, and found that it was present in the nucleus and cytosol in both *RNA1* and *rna1-1* at 21°C and at 37°C. These findings led me to question if the accumulation of GFP-Ub in the nucleus in *sts1-2* might be explained by its conjugation to substrates. To test this idea I characterized RFP-ub$^{\Delta RGG}$; a mutant that cannot be ligated to lysine side-chains on substrates, or polyubiquitin chains. RFP-ub$^{\Delta RGG}$ was co-expressed with GFP-Ub in *STS1*, *sts1-1*, *RNA1*, and *rna1-1*. Whereas GFP-Ub accumulated in the nucleus in *sts1-2*, RFP-ub$^{\Delta RGG}$ remained cytosolic. In *rna1-1*, RFP-ub$^{\Delta RGG}$ was located in the cytosol in both *RNA1* and *rna1-1* at 21°C and 37°C, while GFP-Ub was present in the nucleus and cytoplasm. These findings suggest that ubiquitin is conjugated to nuclear substrates in *sts1-2*, and that these polyUb proteins are bound to shuttle-factors, such as Rad23 (APPENDIX II, – Okeke et. al., manuscript in review).

CHAPTER IV

Summary/Discussion

4.1 Summary

Presented here is evidence in support of my hypothesis that Rad23 plays a key role in targeting nuclear polyUb substrates to the proteasome at the nuclear surface; thus suggesting the existence of a transport mechanism that guides substrates from the nucleus to the proteasome. Emerging studies indicate that proteasomes are tethered at the nuclear surface. I confirmed proteasome mislocalization, and examined localization of Rad23 in the *sts1-2* yeast mutant. I found that Rad23 is enriched in the nucleus in *sts1-2*. Based on previously reported data that substrates are stabilized in *sts1-2*, I examined Rad23 interaction with polyUb substrates while trapped inside the nucleus. I determined that Rad23 binds higher levels of polyUb substrates in the nucleus. In contrast, Rad23 is enriched in the cytosol in *rna1-1*. I determined that Rad23 interaction with polyUb substrates is decreased in *rna1-1*. This suggests that once Rad23 exits the nucleus, it rapidly delivers polyUb substrates to the proteasome, and is free to re-enter the nucleus to repeat this transport cycle. Interestingly, the shuttle factor Ddi1 is also enriched in the nucleus and cytosol in *sts1-2* and *rna1-1* respectively. In addition, Ddi1 showed the same polyUb binding properties in these mutants; high level binding to polyUb substrates in *sts1-2* and low level association in *rna1-1*. This finding demonstrates that shuttle factors operate in a mechanistically similar way, and may have overlapping functions.

To investigate if Rad23's domains, including its UbL and UBA domains, play a key role in its ability to shuttle in and out of the nucleus, I examined the localization of three specific Rad23 mutants. The availability of the *sts1-2* and

rna1-1 mutants allowed me to examine their localization. I found that Rad23 mutants that are unable to bind the proteasome localize to the nucleus or cytoplasm in *sts1-2* and *rna1-1* respectively. Similarly, a Rad23 mutant that is unable to bind polyUb substrates shows the same subcellular distribution as wildtype Rad23. This suggests that Rad23 can oscillate between the nucleus and cytoplasm without a requirement for binding polyUb proteins, or the proteasome.

There are only a few known physiological substrates of Rad23, and because extensive experimental manipulation was required, they were not considered for further study. Instead, I sought more suitable physiological substrates of Rad23 that are known to be degraded in a Ub-proteasome dependent manner. I examined nuclear substrates Ho-endonuclease, Matα2, and Clb2. Each of these proteins were stabilized inside the nucleus in *sts1-2*, and accumulated in aggregates in the cytosol in *rna1-1*. Because Ho requires the shuttle factor Ddi1 for its turnover, I examined if other shuttle factors were also able to bind Ho through its polyUb chain. I discovered that Ho formed a much more favorable interaction with Rad23, than with Ddi1. No binding was detected with Dsk2. To determine if Rad23 and Ddi1 exhibited specificity towards Ho, I swapped the key UBA domains in these proteins. Specifically, I exchanged Ddi1's single C-terminal UBA domain with UBA1 from Rad23, and replaced Rad23's UBA1 domain with the UBA domain from Ddi1. A co-immunoprecipitation experiment showed that Rad23, containing the UBA domain from Ddi1, continued to form a significant interaction with Ho. Similarly, Ddi1 containing the UBA1 domain from Rad23

continued to form a weaker interaction with Ho. One explanation for this difference is that Rad23 contains two UBA domains, whereas Ddi1 contains only one.

Based on my characterization of Rad23 movement between the nucleus and the cytosol, and its nuclear-specific binding to polyUb proteins, I investigated if Rad23 interaction with Ho-endo was similarly strong in the nucleus, but weak in the cytosol. I found that Rad23 binds high levels of Ho in the nucleus in *sts1-2*, but in *rna1-1*, when Rad23 is enriched in the cytosol, this interaction is diminished.

Using a Ho as the physiological substrate, I wanted to determine if levels of binding are altered when Rad23's domains are compromised. I studied the interaction of Rad23 with Ho using the proteasome binding mutant rad23$^{\Delta UbL}$, and rad23^{K7A}, as well as rad23^{uba1}, a mutant that is unable to interact with polyUb chains. While similar levels of Ho were co-purified with Rad23, rad23$^{\Delta UbL}$, and rad23^{K7A}, only low levels were detected in association with rad23^{uba1}. In a separate experiment, I compared Ho binding to GST-UBA1 and GST-UBA2, and found that GST-UBA1 co-purified high levels of polyUb Ho; even higher than Rad23 (APPENDIX I, Fig. 37). In contrast, UBA2 showed no significant binding to Ho (APPENDIX I, Fig. 37). This confirms, that the UBA1 domain in Rad23 is the primary domain interacting with polyUb substrates, as reported earlier. In addition, it suggests that Rad23 may function as the primary shuttle factor in yeast.

In my studies, I confirmed that Ho is a polyUb substrate of the proteasome. I showed for the first time that Ho specifically binds the shuttle factor Rad23; which defines a new a physiological substrate of Rad23. This discovery allowed me to examine Rad23's role as a shuttle factor, using Ho. Moreover, the characterization

of *sts1-2* and *rna1-1* genetic mutants allowed me to test Rad23 interactions with polyUb substrates, based on its subcellular localization. I have shown for the first time that Rad23 forms variable interactions with polyUb substrate, based on its location in the cell. Similarly, using Ho as physiological substrate of Rad23, I have confirmed that Rad23 binds higher levels of Ho when in nucleus, and lower levels when in the cytosol. I also determined that Rad23 may have overlapping function with other shuttle factors (Ddi1), but it is the primary shuttle factor for transporting nuclear substrates.

4.2 Discussion

4.2.1 Nuclear substrates are exported from the nucleus

Numerous reports have proposed that nuclear substrates of the proteasome are degraded inside the nucleus. However, these studies have not convincingly demonstrated that catalytically active proteasome are present inside the nucleus and promote protein degradation. While subunits of the proteasome have been found inside the nucleus, and shown to perform non-proteolytic functions in transcription and DNA repair, it has not been demonstrated that these subunits assemble into 26*S* proteasomes that have peptidase activity. In contrast, the Madura group reported that catalytic active proteasomes are detected primarily in the cytosol (Dang et al., 2016). Moreover, only the cytosol contained intact 26*S* proteasomes (Dang et al., 2016). In contrast to the idea that protein degradation

can occur inside the nucleus many studies have reported that nuclear substrates are exported from the nucleus to be degraded. These are summarized below.

Levine and coworkers showed that the nuclear tumor suppressor protein p53 was stabilized when nuclear export was blocked (Freedman et al., 1998). Specifically, p53 was stabilized in cells treated with LMB, an inhibitor of the nuclear export factor Xpo1/Crm1 (Freedman et al., 1998). These investigators also reported that p53 accumulated inside the nucleus and remained transcriptionally active, implicating a lack of active proteasomes inside the nucleus (Freedman et al., 1998).

Wiechens *et al.,* characterized the export of β-catenin, a nuclear protein with dual functions in gene transcription and in cell-cell adhesion (Wiechens et al., 2001). The export of β-catenin was independent of RanGTP and the Crm1-mediated export pathway, suggesting that its turnover occurred independently of the primary nuclear export factors (Wiechens et al., 2001). However, blocking nuclear export in *Xenopus* oocytes stabilized β-catenin, and as a result it accumulated inside the nucleus (Wiechens et al., 2001). These results showed that β-catenin requires nuclear export, and its degradation occurred in the cytoplasm (Wiechens et al., 2001).

The degradation of TRIP-Br2 also requires export from the nucleus (Cheong et al., 2008). TRIP-Br2 promotes tumorigenesis, and its removal arrests cell growth (Cheong et al., 2008). Cheong *et al.,* demonstrated that TRIP-Br2 is a short-lived protein that is expressed in G1/S phase of the cell cycle. Significantly, the degradation of TRIP-Br2 requires the proteasome (Cheong et al., 2008). TRIP-Br2

was stabilized when nuclear export was inhibited by LMB, and also by deleting its export (NES) motif (Cheong et al., 2008).

Collectively, these observation strongly suggest that the degradation of many nuclear substrates requires export to cytosolic proteasomes. Moreover, since blocking nuclear export does not affect import, proteasomes should have entered the nucleus to degrade nuclear substrate, based on the current model. However, this was not observed, supporting my view that many nuclear proteins are exported and degraded by cytoplasmic proteasomes.

4.2.2 Proteasome is predicted to be located on the nuclear surface

The localization of the 26*S* proteasome is an important requirement for the degradation of nuclear proteins. It was previously reported that when proteasomes are mislocalized to the cytosol in *sts1-2* multiple nuclear substrates become stabilized (L. Chen et al., 2011; L. Chen et al., 2014a). Similarly, the failure to properly localize proteasomes in *srp1-49* causes nuclear substrates to become stabilized and to accumulate in the nucleus (L. Chen et al., 2014b). These studies suggest that the availability of proteasomes at the nuclear surface is important for the degradation of nuclear proteins. In agreement with this idea, a number of studies showed that catalytically active 26*S* proteasomes are enriched at the nuclear surface (Enenkel et al., 1998; Fabunmi et al., 2000; Laporte et al., 2008; Niepel et al., 2013).

The nucleus and cytoplasm are separated by the nuclear envelope, a double membrane structure that partitions the DNA in the nucleus from the

cytoplasm. The nuclear envelope is characterized by its many nuclear pore complexes (NPCs), which span the two lipid bilayers, and through which molecules are transported bi-directionally employing nuclear transport factors. The NPCs consists of a cytoplasmic ring bearing cytoplasmic filaments, a central pore, and a nuclear ring attached to a proteinaceous nuclear basket extending into the interior of the nucleus. Niepel *et al*., showed that yeast proteins Mlp1 and Mlp2 are located in the nuclear basket, and interact with proteasomes in the NPC (Niepel et al., 2013). This observation is consistent with a previous study, which showed that proteasomes are enriched in the nuclear envelope (Enenkel et al., 1998). Niepel demonstrated that the 26*S* proteasome is linked *via* its 19*S* regulatory subunit to Esc1p, a nuclear envelope-associated protein that binds Mlp1 and Mlp2. These findings suggested that proteasomes are located near the nuclear periphery (Niepel et al., 2013). Another study showed high levels of proteasomes in association with the centrosome (Fabunmi et al., 2000). Significantly, the centrosome could be co-purified with high levels of active 26*S* proteasomes (Fabunmi et al., 2000). Because the centrosome is present on the outer membrane of the nuclear envelope, its association with proteasomes suggests that a major fraction of cytosolic proteasomes are located near the nuclear periphery.

Laporte *et al*., reported that in non-proliferating yeast cells nuclear surface localized proteasomes are rapidly redistributed to cytoplasmic aggregates termed proteasome storage granules (PSGs) (Laporte et al., 2008). Although it was reported that the 26*S* proteasome is disassembled when cells enter the stationary phase, Laporte and colleagues showed that different subunits of the 19*S* and 20*S*

subunits all co-localize to cytoplasmic PSGs (Laporte et al., 2008). Intriguingly, the 20*S* complex remained assembled throughout stationary stage (Laporte et al., 2008). Laporte proposed that PSGs function to store proteasomes when they are not needed. However, the PSGs provide a way to rapidly release preassembled complexes once the cells begin proliferating (Laporte et al., 2008). Laporte showed that proteasome subcomplexes are rapidly mobilized from the PSGs to intact 26*S* proteasomes at the nuclear periphery (Laporte et al., 2008).

These important observations support my model that proteasome targeting to the nuclear periphery plays a key role in nuclear substrate turnover.

4.2.3 Proteasome is targeted to the nuclear surface

Proteasome localization is an essential part of the Ub-proteasome dependent turnover of nuclear substrate. However, the mechanism of its targeting is not well understood.

The Yanagida group described a mechanism for targeting the proteasome to the nuclear periphery in the fission yeast *S. pombe* (Takeda et al., 2005). Cut8, a distant relative of the yeast Sts1 protein, was found to physically interact with the proteasomes (Takeda et al., 2005). It has been shown to tether the proteasome to the nuclear surface (Takeda et al., 2005). Cut8 is highly unstable and its first 72 residues act as the degron that is recognized by Ubc2 and Ubr1 (E2 and E3, respectively). The degradation of Cut8 is important for nuclear enrichment of the 26*S* proteasome (Takeda et al., 2005). In agreement, when all lysine residues in the Cut8 degron were replaced with arginine, the mutant Cut8 exhibited weak

interaction with proteasome, and was associated with the failure in proteasomal targeting (Takeda et al., 2005). Similarly, this failure was also observed in *ubc2* and *ubr1* null mutants (Takeda et al., 2005). These mutants also exhibited sensitivity to DNA damage, which might be due to improperly localized proteasomes (Takeda et al., 2005). The proteasome tethering mechanism was predicted to be a conserved because Cut8 homologs are present in *S. cerevisiae, Neurospora*, and *D. melanogaster* (Takeda et al., 2005).

Tabb *et al.,* reported about Sts1, a protein of unknown function that was found to contain an NLS domain (Tabb et al., 2000). It was described that Sts1, the import factor Srp1, and the 19*S* proteasome subunit Rpn11 are able to interact (Tabb et al., 2000). The Madura group demonstrated that Sts1 plays a key role in targeting the proteasome to the nuclear periphery in *S. cerevisiae* (L. Chen et al., 2011). As observed with Cut8 in *S. pombe*, Sts1 is highly unstable (L. Chen et al., 2011). It was found that proteasomes were not targeted to the nucleus in *sts1-2*, a temperature sensitive mutant (L. Chen et al., 2011). The mislocalized proteasomes were intact and catalytically active, indicating that only its localization to the nucleus was disrupted in *sts1-2* (L. Chen et al., 2011). This defect was fully rescued by expressing wildtype Sts1 in *sts1-2* (L. Chen et al., 2011). Sts1 was shown to bind Srp1, a classic importin-α subunit, through its NLS domain (Tabb et al., 2000). Importantly, this interaction was required for the targeting of the proteasome to the nuclear periphery, thus demonstrating a role for the nucleocytoplasmic transport system in targeting proteasomes to the nucleus (L. Chen et al., 2011). The Madura group reported that the targeting of the proteasome

to the nucleus was distinct from the import function of Srp1 (L. Chen et al., 2014b).

A recent report from Albert *et al*., showed that proteasomes are detected in two distinct sites within the nuclear pore complex. They used cryo-electron tomography to locate proteasomes in the native cellular environment in *C. reinhardtii* (Albert et al., 2017). These studies suggested that the proteasome subunit Rpn9, functioned to anchor proteasomes to these two distinct NPC locations (Albert et al., 2017). A fraction of proteasomes were found to be tethered to the nuclear basket, while a more abundant binding site was observed at the inner nuclear membrane that encircles the NPC (Albert et al., 2017). Based on these data it was proposed that the 26S proteasome binds the NPCs to establish a cellular hub for protein degradation at the interface between nucleus and cytoplasm (Albert et al., 2017). These findings are significant because they are consistent with my hypothesis that many nuclear substrates are exported and degraded by cytosolic proteasomes. Since the NPC and its associated nuclear basket define cytosolic volume (although they penetrate deep into the nucleus), it is expected that an export mechanism would be required.

4.2.4 The role of shuttle factors

In my study, I show that shuttle factors play key role in nuclear substrate turnover. I determined that the subcellular location of Rad23 affects the turnover of Ho-endonuclease, a nuclear protein that is degraded by the proteasome, in an export-dependent mechanism (Fig. 25, Fig. 27, Fig. 32, Fig. 35, and Fig. 36). I also found that Rad23 and Ddi1 were similarly localized to the nucleus or cytoplasm in

yeast genetic mutants *sts1-2* and *rna1-1* (Fig. 11, Fig. 14, Fig. 18, and Fig. 20). A previous report showed that the degradation of Ho required export and the Ddi1 substrate shuttle factor (Kaplun et al., 2005). Although Kaplun *et al*., proposed that Ddi1 was the sole shuttle factor trafficking Ho (Kaplun et al., 2005). I determined that Rad23 can also bind Ho efficiently (Fig. 29, 31, 32, 33, and 34). Moreover, I discovered that Rad23 binds higher levels of Ho than Ddi1 (Fig. 31, and Fig. 33). The Rad23/Ho interaction was confirmed by placing different epitopes on both Rad23 (FLAG; GST) and Ho (HA; GFP). The experimental disparity could be due to different methodological approaches. For instance, Kaplun *et al*., characterized a beta-galactosidase-Ho fusion protein, which yields a chimera of over 700 MDa, since beta-galactosidase is a tetramer (Kaplun et al., 2005). This large appendage could sterically disrupt Ho binding to Rad23. Moreover, Kaplun *et al*., mixed lysates containing Ho-LacZ and either Rad23 or Ddi1 to test the binding *in vitro*. In contrast, I fused Ho-endo to smaller epitopes (GFP; HA) and characterized binding to shuttle factors by performing co-purification studies using yeast cell lysates. My data, and the conserved domain structures of shuttle factors suggest that they operate in similar ways and may have overlapping function.

Rad23 exhibits a more robust interaction with polyUb Ho than Ddi1. This difference could be due to different substrate specificity among shuttle factors. To test this idea I replaced the UBA1 domain in Rad23, with the UBA domain in Ddi1. A reciprocal construct was also made. I found that Rad23 containing UBA^{Ddi1} in place of the UBA1 continued to bind high levels of polyUb Ho, similar to native Rad23. In addition, Ddi1 containing the UBA1 domain from Rad23 did not show

improved binding to polyUb proteins (Fig. 33). Therefore, the more robust interaction with polyUb Ho observed with Rad23 could be due to the presence of two UBA domains. In agreement with this view, a Rad23 mutant containing only a single functioning UBA2 domain was unable to bind Ho efficiently, suggesting that it is the primary shuttle factor for this, and possibly other nuclear substrates (Fig. 34.). The idea that shuttle factors perform distinct roles in the UPP is consistent with the failure of the Dsk2 shuttle factor to bind Ho (Fig. 31). Dsk2 was reported to play a role in organizing the microtubule organizing center; known as the spindle pole body (SBP) in yeast (Biggins et al., 1996). Dsk2 was also reported to play a role in the endoplasmic reticulum-associated protein degradation (ERAD) (Medicherla et al., 2004). Although the ER contains an efficient protein quality control system to recognize misfolded proteins, there is no proteolytic system in the ER. Therefore, misfolded proteins are captured and retrotranslocated to cytosolic proteasomes; reminiscent of the nuclear export model I have proposed. ERAD defines a highly conserved mechanism to ensure the timely elimination of damaged proteins (Medicherla et al., 2004). Finally, Dsk2 was shown to interact with polyUb substrates *via* its UBA domain to target them to the proteasome for degradation (Medicherla et al., 2004). This study suggested that shuttle factors can perform compartment specific roles within the UPP. Significantly, ERAD demonstrates that the degradation of certain substrates requires translocation across a membrane barrier, to be trafficked to cytosolic proteasomes. Moreover, this event can require dedicated shuttle factors to traffic the polyUb substrates to the proteasome.

I proposed that the Rad23 shuttle factor transports polyUb proteins to the proteasome (L. Chen et al., 2002). This model envisions that the shuttle factor initially binds a polyUb substrate, and subsequently traffics it to the proteasome. Elsasser et al. proposed an alternative model. They speculated that Rad23 was located in the proteasome, where it operated as a polyUb receptor (Elsasser et al., 2004). In agreement with other studies, Elsasser reported that the proteasome interacted with polyUb chains through Rpn10, a well-characterized polyUb receptor in the proteasome (Elsasser et al., 2004). However, Rpn10 also interacted with these polyUb chains through Rad23. Therefore, Rad23 was proposed to form reversible interactions with the proteasome (Elsasser et al., 2004). The key distinction between my model, and that proposed by Elsasser *et al*., is that I predict Rad23 binds polyUb substrates first, and then the proteasome, whereas Elsasser argues that Rad23 binds the proteasome first, and then the polyUb substrate (Elsasser et al., 2004). More significantly, Rad23 is present in both the nucleus and cytoplasm (Fig. 11, and Fig. 14), and its movement is independent of its ability to bind the proteasome, or polyUb chains (Fig. 17). I found that Rad23 binds high levels of polyUb substrates when it is trapped inside the nucleus (Fig. 13), where proteasomes are absent. In addition, it forms a weak interaction with polyUb proteins when it is trapped in the cytosol (Fig. 16); the location of proteasomes. This is in agreement with the idea that Rad23 functions predominantly to deliver nuclear substrates to proteasomes at the nuclear surface, and refutes the model that Rad23 functions as a transient receptor in the proteasome. My model also predicts an efficient way to target polyUb substrates

to the proteasome *via* shuttle factors, rather than capturing them as they traffic out of the nucleus. To strengthen the idea that Rad23 exits the nucleus to deliver substrates to the proteasome it will be important to examine the interaction between rad23$^{\Delta UbL}$ and polyUb substrates in *rna1-1*; rad23$^{\Delta UbL}$ is enriched in the cytosol in this mutant. If Rad23 function as I hypothesized, rad23$^{\Delta UbL}$ unable to deliver its substrate to the proteasome should be bound to high levels of polyUb substrates in the cytosol, unlike wildtype Rad23.

Because components of the UPP, as well as shuttle factors are conserved across eukaryotic evolution my studies will be broadly applicable, from yeast to humans. For instance, Rad23 has been identified in fruit fly, mouse, and humans. Chen *et al*., examined the two isoforms of human Rad23 (hHR23A and hHR23B). It was discovered that human Rad23 functions in a similar way to yeast Rad23, since they are also involved in DNA repair and protein degradation. However, hHR23A and hHR23B formed distinct interactions with the proteasome and polyUb chains, which could suggest functional divergence in humans (L. Chen et al., 2006). A more recent study in support of my studies described a transport mechanism for nuclear polyUb substrates using a human cell based system and *C. elegans* (Hirayama et al., 2018). In this study, a complex that mediates the export of polyUb substrates from the nucleus to the cytosol was found to consist of a UBA domain-containing protein, called UBIN that shuttles between the nucleus and cytosol in a Crm1-dependent manner despite the lack of an NES motif (Hirayama et al., 2018). Instead, the UBIN binding protein polyUb substrate transporter, called POST that contains the NES domain, translocates UBIN across

the nuclear pore (Hirayama et al., 2018). It was demonstrated that UBIN interacts with polyUb substrates through it UBA domains, and that the UBIN-POST complex shuttled the polyUb substrates out of the nucleus (Hirayama et al., 2018). Furthermore, nuclear substrates accumulated in the cytosol when the proteasome was inhibited, while a Crm1 inhibition resulted in the nuclear accumulation of polyUb substrates (Hirayama et al., 2018). Taken together these results are consistent with my findings that export of nuclear proteins is essential for the maintenance of nuclear protein homeostasis (Hirayama et al., 2018).

My studies have potential clinical implications. Since high levels of proteasome activity is associated with disease, including cancer, a number of, chemotherapy drugs have been developed to inhibit the proteasome. However, these drugs are highly toxic, because they also inhibit proteasomes in healthy cells. By defining the important role Rad23 performs as a substrate shuttle factor it is possible that controlling its activity could have a therapeutic benefit. Moreover, since nuclear substrates are exported to cytosolic proteasomes new cancer drugs may be developed to specifically control its nuclear localization, and the export mechanism. Because Rad23 exhibits a preferred interaction with Ho-endonuclease, in contrast to Ddi1, substrate-specificity provides a basis for developing drugs that alter the targeting properties of shuttle factors.

BIBLIOGRAPHY

Albert, S., Schaffer, M., Beck, F., Mosalaganti, S., Asano, S., Thomas, H. F., Plitzko, J. M., Beck, M., Baumeister, W., & Engel, B. D. (2017). Proteasomes tether to two distinct sites at the nuclear pore complex. *Proc Natl Acad Sci U S A, 114*(52), 13726-13731. doi:10.1073/pnas.1716305114

Almond, J. B., & Cohen, G. M. (2002). The proteasome: a novel target for cancer chemotherapy. *Leukemia, 16*(4), 433-443. doi:10.1038/sj.leu.2402417

Amerik, A. Y., Li, S. J., & Hochstrasser, M. (2000). Analysis of the deubiquitinating enzymes of the yeast Saccharomyces cerevisiae. *Biol Chem, 381*(9-10), 981-992. doi:10.1515/BC.2000.121

Aravind, L., & Ponting, C. P. (1998). Homologues of 26S proteasome subunits are regulators of transcription and translation. *Protein Sci, 7*(5), 1250-1254. doi:10.1002/pro.5560070521

Arendt, C. S., & Hochstrasser, M. (1997). Identification of the yeast 20S proteasome catalytic centers and subunit interactions required for active-site formation. *Proc Natl Acad Sci U S A, 94*(14), 7156-7161. doi:10.1073/pnas.94.14.7156

Bajorek, M., Finley, D., & Glickman, M. H. (2003). Proteasome disassembly and downregulation is correlated with viability during stationary phase. *Curr Biol, 13*(13), 1140-1144. doi:10.1016/s0960-9822(03)00417-2

Bertolaet, B. L., Clarke, D. J., Wolff, M., Watson, M. H., Henze, M., Divita, G., & Reed, S. I. (2001). UBA domains mediate protein-protein interactions between two DNA damage-inducible proteins. *J Mol Biol, 313*(5), 955-963. doi:10.1006/jmbi.2001.5105

Biggins, S., Ivanovska, I., & Rose, M. D. (1996). Yeast ubiquitin-like genes are involved in duplication of the microtubule organizing center. *J Cell Biol, 133*(6), 1331-1346. doi:10.1083/jcb.133.6.1331

Blondel, M., Galan, J. M., Chi, Y., Lafourcade, C., Longaretti, C., Deshaies, R. J., & Peter, M. (2000). Nuclear-specific degradation of Far1 is controlled by the localization of the F-box protein Cdc4. *EMBO J, 19*(22), 6085-6097. doi:10.1093/emboj/19.22.6085

Bochtler, M., Ditzel, L., Groll, M., Hartmann, C., & Huber, R. (1999). The proteasome. *Annu Rev Biophys Biomol Struct, 28*, 295-317. doi:10.1146/annurev.biophys.28.1.295

Boiteux, S., & Jinks-Robertson, S. (2013). DNA repair mechanisms and the bypass of DNA damage in Saccharomyces cerevisiae. *Genetics, 193*(4), 1025-1064. doi:10.1534/genetics.112.145219

Boyd, S. D., Tsai, K. Y., & Jacks, T. (2000). An intact HDM2 RING-finger domain is required for nuclear exclusion of p53. *Nat Cell Biol, 2*(9), 563-568. doi:10.1038/35023500

Cadet, J., Sage, E., & Douki, T. (2005). Ultraviolet radiation-mediated damage to cellular DNA. *Mutat Res, 571*(1-2), 3-17. doi:10.1016/j.mrfmmm.2004.09.012

Chen, L., & Madura, K. (2002). Rad23 promotes the targeting of proteolytic substrates to the proteasome. *Mol Cell Biol, 22*(13), 4902-4913. doi:10.1128/mcb.22.13.4902-4913.2002

Chen, L., & Madura, K. (2006). Evidence for distinct functions for human DNA repair factors hHR23A and hHR23B. *FEBS Lett, 580*(14), 3401-3408. doi:10.1016/j.febslet.2006.05.012

Chen, L., & Madura, K. (2014a). Degradation of specific nuclear proteins occurs in the cytoplasm in Saccharomyces cerevisiae. *Genetics, 197*(1), 193-197. doi:10.1534/genetics.114.163824

Chen, L., & Madura, K. (2014b). Yeast importin-alpha (Srp1) performs distinct roles in the import of nuclear proteins and in targeting proteasomes to the nucleus. *J Biol Chem, 289*(46), 32339-32352. doi:10.1074/jbc.M114.582023

Chen, L., Romero, L., Chuang, S. M., Tournier, V., Joshi, K. K., Lee, J. A., Kovvali, G., & Madura, K. (2011). Sts1 plays a key role in targeting proteasomes to the nucleus. *J Biol Chem, 286*(4), 3104-3118. doi:10.1074/jbc.M110.135863

Chen, L., Shinde, U., Ortolan, T. G., & Madura, K. (2001). Ubiquitin-associated (UBA) domains in Rad23 bind ubiquitin and promote inhibition of multi-ubiquitin chain assembly. *EMBO Rep, 2*(10), 933-938. doi:10.1093/embo-reports/kve203

Chen, P., & Hochstrasser, M. (1996). Autocatalytic subunit processing couples active site formation in the 20S proteasome to completion of assembly. *Cell, 86*(6), 961-972. doi:10.1016/s0092-8674(00)80171-3

Chen, P., Johnson, P., Sommer, T., Jentsch, S., & Hochstrasser, M. (1993). Multiple ubiquitin-conjugating enzymes participate in the in vivo degradation of the yeast MAT alpha 2 repressor. *Cell, 74*(2), 357-369.

Cheong, J. K., Gunaratnam, L., & Hsu, S. I. (2008). CRM1-mediated nuclear export is required for 26 S proteasome-dependent degradation of the TRIP-Br2 proto-oncoprotein. *J Biol Chem, 283*(17), 11661-11676. doi:10.1074/jbc.M708365200

Chernova, T. A., Allen, K. D., Wesoloski, L. M., Shanks, J. R., Chernoff, Y. O., & Wilkinson, K. D. (2003). Pleiotropic effects of Ubp6 loss on drug sensitivities and yeast prion are due to depletion of the free ubiquitin pool. *J Biol Chem, 278*(52), 52102-52115. doi:10.1074/jbc.M310283200

Chuang, L. C., & Yew, P. R. (2001). Regulation of nuclear transport and degradation of the Xenopus cyclin-dependent kinase inhibitor, p27Xic1. *J Biol Chem, 276*(2), 1610-1617. doi:10.1074/jbc.M008896200

Clague, M. J., Urbe, S., & Komander, D. (2019). Breaking the chains: deubiquitylating enzyme specificity begets function. *Nat Rev Mol Cell Biol, 20*(6), 338-352. doi:10.1038/s41580-019-0099-1

Dang, F. W., Chen, L., & Madura, K. (2016). Catalytically Active Proteasomes Function Predominantly in the Cytosol. *J Biol Chem, 291*(36), 18765-18777. doi:10.1074/jbc.M115.712406

Dantuma, N. P., Heinen, C., & Hoogstraten, D. (2009). The ubiquitin receptor Rad23: at the crossroads of nucleotide excision repair and proteasomal

degradation. *DNA Repair (Amst), 8*(4), 449-460. doi:10.1016/j.dnarep.2009.01.005

Darwin, K. H. (2009). Prokaryotic ubiquitin-like protein (Pup), proteasomes and pathogenesis. *Nat Rev Microbiol, 7*(7), 485-491. doi:10.1038/nrmicro2148

Depre, C., Wang, Q., Yan, L., Hedhli, N., Peter, P., Chen, L., Hong, C., Hittinger, L., Ghaleb, B., Sadoshima, J., Vatner, D. E., Vatner, S. F., & Madura, K. (2006). Activation of the cardiac proteasome during pressure overload promotes ventricular hypertrophy. *Circulation, 114*(17), 1821-1828. doi:10.1161/CIRCULATIONAHA.106.637827

Dieckmann, T., Withers-Ward, E. S., Jarosinski, M. A., Liu, C. F., Chen, I. S., & Feigon, J. (1998). Structure of a human DNA repair protein UBA domain that interacts with HIV-1 Vpr. *Nat Struct Biol, 5*(12), 1042-1047. doi:10.1038/4220

Elsasser, S., Chandler-Militello, D., Muller, B., Hanna, J., & Finley, D. (2004). Rad23 and Rpn10 serve as alternative ubiquitin receptors for the proteasome. *J Biol Chem, 279*(26), 26817-26822. doi:10.1074/jbc.M404020200

Elsasser, S., Gali, R. R., Schwickart, M., Larsen, C. N., Leggett, D. S., Muller, B., Feng, M. T., Tubing, F., Dittmar, G. A., & Finley, D. (2002). Proteasome subunit Rpn1 binds ubiquitin-like protein domains. *Nat Cell Biol, 4*(9), 725-730. doi:10.1038/ncb845

Enenkel, C., Lehmann, A., & Kloetzel, P. M. (1998). Subcellular distribution of proteasomes implicates a major location of protein degradation in the nuclear envelope-ER network in yeast. *EMBO J, 17*(21), 6144-6154. doi:10.1093/emboj/17.21.6144

Fabunmi, R. P., Wigley, W. C., Thomas, P. J., & DeMartino, G. N. (2000). Activity and regulation of the centrosome-associated proteasome. *J Biol Chem, 275*(1), 409-413. doi:10.1074/jbc.275.1.409

Finley, D., Ozkaynak, E., & Varshavsky, A. (1987). The yeast polyubiquitin gene is essential for resistance to high temperatures, starvation, and other stresses. *Cell, 48*(6), 1035-1046. doi:10.1016/0092-8674(87)90711-2

Finley, D., Ulrich, H. D., Sommer, T., & Kaiser, P. (2012). The ubiquitin-proteasome system of Saccharomyces cerevisiae. *Genetics, 192*(2), 319-360. doi:10.1534/genetics.112.140467

Floyd, Z. E., Trausch-Azar, J. S., Reinstein, E., Ciechanover, A., & Schwartz, A. L. (2001). The nuclear ubiquitin-proteasome system degrades MyoD. *J Biol Chem, 276*(25), 22468-22475. doi:10.1074/jbc.M009388200

Freedman, D. A., & Levine, A. J. (1998). Nuclear export is required for degradation of endogenous p53 by MDM2 and human papillomavirus E6. *Mol Cell Biol, 18*(12), 7288-7293. doi:10.1128/mcb.18.12.7288

Friedberg, E. C., Aguilera, A., Gellert, M., Hanawalt, P. C., Hays, J. B., Lehmann, A. R., Lindahl, T., Lowndes, N., Sarasin, A., & Wood, R. D. (2006). DNA repair: from molecular mechanism to human disease. *DNA Repair (Amst), 5*(8), 986-996.

Fu, Y., Zhu, Y., Zhang, K., Yeung, M., Durocher, D., & Xiao, W. (2008). Rad6-Rad18 mediates a eukaryotic SOS response by ubiquitinating the 9-1-1 checkpoint clamp. *Cell, 133*(4), 601-611. doi:10.1016/j.cell.2008.02.050

Funakoshi, M., Tomko, R. J., Jr., Kobayashi, H., & Hochstrasser, M. (2009). Multiple assembly chaperones govern biogenesis of the proteasome regulatory particle base. *Cell, 137*(5), 887-899. doi:10.1016/j.cell.2009.04.061

Geyer, R. K., Yu, Z. K., & Maki, C. G. (2000). The MDM2 RING-finger domain is required to promote p53 nuclear export. *Nat Cell Biol, 2*(9), 569-573. doi:10.1038/35023507

Giglia-Mari, G., Zotter, A., & Vermeulen, W. (2011). DNA damage response. *Cold Spring Harb Perspect Biol, 3*(1), a000745. doi:10.1101/cshperspect.a000745

Glickman, M. H., & Ciechanover, A. (2002). The ubiquitin-proteasome proteolytic pathway: destruction for the sake of construction. *Physiol Rev, 82*(2), 373-428. doi:10.1152/physrev.00027.2001

Glickman, M. H., Rubin, D. M., Coux, O., Wefes, I., Pfeifer, G., Cjeka, Z., Baumeister, W., Fried, V. A., & Finley, D. (1998a). A subcomplex of the proteasome regulatory particle required for ubiquitin-conjugate degradation and related to the COP9-signalosome and eIF3. *Cell, 94*(5), 615-623. doi:10.1016/s0092-8674(00)81603-7

Glickman, M. H., Rubin, D. M., Fried, V. A., & Finley, D. (1998b). The regulatory particle of the Saccharomyces cerevisiae proteasome. *Mol Cell Biol, 18*(6), 3149-3162. doi:10.1128/mcb.18.6.3149

Goldberg, A. L., & Rock, K. L. (1992). Proteolysis, proteasomes and antigen presentation. *Nature, 357*(6377), 375-379. doi:10.1038/357375a0

Groll, M., Bajorek, M., Kohler, A., Moroder, L., Rubin, D. M., Huber, R., Glickman, M. H., & Finley, D. (2000). A gated channel into the proteasome core particle. *Nat Struct Biol, 7*(11), 1062-1067. doi:10.1038/80992

Groll, M., Bochtler, M., Brandstetter, H., Clausen, T., & Huber, R. (2005). Molecular machines for protein degradation. *Chembiochem, 6*(2), 222-256. doi:10.1002/cbic.200400313

Groll, M., Ditzel, L., Lowe, J., Stock, D., Bochtler, M., Bartunik, H. D., & Huber, R. (1997). Structure of 20S proteasome from yeast at 2.4 A resolution. *Nature, 386*(6624), 463-471. doi:10.1038/386463a0

Guzder, S. N., Habraken, Y., Sung, P., Prakash, L., & Prakash, S. (1995). Reconstitution of yeast nucleotide excision repair with purified Rad proteins, replication protein A, and transcription factor TFIIH. *J Biol Chem, 270*(22), 12973-12976. doi:10.1074/jbc.270.22.12973

Guzzo, C. M., & Matunis, M. J. (2013). Expanding SUMO and ubiquitin-mediated signaling through hybrid SUMO-ubiquitin chains and their receptors. *Cell Cycle, 12*(7), 1015-1017. doi:10.4161/cc.24332

Hanna, J., Leggett, D. S., & Finley, D. (2003). Ubiquitin depletion as a key mediator of toxicity by translational inhibitors. *Mol Cell Biol, 23*(24), 9251-9261. doi:10.1128/mcb.23.24.9251-9261.2003

Hanna, J., Meides, A., Zhang, D. P., & Finley, D. (2007). A ubiquitin stress response induces altered proteasome composition. *Cell, 129*(4), 747-759. doi:10.1016/j.cell.2007.03.042

Hartmann-Petersen, R., Hendil, K. B., & Gordon, C. (2003). Ubiquitin binding proteins protect ubiquitin conjugates from disassembly. *FEBS Lett, 535*(1-3), 77-81. doi:10.1016/s0014-5793(02)03874-7

Herrmann, J., Lerman, L. O., & Lerman, A. (2007). Ubiquitin and ubiquitin-like proteins in protein regulation. *Circ Res, 100*(9), 1276-1291. doi:10.1161/01.RES.0000264500.11888.f0

Hershko, A., Heller, H., Elias, S., & Ciechanover, A. (1983). Components of ubiquitin-protein ligase system. Resolution, affinity purification, and role in protein breakdown. *J Biol Chem, 258*(13), 8206-8214.

Hicke, L., & Riezman, H. (1996). Ubiquitination of a yeast plasma membrane receptor signals its ligand-stimulated endocytosis. *Cell, 84*(2), 277-287. doi:10.1016/s0092-8674(00)80982-4

Hicke, L., Schubert, H. L., & Hill, C. P. (2005). Ubiquitin-binding domains. *Nat Rev Mol Cell Biol, 6*(8), 610-621. doi:10.1038/nrm1701

Hirayama, S., Sugihara, M., Morito, D., Iemura, S. I., Natsume, T., Murata, S., & Nagata, K. (2018). Nuclear export of ubiquitinated proteins via the UBIN-POST system. *Proc Natl Acad Sci U S A, 115*(18), E4199-E4208. doi:10.1073/pnas.1711017115

Humbard, M. A., & Maupin-Furlow, J. A. (2013). Prokaryotic proteasomes: nanocompartments of degradation. *J Mol Microbiol Biotechnol, 23*(4-5), 321-334. doi:10.1159/000351348

Husnjak, K., Elsasser, S., Zhang, N., Chen, X., Randles, L., Shi, Y., Hofmann, K., Walters, K. J., Finley, D., & Dikic, I. (2008). Proteasome subunit Rpn13 is a novel ubiquitin receptor. *Nature, 453*(7194), 481-488. doi:10.1038/nature06926

Isasa, M., Katz, E. J., Kim, W., Yugo, V., Gonzalez, S., Kirkpatrick, D. S., Thomson, T. M., Finley, D., Gygi, S. P., & Crosas, B. (2010). Monoubiquitination of RPN10 regulates substrate recruitment to the proteasome. *Mol Cell, 38*(5), 733-745. doi:10.1016/j.molcel.2010.05.001

Ishii, T., Funakoshi, M., & Kobayashi, H. (2006). Yeast Pth2 is a UBL domain-binding protein that participates in the ubiquitin-proteasome pathway. *EMBO J, 25*(23), 5492-5503. doi:10.1038/sj.emboj.7601418

Jansen, L. E., Verhage, R. A., & Brouwer, J. (1998). Preferential binding of yeast Rad4.Rad23 complex to damaged DNA. *J Biol Chem, 273*(50), 33111-33114. doi:10.1074/jbc.273.50.33111

Kaneko, T., Hamazaki, J., Iemura, S., Sasaki, K., Furuyama, K., Natsume, T., Tanaka, K., & Murata, S. (2009). Assembly pathway of the Mammalian proteasome base subcomplex is mediated by multiple specific chaperones. *Cell, 137*(5), 914-925. doi:10.1016/j.cell.2009.05.008

Kang, Y., Vossler, R. A., Diaz-Martinez, L. A., Winter, N. S., Clarke, D. J., & Walters, K. J. (2006). UBL/UBA ubiquitin receptor proteins bind a common tetraubiquitin chain. *J Mol Biol, 356*(4), 1027-1035. doi:10.1016/j.jmb.2005.12.001

Kaplun, L., Ivantsiv, Y., Kornitzer, D., & Raveh, D. (2000). Functions of the DNA damage response pathway target Ho endonuclease of yeast for degradation via the ubiquitin-26S proteasome system. *Proc Natl Acad Sci U S A, 97*(18), 10077-10082. doi:10.1073/pnas.97.18.10077

Kaplun, L., Tzirkin, R., Bakhrat, A., Shabek, N., Ivantsiv, Y., & Raveh, D. (2005). The DNA damage-inducible UbL-UbA protein Ddi1 participates in Mec1-mediated degradation of Ho endonuclease. *Mol Cell Biol, 25*(13), 5355-5362. doi:10.1128/MCB.25.13.5355-5362.2005

Kerscher, O., Felberbaum, R., & Hochstrasser, M. (2006). Modification of proteins by ubiquitin and ubiquitin-like proteins. *Annu Rev Cell Dev Biol, 22*, 159-180. doi:10.1146/annurev.cellbio.22.010605.093503

Kim, I., Ahn, J., Liu, C., Tanabe, K., Apodaca, J., Suzuki, T., & Rao, H. (2006). The Png1-Rad23 complex regulates glycoprotein turnover. *J Cell Biol, 172*(2), 211-219. doi:10.1083/jcb.200507149

Kim, I., Mi, K., & Rao, H. (2004). Multiple interactions of rad23 suggest a mechanism for ubiquitylated substrate delivery important in proteolysis. *Mol Biol Cell, 15*(7), 3357-3365. doi:10.1091/mbc.e03-11-0835

Kimura, Y., Yashiroda, H., Kudo, T., Koitabashi, S., Murata, S., Kakizuka, A., & Tanaka, K. (2009). An inhibitor of a deubiquitinating enzyme regulates ubiquitin homeostasis. *Cell, 137*(3), 549-559. doi:10.1016/j.cell.2009.02.028

Kloetzel, P. M. (2001). Antigen processing by the proteasome. *Nat Rev Mol Cell Biol, 2*(3), 179-187. doi:10.1038/35056572

Kodadek, T. (2010). No Splicing, no dicing: non-proteolytic roles of the ubiquitin-proteasome system in transcription. *J Biol Chem, 285*(4), 2221-2226. doi:10.1074/jbc.R109.077883

Kohler, A., Cascio, P., Leggett, D. S., Woo, K. M., Goldberg, A. L., & Finley, D. (2001). The axial channel of the proteasome core particle is gated by the Rpt2 ATPase and controls both substrate entry and product release. *Mol Cell, 7*(6), 1143-1152.

Komander, D., & Rape, M. (2012). The ubiquitin code. *Annu Rev Biochem, 81*, 203-229. doi:10.1146/annurev-biochem-060310-170328

Krylov, D. M., & Koonin, E. V. (2001). A novel family of predicted retroviral-like aspartyl proteases with a possible key role in eukaryotic cell cycle control. *Curr Biol, 11*(15), R584-587. doi:10.1016/s0960-9822(01)00357-8

Kunjappu, M. J., & Hochstrasser, M. (2014). Assembly of the 20S proteasome. *Biochim Biophys Acta, 1843*(1), 2-12. doi:10.1016/j.bbamcr.2013.03.008

Kusmierczyk, A. R., & Hochstrasser, M. (2008). Some assembly required: dedicated chaperones in eukaryotic proteasome biogenesis. *Biol Chem, 389*(9), 1143-1151. doi:10.1515/BC.2008.130

Kusmierczyk, A. R., Kunjappu, M. J., Kim, R. Y., & Hochstrasser, M. (2011). A conserved 20S proteasome assembly factor requires a C-terminal HbYX motif for proteasomal precursor binding. *Nat Struct Mol Biol, 18*(5), 622-629. doi:10.1038/nsmb.2027

Lai, Z., Ferry, K. V., Diamond, M. A., Wee, K. E., Kim, Y. B., Ma, J., Yang, T., Benfield, P. A., Copeland, R. A., & Auger, K. R. (2001). Human mdm2

mediates multiple mono-ubiquitination of p53 by a mechanism requiring enzyme isomerization. *J Biol Chem, 276*(33), 31357-31367. doi:10.1074/jbc.M011517200

Lambertson, D., Chen, L., & Madura, K. (1999). Pleiotropic defects caused by loss of the proteasome-interacting factors Rad23 and Rpn10 of Saccharomyces cerevisiae. *Genetics, 153*(1), 69-79.

Lambertson, D., Chen, L., & Madura, K. (2003). Investigating the importance of proteasome-interaction for Rad23 function. *Curr Genet, 42*(4), 199-208. doi:10.1007/s00294-002-0350-7

Lander, G. C., Estrin, E., Matyskiela, M. E., Bashore, C., Nogales, E., & Martin, A. (2012). Complete subunit architecture of the proteasome regulatory particle. *Nature, 482*(7384), 186-191. doi:10.1038/nature10774

Laporte, D., Salin, B., Daignan-Fornier, B., & Sagot, I. (2008). Reversible cytoplasmic localization of the proteasome in quiescent yeast cells. *J Cell Biol, 181*(5), 737-745. doi:10.1083/jcb.200711154

Larsen, C. N., & Finley, D. (1997). Protein translocation channels in the proteasome and other proteases. *Cell, 91*(4), 431-434. doi:10.1016/s0092-8674(00)80427-4

Le Tallec, B., Barrault, M. B., Guerois, R., Carre, T., & Peyroche, A. (2009). Hsm3/S5b participates in the assembly pathway of the 19S regulatory particle of the proteasome. *Mol Cell, 33*(3), 389-399. doi:10.1016/j.molcel.2009.01.010

Lecker, S. H., Goldberg, A. L., & Mitch, W. E. (2006). Protein degradation by the ubiquitin-proteasome pathway in normal and disease states. *J Am Soc Nephrol, 17*(7), 1807-1819. doi:10.1681/ASN.2006010083

Leggett, D. S., Hanna, J., Borodovsky, A., Crosas, B., Schmidt, M., Baker, R. T., Walz, T., Ploegh, H., & Finley, D. (2002). Multiple associated proteins regulate proteasome structure and function. *Mol Cell, 10*(3), 495-507.

Lilienbaum, A. (2013). Relationship between the proteasomal system and autophagy. *Int J Biochem Mol Biol, 4*(1), 1-26.

Liu, C., van Dyk, D., Li, Y., Andrews, B., & Rao, H. (2009). A genome-wide synthetic dosage lethality screen reveals multiple pathways that require the functioning of ubiquitin-binding proteins Rad23 and Dsk2. *BMC Biol, 7*, 75. doi:10.1186/1741-7007-7-75

Liu, Y., Dai, H., & Xiao, W. (1997a). UAS(MAG1), a yeast cis-acting element that regulates the expression of MAG1, is located within the protein coding region of DDI1. *Mol Gen Genet, 255*(5), 533-542. doi:10.1007/s004380050526

Liu, Y., & Xiao, W. (1997b). Bidirectional regulation of two DNA-damage-inducible genes, MAG1 and DDI1, from Saccharomyces cerevisiae. *Mol Microbiol, 23*(4), 777-789. doi:10.1046/j.1365-2958.1997.2701631.x

Lommel, L., Ortolan, T., Chen, L., Madura, K., & Sweder, K. S. (2002). Proteolysis of a nucleotide excision repair protein by the 26 S proteasome. *Curr Genet, 42*(1), 9-20. doi:10.1007/s00294-002-0332-9

Lotz, K., Pyrowolakis, G., & Jentsch, S. (2004). BRUCE, a giant E2/E3 ubiquitin ligase and inhibitor of apoptosis protein of the trans-Golgi network, is

required for normal placenta development and mouse survival. *Mol Cell Biol, 24*(21), 9339-9350. doi:10.1128/MCB.24.21.9339-9350.2004

Lustgarten, V., & Gerst, J. E. (1999). Yeast VSM1 encodes a v-SNARE binding protein that may act as a negative regulator of constitutive exocytosis. *Mol Cell Biol, 19*(6), 4480-4494. doi:10.1128/mcb.19.6.4480

Madura, K., & Prakash, S. (1990). Transcript levels of the Saccharomyes cerevisiae DNA repair gene RAD23 increase in response to UV light and in meiosis but remain constant in the mitotic cell cycle. *Nucleic Acids Res, 18*(16), 4737-4742. doi:10.1093/nar/18.16.4737

Madura, K., & Varshavsky, A. (1994). Degradation of G alpha by the N-end rule pathway. *Science, 265*(5177), 1454-1458. doi:10.1126/science.8073290

Marash, M., & Gerst, J. E. (2003). Phosphorylation of the autoinhibitory domain of the Sso t-SNAREs promotes binding of the Vsm1 SNARE regulator in yeast. *Mol Biol Cell, 14*(8), 3114-3125. doi:10.1091/mbc.e02-12-0804

Mayor, T., Graumann, J., Bryan, J., MacCoss, M. J., & Deshaies, R. J. (2007). Quantitative profiling of ubiquitylated proteins reveals proteasome substrates and the substrate repertoire influenced by the Rpn10 receptor pathway. *Mol Cell Proteomics, 6*(11), 1885-1895. doi:10.1074/mcp.M700264-MCP200

McGrath, J. P., Jentsch, S., & Varshavsky, A. (1991). UBA 1: an essential yeast gene encoding ubiquitin-activating enzyme. *EMBO J, 10*(1), 227-236.

Medicherla, B., Kostova, Z., Schaefer, A., & Wolf, D. H. (2004). A genomic screen identifies Dsk2p and Rad23p as essential components of ER-associated degradation. *EMBO Rep, 5*(7), 692-697. doi:10.1038/sj.embor.7400164

Mueller, T. D., & Feigon, J. (2002). Solution structures of UBA domains reveal a conserved hydrophobic surface for protein-protein interactions. *J Mol Biol, 319*(5), 1243-1255. doi:10.1016/S0022-2836(02)00302-9

Mueller, T. D., Kamionka, M., & Feigon, J. (2004). Specificity of the interaction between ubiquitin-associated domains and ubiquitin. *J Biol Chem, 279*(12), 11926-11936. doi:10.1074/jbc.M312865200

Niepel, M., Molloy, K. R., Williams, R., Farr, J. C., Meinema, A. C., Vecchietti, N., Cristea, I. M., Chait, B. T., Rout, M. P., & Strambio-De-Castillia, C. (2013). The nuclear basket proteins Mlp1p and Mlp2p are part of a dynamic interactome including Esc1p and the proteasome. *Mol Biol Cell, 24*(24), 3920-3938. doi:10.1091/mbc.E13-07-0412

Ortolan, T. G., Chen, L., Tongaonkar, P., & Madura, K. (2004). Rad23 stabilizes Rad4 from degradation by the Ub/proteasome pathway. *Nucleic Acids Res, 32*(22), 6490-6500. doi:10.1093/nar/gkh987

Ortolan, T. G., Tongaonkar, P., Lambertson, D., Chen, L., Schauber, C., & Madura, K. (2000). The DNA repair protein rad23 is a negative regulator of multi-ubiquitin chain assembly. *Nat Cell Biol, 2*(9), 601-608. doi:10.1038/35023547

Ozkaynak, E., Finley, D., & Varshavsky, A. (1984). The yeast ubiquitin gene: head-to-tail repeats encoding a polyubiquitin precursor protein. *Nature, 312*(5995), 663-666. doi:10.1038/312663a0

Pagan, J., Seto, T., Pagano, M., & Cittadini, A. (2013). Role of the ubiquitin proteasome system in the heart. *Circ Res, 112*(7), 1046-1058. doi:10.1161/CIRCRESAHA.112.300521

Park, S., Roelofs, J., Kim, W., Robert, J., Schmidt, M., Gygi, S. P., & Finley, D. (2009). Hexameric assembly of the proteasomal ATPases is templated through their C termini. *Nature, 459*(7248), 866-870. doi:10.1038/nature08065

Park, S. H., Kukushkin, Y., Gupta, R., Chen, T., Konagai, A., Hipp, M. S., Hayer-Hartl, M., & Hartl, F. U. (2013). PolyQ proteins interfere with nuclear degradation of cytosolic proteins by sequestering the Sis1p chaperone. *Cell, 154*(1), 134-145. doi:10.1016/j.cell.2013.06.003

Pathare, G. R., Nagy, I., Bohn, S., Unverdorben, P., Hubert, A., Korner, R., Nickell, S., Lasker, K., Sali, A., Tamura, T., Nishioka, T., Forster, F., Baumeister, W., & Bracher, A. (2012). The proteasomal subunit Rpn6 is a molecular clamp holding the core and regulatory subcomplexes together. *Proc Natl Acad Sci U S A, 109*(1), 149-154. doi:10.1073/pnas.1117648108

Pearce, M. J., Mintseris, J., Ferreyra, J., Gygi, S. P., & Darwin, K. H. (2008). Ubiquitin-like protein involved in the proteasome pathway of Mycobacterium tuberculosis. *Science, 322*(5904), 1104-1107. doi:10.1126/science.1163885

Pickart, C. M., & Eddins, M. J. (2004). Ubiquitin: structures, functions, mechanisms. *Biochim Biophys Acta, 1695*(1-3), 55-72. doi:10.1016/j.bbamcr.2004.09.019

Prasad, R., Kawaguchi, S., & Ng, D. T. (2010). A nucleus-based quality control mechanism for cytosolic proteins. *Mol Biol Cell, 21*(13), 2117-2127. doi:10.1091/mbc.E10-02-0111

Raasi, S., & Pickart, C. M. (2003). Rad23 ubiquitin-associated domains (UBA) inhibit 26 S proteasome-catalyzed proteolysis by sequestering lysine 48-linked polyubiquitin chains. *J Biol Chem, 278*(11), 8951-8959. doi:10.1074/jbc.m212841200

Raasi, S., Varadan, R., Fushman, D., & Pickart, C. M. (2005). Diverse polyubiquitin interaction properties of ubiquitin-associated domains. *Nat Struct Mol Biol, 12*(8), 708-714. doi:10.1038/nsmb962

Rahimi, N. (2012). The ubiquitin-proteasome system meets angiogenesis. *Mol Cancer Ther, 11*(3), 538-548. doi:10.1158/1535-7163.MCT-11-0555

Ramos, P. C., Hockendorff, J., Johnson, E. S., Varshavsky, A., & Dohmen, R. J. (1998). Ump1p is required for proper maturation of the 20S proteasome and becomes its substrate upon completion of the assembly. *Cell, 92*(4), 489-499. doi:10.1016/s0092-8674(00)80942-3

Rao, H., & Sastry, A. (2002). Recognition of specific ubiquitin conjugates is important for the proteolytic functions of the ubiquitin-associated domain proteins Dsk2 and Rad23. *J Biol Chem, 277*(14), 11691-11695. doi:10.1074/jbc.M200245200

Roelofs, J., Park, S., Haas, W., Tian, G., McAllister, F. E., Huo, Y., Lee, B. H., Zhang, F., Shi, Y., Gygi, S. P., & Finley, D. (2009). Chaperone-mediated

pathway of proteasome regulatory particle assembly. *Nature, 459*(7248), 861-865. doi:10.1038/nature08063

Romero-Perez, L., Chen, L., Lambertson, D., & Madura, K. (2007). Sts1 can overcome the loss of Rad23 and Rpn10 and represents a novel regulator of the ubiquitin/proteasome pathway. *J Biol Chem, 282*(49), 35574-35582. doi:10.1074/jbc.M704857200

Rosenzweig, R., Osmulski, P. A., Gaczynska, M., & Glickman, M. H. (2008). The central unit within the 19S regulatory particle of the proteasome. *Nat Struct Mol Biol, 15*(6), 573-580. doi:10.1038/nsmb.1427

Russell, S. J., & Johnston, S. A. (2001). Evidence that proteolysis of Gal4 cannot explain the transcriptional effects of proteasome ATPase mutations. *J Biol Chem, 276*(13), 9825-9831. doi:10.1074/jbc.M010889200

Russell, S. J., Reed, S. H., Huang, W., Friedberg, E. C., & Johnston, S. A. (1999). The 19S regulatory complex of the proteasome functions independently of proteolysis in nucleotide excision repair. *Mol Cell, 3*(6), 687-695.

Saeki, Y., Sone, T., Toh-e, A., & Yokosawa, H. (2002). Identification of ubiquitin-like protein-binding subunits of the 26S proteasome. *Biochem Biophys Res Commun, 296*(4), 813-819. doi:10.1016/s0006-291x(02)02002-8

Saeki, Y., Toh-e, A., & Yokosawa, H. (2000). Rapid isolation and characterization of the yeast proteasome regulatory complex. *Biochem Biophys Res Commun, 273*(2), 509-515. doi:10.1006/bbrc.2000.2980

Saeki, Y., Toh, E. A., Kudo, T., Kawamura, H., & Tanaka, K. (2009). Multiple proteasome-interacting proteins assist the assembly of the yeast 19S regulatory particle. *Cell, 137*(5), 900-913. doi:10.1016/j.cell.2009.05.005

Sakata, E., Bohn, S., Mihalache, O., Kiss, P., Beck, F., Nagy, I., Nickell, S., Tanaka, K., Saeki, Y., Forster, F., & Baumeister, W. (2012). Localization of the proteasomal ubiquitin receptors Rpn10 and Rpn13 by electron cryomicroscopy. *Proc Natl Acad Sci U S A, 109*(5), 1479-1484. doi:10.1073/pnas.1119394109

Schauber, C., Chen, L., Tongaonkar, P., Vega, I., Lambertson, D., Potts, W., & Madura, K. (1998). Rad23 links DNA repair to the ubiquitin/proteasome pathway. *Nature, 391*(6668), 715-718. doi:10.1038/35661

Schlenstedt, G., Saavedra, C., Loeb, J. D., Cole, C. N., & Silver, P. A. (1995). The GTP-bound form of the yeast Ran/TC4 homologue blocks nuclear protein import and appearance of poly(A)+ RNA in the cytoplasm. *Proc Natl Acad Sci U S A, 92*(1), 225-229. doi:10.1073/pnas.92.1.225

Smith, D. M., Chang, S. C., Park, S., Finley, D., Cheng, Y., & Goldberg, A. L. (2007). Docking of the proteasomal ATPases' carboxyl termini in the 20S proteasome's alpha ring opens the gate for substrate entry. *Mol Cell, 27*(5), 731-744. doi:10.1016/j.molcel.2007.06.033

Spence, J., Sadis, S., Haas, A. L., & Finley, D. (1995). A ubiquitin mutant with specific defects in DNA repair and multiubiquitination. *Mol Cell Biol, 15*(3), 1265-1273. doi:10.1128/mcb.15.3.1265

Svoboda, M., Konvalinka, J., Trempe, J. F., & Grantz Saskova, K. (2019). The yeast proteases Ddi1 and Wss1 are both involved in the DNA replication

stress response. *DNA Repair (Amst), 80*, 45-51. doi:10.1016/j.dnarep.2019.06.008

Swaminathan, S., Amerik, A. Y., & Hochstrasser, M. (1999). The Doa4 deubiquitinating enzyme is required for ubiquitin homeostasis in yeast. *Mol Biol Cell, 10*(8), 2583-2594. doi:10.1091/mbc.10.8.2583

Tabb, M. M., Tongaonkar, P., Vu, L., & Nomura, M. (2000). Evidence for separable functions of Srp1p, the yeast homolog of importin alpha (Karyopherin alpha): role for Srp1p and Sts1p in protein degradation. *Mol Cell Biol, 20*(16), 6062-6073. doi:10.1128/mcb.20.16.6062-6073.2000

Takeda, K., & Yanagida, M. (2005). Regulation of nuclear proteasome by Rhp6/Ubc2 through ubiquitination and destruction of the sensor and anchor Cut8. *Cell, 122*(3), 393-405. doi:10.1016/j.cell.2005.05.023

Tanaka, K., Suzuki, T., & Chiba, T. (1998). The ligation systems for ubiquitin and ubiquitin-like proteins. *Mol Cells, 8*(5), 503-512.

Tatebe, H., & Yanagida, M. (2000). Cut8, essential for anaphase, controls localization of 26S proteasome, facilitating destruction of cyclin and Cut2. *Curr Biol, 10*(21), 1329-1338. doi:10.1016/s0960-9822(00)00773-9

Tian, G., Park, S., Lee, M. J., Huck, B., McAllister, F., Hill, C. P., Gygi, S. P., & Finley, D. (2011). An asymmetric interface between the regulatory and core particles of the proteasome. *Nat Struct Mol Biol, 18*(11), 1259-1267. doi:10.1038/nsmb.2147

Tomko, R. J., Jr., Funakoshi, M., Schneider, K., Wang, J., & Hochstrasser, M. (2010). Heterohexameric ring arrangement of the eukaryotic proteasomal ATPases: implications for proteasome structure and assembly. *Mol Cell, 38*(3), 393-403. doi:10.1016/j.molcel.2010.02.035

Trempe, J. F., Saskova, K. G., Siva, M., Ratcliffe, C. D., Veverka, V., Hoegl, A., Menade, M., Feng, X., Shenker, S., Svoboda, M., Kozisek, M., Konvalinka, J., & Gehring, K. (2016). Structural studies of the yeast DNA damage-inducible protein Ddi1 reveal domain architecture of this eukaryotic protein family. *Sci Rep, 6*, 33671. doi:10.1038/srep33671

Ulrich, H. D. (2005). Mutual interactions between the SUMO and ubiquitin systems: a plea of no contest. *Trends Cell Biol, 15*(10), 525-532. doi:10.1016/j.tcb.2005.08.002

Verma, R., Oania, R., Graumann, J., & Deshaies, R. J. (2004). Multiubiquitin chain receptors define a layer of substrate selectivity in the ubiquitin-proteasome system. *Cell, 118*(1), 99-110. doi:10.1016/j.cell.2004.06.014

Wade, S. L., & Auble, D. T. (2010). The Rad23 ubiquitin receptor, the proteasome and functional specificity in transcriptional control. *Transcription, 1*(1), 22-26. doi:10.4161/trns.1.1.12201

Watkins, J. F., Sung, P., Prakash, L., & Prakash, S. (1993). The Saccharomyces cerevisiae DNA repair gene RAD23 encodes a nuclear protein containing a ubiquitin-like domain required for biological function. *Mol Cell Biol, 13*(12), 7757-7765. doi:10.1128/mcb.13.12.7757

Welchman, R. L., Gordon, C., & Mayer, R. J. (2005). Ubiquitin and ubiquitin-like proteins as multifunctional signals. *Nat Rev Mol Cell Biol, 6*(8), 599-609. doi:10.1038/nrm1700

Whitby, F. G., Masters, E. I., Kramer, L., Knowlton, J. R., Yao, Y., Wang, C. C., & Hill, C. P. (2000). Structural basis for the activation of 20S proteasomes by 11S regulators. *Nature, 408*(6808), 115-120. doi:10.1038/35040607

White, R. E., Dickinson, J. R., Semple, C. A., Powell, D. J., & Berry, C. (2011). The retroviral proteinase active site and the N-terminus of Ddi1 are required for repression of protein secretion. *FEBS Lett, 585*(1), 139-142. doi:10.1016/j.febslet.2010.11.026

Wiechens, N., & Fagotto, F. (2001). CRM1- and Ran-independent nuclear export of beta-catenin. *Curr Biol, 11*(1), 18-27. doi:10.1016/s0960-9822(00)00045-2

Wilkinson, C. R., Seeger, M., Hartmann-Petersen, R., Stone, M., Wallace, M., Semple, C., & Gordon, C. (2001). Proteins containing the UBA domain are able to bind to multi-ubiquitin chains. *Nat Cell Biol, 3*(10), 939-943. doi:10.1038/ncb1001-939

Withers-Ward, E. S., Jowett, J. B., Stewart, S. A., Xie, Y. M., Garfinkel, A., Shibagaki, Y., Chow, S. A., Shah, N., Hanaoka, F., Sawitz, D. G., Armstrong, R. W., Souza, L. M., & Chen, I. S. (1997). Human immunodeficiency virus type 1 Vpr interacts with HHR23A, a cellular protein implicated in nucleotide excision DNA repair. *J Virol, 71*(12), 9732-9742.

Withers-Ward, E. S., Mueller, T. D., Chen, I. S., & Feigon, J. (2000). Biochemical and structural analysis of the interaction between the UBA(2) domain of the DNA repair protein HHR23A and HIV-1 Vpr. *Biochemistry, 39*(46), 14103-14112. doi:10.1021/bi0017071

Worden, E. J., Dong, K. C., & Martin, A. (2017). An AAA Motor-Driven Mechanical Switch in Rpn11 Controls Deubiquitination at the 26S Proteasome. *Mol Cell, 67*(5), 799-811 e798. doi:10.1016/j.molcel.2017.07.023

Xie, Z., Liu, S., Zhang, Y., & Wang, Z. (2004). Roles of Rad23 protein in yeast nucleotide excision repair. *Nucleic Acids Res, 32*(20), 5981-5990. doi:10.1093/nar/gkh934

Yewdell, J. W., & Bennink, J. R. (2001). Cut and trim: generating MHC class I peptide ligands. *Curr Opin Immunol, 13*(1), 13-18.

Zhu, Q., Wani, G., Wani, M. A., & Wani, A. A. (2001). Human homologue of yeast Rad23 protein A interacts with p300/cyclic AMP-responsive element binding (CREB)-binding protein to down-regulate transcriptional activity of p53. *Cancer Res, 61*(1), 64-70.

Zhu, Y., & Xiao, W. (1998). Differential regulation of two closely clustered yeast genes, MAG1 and DDI1, by cell-cycle checkpoints. *Nucleic Acids Res, 26*(23), 5402-5408. doi:10.1093/nar/26.23.5402

Zhu, Y., & Xiao, W. (2001). Two alternative cell cycle checkpoint pathways differentially control DNA damage-dependent induction of MAG1 and DDI1 expression in yeast. *Mol Genet Genomics, 266*(3), 436-444. doi:10.1007/s004380100538

APPENDIX I

APPENDIX I

Previous studies have shown that overexpression of Rad23's UbL (UbL^{Rad23}) domain leads to stabilization of a test substrate examined. In this study, GST-UbL was co-expressed with the artificial substrates Ub-Pro-β-Galactosidase (Ub-Pro-β-Gal), and protein levels over time were examined. This can be explained that the UbL^{Rad23} domain competes for binding sites in the19S subunit with shuttle factors, and by overexpressing UbL^{Rad23} will outcompete other 19S binding partners. I wanted to examine the subcellular localization of GFP-UbL to elucidate in this observation. I expressed GFP-UbL in either *sts1-2*, in which proteasome are stabilized and nuclear substrates stabilized, as well as in *rna1-1*, which exhibits a significant nuclear transport defect. I found that GFP-UbL localized to the cytosol in wildtype, *sts1-2* and *rna1-1* at permissive (21°C) and the non-permissive temperature (37°C) (Fig 35). Additionally, I wanted to examine a physiological nuclear substrates, since other studies examined only artificial substrate in conjunction with the overexpression of GST-UbL. I selected Ho because I discovered robust binding to Rad23 (Fig. 29). I co-expressed GFP-Ho with GST-UbL in *rad23Δ* cells. I overserved an increased fluorescent signal of GFP-Ho in cells expressing GST-UbL when compared to wildtype, suggesting Ho becomes stabilized (Fig. 36). The observations that GFP-UbL localizes to the cytosol, and GFP-Ho appears to be stabilized when co-expressed with GST-UbL are in agreement with the idea that nuclear substrates are exported to the cytosolic proteasome.

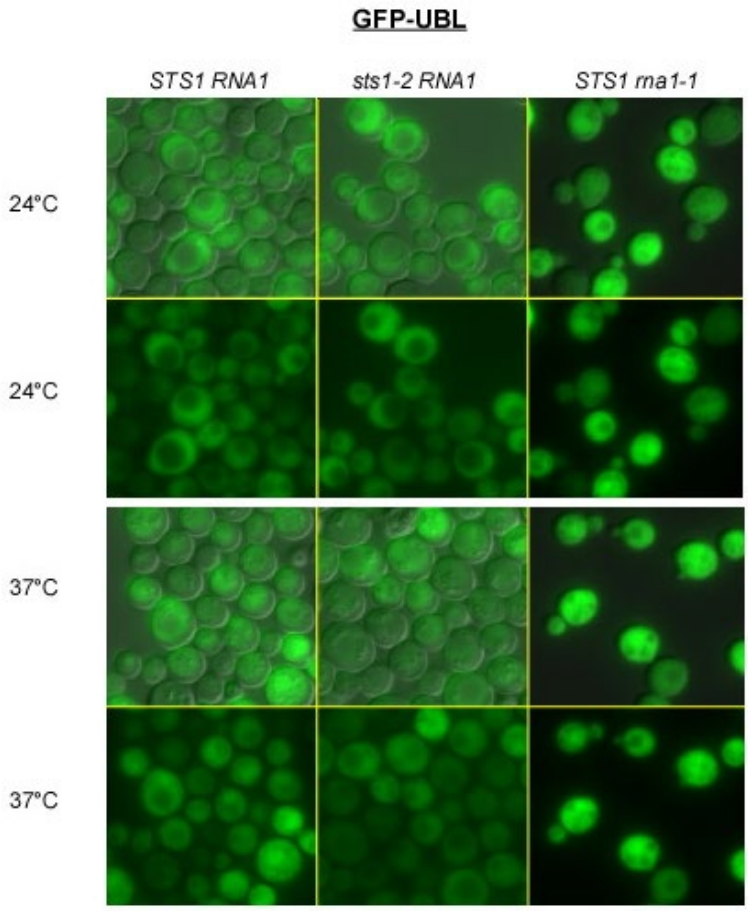

Figure 37. GFP-UbL localizes to the cytosol. GFP-UbL was expressed in *STS1, RNA1*, *sts1-2*, and *rna1-1*. Cells were grown in 10 ml of SM for 16 hours at 21°C. Cultures were diluted into fresh SM and incubated at for either 5 hours (*sts1-2*), or 1 hours (*rna1-1*) at 21°C and 37°C. One ml aliquots were withdrawn from exponentially growing culture, pelleted, and re-suspended in residual liquid. For imaging, 2.5 µl aliquots from each sample was withdrawn, spotted on Poly-Prep slides, and cells were imaged live.

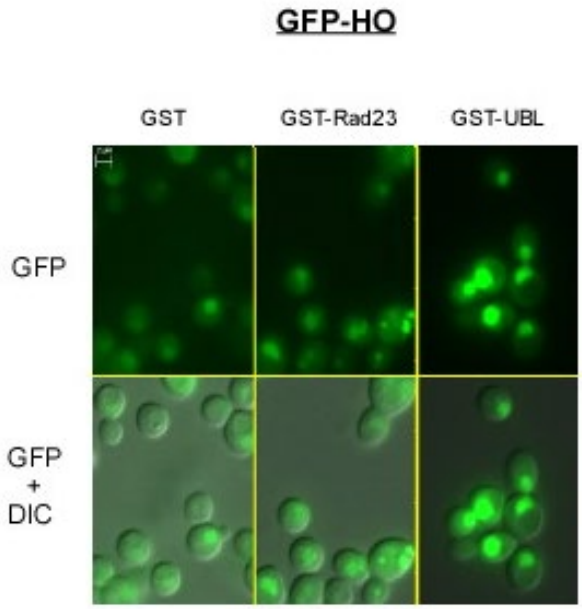

Figure 38. GFP-Ho is stabilized in the presence of GST-UbL. GFP-Ho was expressed in *rad23Δ*. Cells were grown in 10 ml of SM with 2% raffinose for 16 hours at 30°C. Cultures were diluted into fresh SM with 2% galactose and incubated at for 3 hours 30°C. One ml aliquots were withdrawn from exponentially growing culture, pelleted, and re-suspended in residual liquid. For imaging, 2.5 µl aliquots from each sample was withdrawn, spotted on Poly-Prep slides, and cells were imaged live.

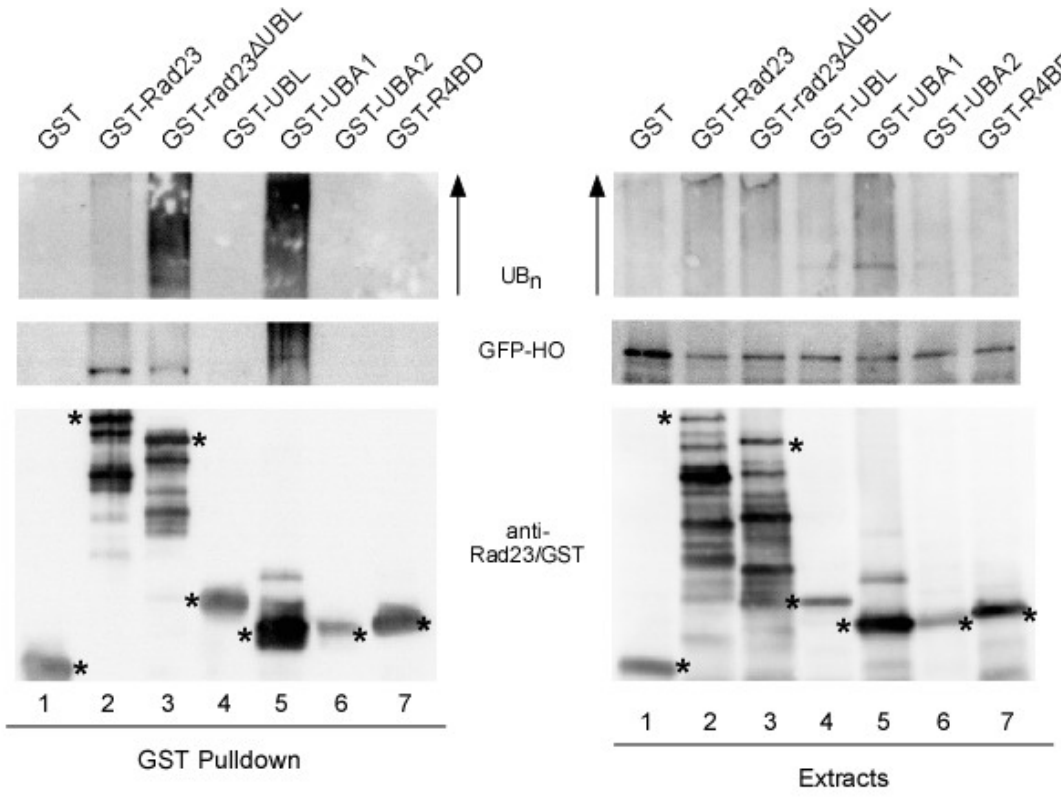

Figure 39. UBA1 domain in Rad23 primarily interacts with Ho and polyUb substrates. GFP-Ho was expressed from the galactose-inducible *GAL1* promoter. Cells were grown in 50 ml SM containing raffinose for 16 hours, and then diluted in fresh non-selective rich media (YP) with galactose for 2 hours. GFP-Ho was co-expressed with GST-tagged Rad23, rad23$^{\Delta UbL}$, UbL, UBA1, UBA2, and R4BD. Yeast lysates were prepared, and equal amount of protein was incubated with anti-FLAG matrix at 4°C for 2 hours. Purified proteins were washed and resolved in a 12 % polyacrylamide SDS-Tricine gel. Gels were transferred to nitrocellulose membrane, and blots were immunoblotted with antibodies against FLAG, GFP, and Ub.

APENDIX II

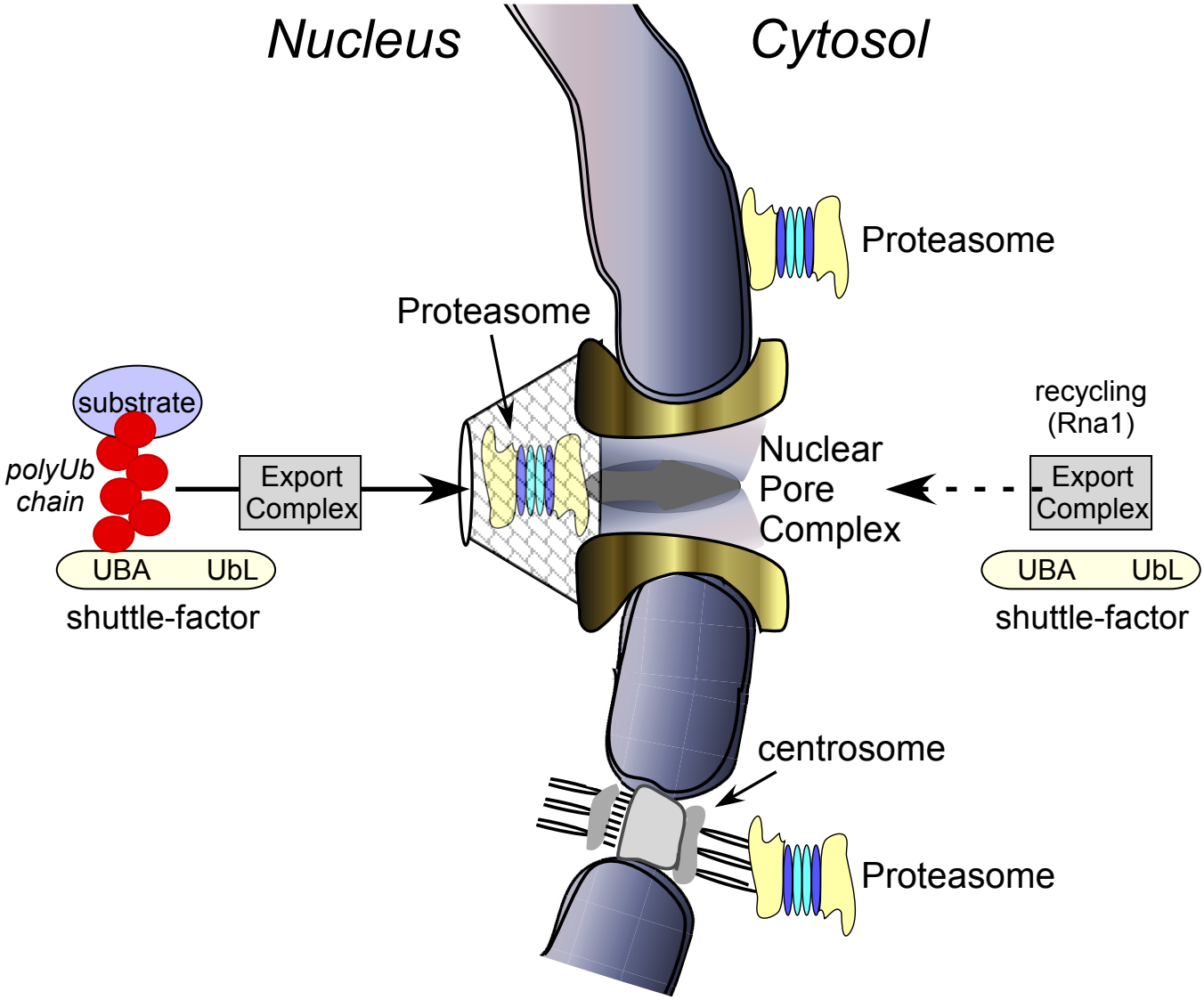
Nucleus
Cytosol
Proteasome
Proteasome
substrate
polyUb
chain
Export
Complex
Nuclear
Pore
Complex
recycling
(Rna1)
Export
Complex
UBA
UbL
shuttle-factor
UBA
UbL
shuttle-factor
centrosome
Proteasome

The cellular location of Rad23, a polyubiquitin chain-binding protein, plays a key role in its interaction with substrates of the proteasome

Evelyn Okeke, Li Chen and Kiran Madura *

Department of Pharmacology – SPH 383

Robert Wood Johnson Medical School

683 Hoes Lane,

Rutgers University.

Piscataway, New Jersey 08854

***: to whom correspondence should be addressed**

Phone: 732-235-5602

Fax: 732-235-4073

Email: maduraki@rwjms.rutgers.edu

Abstract

The Rad23 protein contains structural motifs that allow it to bind polyubiquitin chains and the proteasome; implicating a role in transporting substrates to the proteasome. The validation of this model, however, has been hindered by the lack of specific physiological substrates of Rad23. We have determined that Rad23 can bind Ho-endonuclease (Ho-endo), a nuclear protein that initiates mating-type switching in *Saccharomyces cerevisiae*. We observed that Ho-endo degradation required export from the nucleus, in agreement with a previous report [1]. The subcellular distribution of Rad23 is noticeably altered in genetic mutants that disrupt proteasome localization and nucleocytoplasmic trafficking. We therefore investigated if the location of Rad23 affected its interaction with polyubiquitylated (polyUb) substrates. We report here that mutations in both export and import stabilize nuclear substrates. Significantly, these substrates accumulated in the nucleus and formed an interaction with Rad23. In contrast, Rad23 that was localized to the cytosol showed markedly reduced binding to polyubiquitylated nuclear substrates. These studies show that substrates can be conjugated to polyubiquitin chains in the nucleus, but require an export-dependent mechanism to be degraded by proteasomes. The evolutionarily conservation of Rad23 and similar trafficking proteins suggests that the export mechanism represents a general requirement in the turnover of nuclear proteins.

Keywords: export / degradation / Ho-endonuclease / shuttle factor / ubiquitin

Introduction

It is widely believed that proteasomes are present in the nucleus to degrade proteins [2-5] [6] [7]. However, the preponderance of proteasome peptidase activity is detected in the cytosol [8], and not in the soluble nuclear fraction. Proteasomes have been shown to be located near the nuclear surface [9-11] [12], and are specifically detected in the centrosome, and the nuclear basket of the nuclear pore complex (NPC) [13, 14]. We and others showed that several nuclear proteins are degraded only after export [15] [16] [17] [18]; predicting an important role for the nucleo-cytoplasmic trafficking system. The proteasome-mediated degradation of specific substrates, such as Far1, involves entry into the nucleus [2]. However, this requirement does not exempt a subsequent role for export in Far1 turnover, and the degradation of other nuclear substrates. Although it is possible that nuclear substrates may be degraded either within the nucleus, or after export to cytoplasmic proteasomes, the evidence for intra-nuclear turnover is indirect [2-5] [6] [7]. In contrast, evidence that nuclear proteins are degraded after export has been recognized using by both genetic and pharmacologic strategies [15] [16] [17] [18]. Injection of fluorogenic proteasome substrates directly into nucleoplasm [19] suggested nuclear-specific activity. However, the physiological significance remains to be established since this approach circumvents the role of the nucleocytoplasmic transport system. Our studies indicate that some nuclear proteins are degraded only after exit from the nucleus.

Individual proteasome subunits that are detected in the nucleus may not be engaged in a proteolytic function, because proteasome sub-complexes perform non-proteolytic roles in transcription [20, 21], and DNA repair [22]. Moreover, the detection of proteasome subunits in the nucleus [15, 23, 24], does not indicate that they are assembled in functionally intact proteasomes. We reported that proteasomes are not targeted to the nucleus in *sts1-2*, but accumulate in the cytosol in catalytically active form [23]. Nuclear substrates are stabilized in

sts1-2, demonstrating that the availability of proteasomes at the nuclear periphery is required for degradation. Whether proteasomes enter the nucleus, or remain tethered to the nuclear surface, is uncertain. However, it is notable that in *S. pombe* proteasomes are tethered to the nuclear surface by Cut8 [25]. Similarly, Sts1 in *S. cerevisiae* (a distant homolog of Cut8), also promotes the nuclear targeting of proteasomes [23].

Srp1 is a member of the importin-α family that perform a vital role in the nuclear import of proteins that contain nuclear localization signals (NLS) [26] [27]. Significantly, proteasomes are mislocalized to the cytosol in *srp1-49*, and nuclear substrates are stabilized [28]. Importantly, nuclear import is not impaired in *srp1-49* [28], which suggests that Srp1 does not import proteasomes, but likely localizes them to the nuclear surface. In agreement with this idea, we showed in a different mutant, in which nuclear import defect is inhibited (*srp1-31*), proteasome localization occurred normally [28]. The cytosolic accumulation of proteasomes in *sts1-2* and *srp1-49* causes stabilization of nuclear substrates, and their accumulation in the nucleus. Both Sts1 and Cut8 are cytosolic proteins that are degraded by proteasomes [29] [30], indicating that they do not escort proteasomes into the nucleus.

We used genetic and pharmacological approaches to demonstrate that the degradation of nuclear proteins (Rad4, Clb2, and Cdc17) required export [15] [1]. A similar effect is seen in human cells, where p53 [16], β-catenin [17], TRIP-Br1 [31], and hMSH5 [32] are degraded only after export from the nucleus. These results show that certain substrates are not degraded in the nucleus, but by proteasomes at the periphery, or in the cytosol. Proteasomes were shown to be located in the nuclear basket, which is associated with the NPC [13, 14]. Although an export mechanism is in contravention to the current view, it is conceptually analogous to endoplasmic reticulum associated degradation (ERAD) [33], where damaged proteins are translocated across the ER membrane to proteasomes in the cytosol.

Our findings led us to question how polyubiquitylated (polyUb) nuclear substrates were transported out of the nucleus. A role for the export factor (Xpo1) in trafficking nuclear substrates is suggested by the presence of a functional nuclear export sequence (NES) in Clb2 [34]. However, polyubiquitylated proteins also interact with a family of trafficking proteins, among which Rad23 is the paradigm [35-37]. This family of proteins contain an amino-terminal ubiquitin-like (UbL) domain [38] that binds the 19*S* regulatory particle in the proteasome [37], and two ubiquitin-binding (UBA) motifs that interact with polyUb chains [36, 39, 40]. In Rad23, the UBA1 motif is the primary polyUb-binding determinant [36]. These key structural motifs are also present in other yeast shuttle-factors, Ddi1 and Dsk2, which enable them to transport of polyubiquitylated substrates to the proteasome [35]. The UbL/UBA architecture is conserved across eukaryotic evolution, with mouse and human Rad23 proteins retaining strong functional similarity to their yeast counterpart [41, 42].

We discovered that the subcellular location of Rad23 can be restricted to either the nucleus or the cytosol. Rad23 is completely nuclear localized in *sts1-2*, and is predominantly cytosolic in *rna1-1*, a mutant that regulates the nucleocytoplasmic trafficking system. Nuclear substrates are stabilized in both mutants. This allowed us to investigte the effect of subcellular localization of Rad23 on its interactions with polyUb nuclear substrates. We determined that nuclear Rad23 interacted with total polyUb substrates, and Ho-endonuclease, a specific physiological target. The degradation of another nuclear substrate (Matα2) was similarly affected in these two mutant strains. Taken together with our recently reported studies, we propose that the regulated movement of Rad23, between the nucleus and the cytosol, promotes the export-dependent degradation of nuclear proteins.

Results

Rad23 binds high levels of polyUb substrates in the nucleus

GFP-Rad23 was expressed in *STS1* (wildtype) and *sts1-2* mutant cells. GFP-Rad23 was detected in the nucleus and cytosol in both *STS1* and *sts1-2* at 21°C. However, at 37°C GFP-Rad23 was nuclear-localized in *sts1-2* (Fig. 1a). A merged image (DAPI + GFP) confirmed the nuclear accumulation of GFP-Rad23 in *sts1-2*. We confirmed that the abundance and stability of GFP-Rad23 was not affected in *sts1-2* at both 21°C (Fig. 1b) and 37°C (Fig. 1c). Because FLAG-Rad23 accumulated in the nucleus in *sts1-2* we tested its interaction with polyUb substrates. FLAG-Rad23 was purified from cultures grown at 21°C and 37°C, and the bound proteins were characterized by immunoblotting (Fig. 1d). The overall levels of polyUb species were similar in *STS1* and *sts1-2* at 21°C and 37°C (Extracts; lanes 6-11). Moderately higher levels of polyUb species were co-purified with FLAG-Rad23 at 37°C in *STS1* (Fig. 1d, compare lanes 2 and 4). However, significantly higher amounts were co-purified in *sts1-2* (Fig. 1d, compare lanes 3 and 5). The immunoblot was also treated with antibodies against Rpn10, and equivalent levels were co-purified with FLAG-Rad23 in *STS1* and *sts1-2* (at both 21°C and 37°C). The level of polyUb proteins isolated with FLAG-Rad23 was quantified by densitometry and 2 - 3 fold higher levels were detected in *sts1-2* at 37°C (Fig. 1e).

Cytosolic Rad23 binds low levels of polyUb substrates

Rna1 plays a critical role in controlling nucleocytoplasmic trafficking. We examined the localization of GFP-Rad23 in *rna1-1* and found that it was enriched in the cytosol at 37°C (Fig. 2a). Nuclear import and protein synthesis cease rapidly in *rna1-1* at 37°C [43]. Therefore, the cytosolic accumulation of GFP-Rad23 is most likely due to the movement of nuclear GFP-Rad23 into the cytosol. As we found in *sts1-2* (Fig. 1b, c) GFP-Rad23 levels were unaffected in *RNA1* and *rna1-1* at both 21°C and 37°C (Fig. 2b, c). We examined Rad23 interaction with polyUb proteins in *rna1-1*, as described in Fig. 1d. FLAG-Rad23 was immunopurified from *RNA1* and *rna1-1* to test the level of bound polyUb proteins. Immunoblotting showed FLAG-Rad23 isolated from *rna1-1* (lane 6) failed to display the dramatic increase in polyUb proteins observed in *RNA1* (compare lanes 5). Importantly, similar levels of polyUb proteins were isolated with FLAG-Rad23 from *RNA1* and *rna1-1* at 21°C (lanes 2 and 3). These binding studies were quantified by densitometry (Fig. 2e).

The sub-cellular distribution of ubiquitin is affected in *sts1-2* and *rna1-1*

We examined the cellular distribution of ubiquitin (GFP-Ub) to determine if the stabilization of nuclear substrates was caused by a failure to accurately transport ubiquitin into the nucleus. We found that GFP-Ub was distributed throughout the cell, with no enrichment in the nucleus in *STS1* and *sts1-2* at 21°C (Supplementary Results). However, at 37°C GFP-Ub showed nuclear enrichment in *sts1-2* (Fig. 3a), which is similar to the nuclear accumulation of substrates, and Rad23 (Fig. 1a). The localization of Nup49-RFP identifies the nuclear perimeter. We also determined that GFP-Ub was primarily cytosolic in *RNA1* and *rna1-1* at 21°C (Supplementary Results), and at 37°C (Fig. 3b). These findings led us to question if the nuclear accumulation of GFP-Ub in *sts1-2* (Fig. 3a) might be explained by its conjugation to substrates. To test this we examined RFP-ub$^{\Delta RGG}$; a mutant that cannot be ligated to lysine side-chains on substrates, or polyubiquitin chains. RFP-ub$^{\Delta RGG}$ was co-expressed with GFP-Ub

in *STS1* and *sts1-2*. In contrast to the nuclear accumulation of GFP-Ub in *sts1-2*, RFP-ub$^{\Delta RGG}$ was detected in the cytosol (Fig. 3c). A similar analysis in *rna1-1* showed RFP-ub$^{\Delta RGG}$ located in the cytosol in both *RNA1* and *rna1-1* at 21°C and 37°C (Fig. 3d). These findings suggest that the conjugation of ubiquitin to substrates explains its nuclear accumulation in *sts1-2*. Moreover, these polyubiquitylated proteins bound efficiently to FLAG-Rad23 in *sts1-2* (Fig. 1d).

Rad23 is a major substrate trafficking protein for Ho-endonuclease.

Testing shuttle-factor binding to bulk polyUb proteins does not provide insight on the export-dependent transport of nuclear substrates to the proteasome, because polyubiquitylated substrates are detected throughout the cell. However, characterizing shuttle factor binding to a specific substrate provides a way to monitor this process. Moreover, since the location of Rad23 can be regulated, its compartment-specific binding to physiological substrates can be determined. Nuclear proteins that bind Rad23 include Rad4 [44] and Sic1 [45]. However, due to technical considerations the characterization of their turnover was challenging. We therefore examined Ho-endonuclease (Ho-endo), a nuclear substrate of the proteasome that requires an export mechanism and the Ddi1 shuttle factor [46]. Because shuttle-factors have overlapping substrate specificity we investigated if Rad23 could promote Ho-endo turnover. We co-expressed GFP-Ho with epitope-tagged (FLAG-) derivatives of the three primary yeast shuttle-factors; Rad23, Ddi1, and Dsk2 (Fig. 4a). We observed a strong interaction between GFP-Ho and FLAG-Rad23 (Fig. 4a, lane 2). We detected a surprisingly weak interaction between GFP-Ho and FLAG-Ddi1 (Fig. 4a, lane 3), despite the high expression of this shuttle factor (Fig. 4b; compare lanes 2 and 3). These divergent findings may reflect different experimental conditions; the previous study showing an interaction between Ddi1 and Ho-endo-LacZ used a reconstituted system [46].

We confirmed that GFP-Ho is conjugated to ubiquitin, because this is the key determinant that binds a shuttle-factor. Lysates were prepared from yeast cells co-expressing myc-Ub and Ho-HA, and incubated with antibodies against HA. The purified proteins were separated by SDS/PAGE, transferred to nitrocellulose, and incubated with antibody against the myc epitope (Fig. 4c). An extensive smear was observed, consistent with the polyubiquitylation of Ho-HA (lane 1). Because Rad23 efficiently binds cellular proteins that are conjugated to Ub (see Fig. 1d) its interaction with Ho-endo is likely to occur through polyubiquitin chains.

The localization of Rad23 affects Ho-endo turnover.

As noted in Figures 1 and 2, Rad23 can be enriched in the nucleus (*sts1-2*), or cytosol (*rna1-1*). This offered a unique opportunity to test Rad23 interaction with a physiological substrate. Based on its strong interaction with Ho-endo (Fig. 3a), we investigated if GFP-Ho localization was influenced by the sub-cellular distribution of Rad23. Proteasomes are completely mislocalized to the cytosol in *sts1-2* at 37°C, and nuclear substrates are stabilized [15]. Significantly, Rad23 is enriched in the nucleus in *sts1-2*, where it binds higher levels of polyUb proteins (Fig. 1). We detected higher levels of GFP-Ho fluorescence in the nucleus at 21°C in *sts1-2*, compared to *STS1* (Fig. 5a; left panel). The nuclear level of GFP-Ho increased further at 37°C in *sts1-2* (Fig. 5a; right panel). We previously showed that the stability of artificial substrates increased in *sts1-2* [30]. However, the localization of these engineered substrates was not determined. We therefore investigated if the high level of nuclear GFP-Ho was caused by stabilization. Lysates containing GFP-Ho were prepared from *STS1* and *sts1-2* cells grown at 21°C and 37°C. Immunoblotting showed that GFP-Ho was efficiently degraded at 21°C in both *STS1* and *sts1-2* (Fig. 5b). However, GFP-Ho was stabilized in *sts1-2* at 37°C (Fig. 5c), indicating that the higher GFP signal observed in *sts1-2* is caused by protein stabilization. The relative turnover of GFP-Ho-endo was quantified (Fig. 5d and e).

Similarly, we expressed GFP-Ho in *RNA1* and *rna1-1* mutant. Cells were examined at 21°C and 37°C, and nuclear localization was observed in both wildtype and *rna1-1* at 21°C (Fig. 6a; left panel) After transfer to 37°C GFP-Ho was detected in the nucleus in *RNA1* (Fig. 6a; right panel), but was not observed in the nucleus in *rna1-1*. Instead, GFP-Ho was detected in the cytosol in discrete, punctate aggregates. Interestingly, other reports described the formation of cytosolic aggregates of nuclear proteins in *rna1* mutant [47]. Rna1 plays a vital role in converting GTP-bound Ran protein to GDP-Ran. The failure to catalyze this step prevents dissociation of the export complex, and results in cytosolic aggregation [47, 48]. Immunoblotting showed that GFP-HO-endo was efficiently degraded at 21°C in both *RNA1* and *rna1-1* mutant (Fig. 6b). Antibody reaction against Rpn10 confirmed equal loading. GFP-HO-endo was also degraded at 37°C in *RNA1*, but was stabilized in *rna1-1* (Fig. 6c). These results suggest that the cytosolic aggregates seen in *rna1-1* (Fig. 6a) represent GFP-Ho that exited the nucleus but failed to be degraded. The relative turnover of GFP-HO-endo was quantified (Fig. 6d and e).

Degradation of Matα2 involves the nucleocytoplasmic transport system.

We reported previously that functionally unrelated nuclear proteins (including Rad4, Clb2, and Cdc17), are degraded only after export from the nucleus [15]. However, the shuttle factors that promote turnover of most nuclear substrates of the proteasome have not been described. Therefore we characterized Matα2 protein, a well-studied proteasome substrate [49]. Although we have not identified a shuttle factor for Matα2 we determined that its degradation required nuclear export (L. Chen, unpublished studies). We expressed Matα2-GFP in *sts1-2* and *rna1-1* mutants and in agreement with our studies of GFP-Ho (Fig. 5a), Matα2-GFP was detected in the nucleus in *STS1* at 21°C (Fig. 7a). This GFP signal decreased at 37°C, possibly due to more rapid turnover at the elevated temperature. In contrast, Matα2-GFP levels increased markedly in *sts1-2*, at both 21°C and 37°C, consistent with the stabilization of nuclear proteins in this mutant.

We examined Matα2-GFP in *RNA1* and *rna1-1*. Yeast cells were grown at 21°C and examined by fluorescence microscopy (Fig. 7b). Matα2-GFP was readily detected in the nucleus in both *RNA1* and *rna1-1* at 21°C. Because protein synthesis is rapidly inhibited in *rna1-1* (at 37°C) [43], we blocked translation by transferring both cultures to pre-warmed medium (37°C) containing cycloheximide. The level of nuclear Matα2-GFP was largely unchanged in *RNA1* after transfer from 21°C to 37°C (Fig. 7b). In contrast, in *rna1-1* Matα2-GFP was rapidly depleted from the nucleus (within 15 min), and was seen in discrete deposits in the cytosol at 45 min and 90 min. This finding resembles the accumulation of GFP-Ho in cytosolic aggregates in *rna1-1* (Fig. 6a), and is consistent with our hypothesis that the transport of nuclear substrates to cytoplasmic proteasomes requires an export mechanism. To determine if Matα2-GFP was present in cytosolic aggregates we prepared lysates from cultures described in Fig. 7b. Equal amount of soluble and insoluble proteins, prepared from cells grown at 21°C and 37°C (90 min time point) was examined by immunoblotting with antibody against GFP (Fig. 7c). Whereas equal amount of Matα2-GFP was detected in the soluble (S) and insoluble (P) fractions prepared from *RNA1* and *rna1-1* at 21°C, significantly higher levels were detected at 37°C in *rna1-1* in the insoluble fraction (Fig. 7c, lane 8).

The subcellular location of Rad23 affects its interaction with Ho-endonuclease.

The use of *sts1-2* and *rna1-1* mutants allowed us to manipulate the location of Rad23 and demonstrate that its binding to polyUb proteins increased when it was present in the nucleus (Fig. 1 and 2). Because Rad23 and other shuttle factors transport proteolytic substrates to the proteasome we examined the location of Ho-endonuclease, since its degradation requires nuclear export ([1] and our unpublished studies). FLAG-Rad23 and GFP-Ho were co-expressed in *sts1-2* and *rna1-1* at 21°C and 37°C. Consistent with previous results (Fig. 1), FLAG-Rad23 showed increased binding to GFP-Ho in *sts1-2*, than in *STS1* (Fig. 8a; compare lanes 4 and 5). Differential binding was also evident at 21°C (compare lanes 2 and 3).

Since the nuclear levels of both Rad23 and Ho-endo increases in *sts1-2*, it is to be expected that higher binding is observed in this mutant. Total protein lysates were also examined (Fig. 8b) to confirm equal expression of FLAG-Rad23. The amount of GFP-Ho detected in Fig. 8a were quantified by densitometry, and adjusted to the levels of FLAG-Rad23. In a similar analysis, FLAG-Rad23 and GFP-Ho were co-expressed in *RNA1* and *rna1-1* mutant (Fig. 8d). We detected no interaction between Rad23 and Ho-endo at 37°C in *rna1-1* (lane 5). Although both proteins are cytosolic in *rna1-1*, it is likely that the partitioning of GFP-Ho into the insoluble fractions precludes efficient binding to FLAG-Rad23. Analysis of total protein showed comparable expression of FLAG-Rad23. The results in Fig. 8d were quantified by densitometry (panel f).

Discussion

Proteasomes are mislocalized to the cytosol in *sts1-2* [23], and results in the stabilization of multiple nuclear substrates [23, 30]. However, the degradation of cytosolic substrates is accelerated in *sts1*-2, probably due to the increased availability of proteasomes [23]. We also showed that when proteasomes are mislocalized in *srp1-49* [28], substrates are similarly stabilized. In both *sts1-2* and *srp1-49* substrates accumulate in the nucleus. Since nuclear import is unaffected in these mutants we conclude that proteasomes do not enter the nucleus at appreciable levels. In this report we show that the substrate trafficking protein Rad23 accumulates to high levels in the nucleus in *sts1-2*. Moreover, Rad23 is bound to higher levels of polyUb proteins in the nucleus. Based on these results we propose that polyUb substrates are not transported out of the nucleus if proteasomes are not available at the nuclear periphery. In agreement with this idea we note that proteasomes are located in the nuclear pore complex [13, 14], and are highly enriched in fractionated preparations of the nuclear envelope [9].

Nucleo-cytoplasmic trafficking is regulated by a number of factors, including an evolutionarily conserved GTPase activating enzyme (Rna1) that promotes the recycling of Ran protein [50, 51]. Mutation in *RNA1* (*rna1-1*) disrupts this mechanism and causes a failure in mRNA export [52], which results in the termination of protein synthesis. In *rna1-1* Rad23 is stable but accumulates in the cytosol, which we speculate is due to the failure to reimport it into the nucleus. Therefore, the stabilization of nuclear substrates in *rna1-1* can be attributed, at least in part, to the inability of shuttle factors to reenter the nucleus. Previous studies have shown that nuclear proteins can be detected in the cytosol in punctate aggregates in *rna1-1*. We made a similar observation with both GFP-Ho (Fig. 6a) and Matα2-GFP (Fig. 7b). However, these substrates do not remain bound to cytosolic Rad23 (Fig. 8d).

Rad23 interacted efficiently with polyUb species in *sts1-2* (Fig. 1d), suggesting that the import of ubiquitin and its conjugation to substrates occurred efficiently. In contrast, inhibition of nucleocytoplasmic trafficking in *rna1-1* could prevent ubiquitin import and block protein turnover by hindering polyUb chain assembly. We therefore investigated the localization of ubiquitin in mutants that affected proteasome, Rad23, and substrate localization. GFP-Ub was broadly distirbuted in the cytosol and nucleus in *STS1*, at both 21°C and 37°C. In contrast, GFP-Ub accumulated in the nucleus in *sts1-2*, similar to the high nuclear levels of both Rad23, and proteolytic substrates. In contrast, a ubiquitin mutant that cannot be conjugated to substrates (RFP-ub$^{\Delta RGG}$), remained cytosolic. We speculate that the conjugation of Ub to substrates can explain its nuclear accumulation in *sts1-2*. Similarly, ubiquitin, substrates, and Rad23 accumulated in the nucleus in *srp1-49* (data not shown). It is significant that proteasomes are efficiently localized to the nucleus in *rna1-1* (L. Chen; unpublished studies). However, nuclear substrates and ubiquitin are both present in the cytosol. One interpretation of these results is that in *rna1-1* shuttle-factors (Rad23) are unable to guide nuclear substrates to proteasomes in the nuclear pore complex [13, 14]. An important observation is that E2 and E3 ubiquitin-

conjugating enzymes were readily available in the nucleus in *sts1-2* and *rna1-1*, because the polyubiquitylation of nuclear proteins was unaffected.

Both Ddi1 and Rad23 shuttle-factors can bind Ho-endonuclease. However, we observed that Rad23 formed a much stronger interaction than Ddi1. Rad23/Ho-endo interaction was tested using different epitopes on both Rad23 (FLAG; GST), and Ho-endo (HA; GFP). In contrast, no interaction was detected with Dsk2 (Fig. 4), underscoring significant substrate selectivity among shuttle factors. In contrast to our findings Kaplun *et al* reported that Ddi1 formed a strong interaction with Ho-endo [46]. These experimental disparities could be due to different methodological approaches. Specifically, studies described in Kaplun at al used Ho-LacZ, a tetramer larger than 700 MDa, which could sterically affect binding Rad23 and Ddi1. Moreover, in these previous studies lysates that contained Ho-LacZ were combined with lysates containing either Rad23 or Ddi1, and the binding was tested *in vitro*. Our studies differ in that Ho-endo was fused to a small epitope (GFP; HA), and co-expressed in yeast cells with various shuttle-factors. The UbL domains in yeast shuttle factors bind the Rpn1 subunit in the proteasome [53]. However, we found that Rad23 formed a very robust interaction with the proteasome (Fig. 4a), whereas both Ddi1 and Dsk2 formed very weak interactions. These differential protein-binding properties are consistent with a report showing that a protein domain from Ufo1 containing a UIM motif interacted with all three shuttle-factors (Rad23; Ddi1; Dsk2). However, full-length Ufo1 only bound Ddi1 [54]. Although shuttle-factors may perform broadly overlapping roles, our studies suggest that Ho-endo interaction with shuttle-factors is variable, which could have functionally different effects. It remains to be determined if Ddi1 can form a stronger interaction with Ho-endo and the proteasome in the absence of Rad23.

Mutations in Rna1 can cause cytosolic accumulation of nuclear proteins, frequently in the form of protein aggregates [47]. Similarly, GFP-Ho and GFP-Matα2 were detected in one or more cytosolic aggregates in *rna1-1*, after extensive incubation (~ 90 min) at the restrictive

temperature. We and others found that Ho-endo degradation requires export from the nucleus [1]. However, these nuclear substrates (such as GFP-Ho; GFP-Matα2) were detected in cytosolic aggregates in *rna1-1*, suggesting that they are not targeted to the proteasome (which remained efficiently nuclear localized). The action of Rna1 on the Ran protein results in the conversion of GTP to GDP, which promotes the release of nuclear proteins from the export complex. It is possible that a failure to convert Ran^{GTP} to Ran^{GDP} results in a persistent interaction with exported nuclear proteins, such as GFP-Ho and GFP-Matα2. This association might preclude substrate delivery to the proteasome. We propose that the failure to traffic nuclear substrates to the proteasome underlies the proteolytic defect in *rna1-1*.

Materials and Methods

Yeast strains and plasmids

Yeast transformations were performed using standard techniques to yield strains described in Table 1. The P_{GAL}-GFP-Ho plasmid was a gift from Dr. D Raveh (Ben Gurion University, Israel). The HO gene was amplified by polymerase chain reaction (PCR) using a 5' *Eco*R1 and 3' *Kpn*1 restriction sites. The following oligonucleotides were designed: 5'-GCCGGAATTCATGCTTTCTGAAAACACGAC TATTCTGATG-3' and 5'-ATATAGGTACCTGCAGATGCGCGCACCTGCGTTGTTACCACA-3'. The PCR product was cloned into LEP1004 (Table 2) to generate (EOP83), which was maintained in DH5α (Table 2). To generate P_{GAL}-Ho-HA plasmid EOP83 was digested with *Eco*R1 and *Xba*1 and a DNA fragment containing Ho-2xHA was ligated into LEP591 to yield EOP85 (Table 2). Other relevant constructs are described in Table 2. Expression of genes from the *CUP1* promoter required growth in medium containing 100 μM $CuSO_4$. For genes expressed from the *GAL1* promoter yeast cultures were pre-grown at 30°C in medium containing 2% raffinose, and then induced following transfer to galactose-containing medium. Temperature sensitive yeast mutants were grown at the permissive temperature (21°C), before transfer to the non-permissive temperature (37°C). Protein turnover was determined by immunoblotting following the addition cycloheximide (200 μg/ml; Sigma).

Microscopy

Ten milliliters of yeast cultures were grown in selective media as described above. Cells were spotted on Poly-Prep slides (Sigma), and stained with Hoechst 33342 (Sigma). Following 30 min incubation at 21°C, the cells were washed three times with distilled water (3X), and

examined with a Zeiss Imager M1 microscope. Yeast cell were imaged live and after fixation in paraformaldehyde, using the same setting and exposure times.

Cell fixation

Exponential phase yeast cells were fixed in 4% paraformaldehyde solution (15 min at 21°C). Cells were washed with 500 µl KPO_4/sorbitol buffer before examination by microscopy.

Western blotting

Yeast pellets were suspended in Buffer A (150 mM NaCl, 1% Triton X-100, 50 mM Tris pH 7.5, 5 mM EDTA), containing a protease inhibitor cocktail. Following addition of acid washed glass beads (Sigma) the cells were lysed by disruption using Thermo-Savant Fast Prep FP100. Protein concentration was determined using the Bradford reagent (Bio-Rad), and equal amount of protein lysate was separated in a 12 % polyacrylamide SDS-Tricine gel. Lysates were incubated with anti-Flag (Sigma) or anti-HA (Roche Applied Science) affinity matrix to purify the relevant tagged proteins. Immunoprecipitates were washed with Buffer A, resolved in a 12% polyacrylamide SDS-Tricine gel, and transferred to nitrocellulose.

Antibodies and Reagents

Antibodies against yeast Rpn10 and Rpn12 were kindly provided by Dr. D. Skowyra (St. Louis University). Monoclonal antibodies against HA-HRP were obtained from Roche Applied Science. Monoclonal antibodies against ubiquitin, GFP, myc and Flag-HRP were purchased from Sigma. Polyclonal anti-Ubc4 antibodies were generated by the laboratory. Enhanced chemiluminescent reagents (ECL) were obtained from PerkinElmer Life Science, and analysis was performed using GelLogic 1500 imaging system and software (Eastman Kodak Co.).

Supplementary Material

Figure providing additional information related to Fig. 3 is included as supplementary data.

Acknowledgments

This work was supported by grants to K.M. from the National Institutes of Health (CA083875 and GM104968). E.O. was supported by pre-doctoral fellowships from the National Science Foundation DGE-1842213 and NIH T32-GM008339. We thank Dr. Marc Gartenberg for advice and extensive discussion, and the use of their fluorescence microscope, and Namariq Al-Saadi for generating the plasmid encoding Ho-HA.

References

[1] Kaplun L, Ivantsiv Y, Bakhrat A, Raveh D. DNA damage response-mediated degradation of Ho endonuclease via the ubiquitin system involves its nuclear export. J Biol Chem. 2003;278:48727-34.

[2] Blondel M, Galan JM, Chi Y, Lafourcade C, Longaretti C, Deshaies RJ, et al. Nuclear-specific degradation of Far1 is controlled by the localization of the F-box protein Cdc4. EMBO J. 2000;19:6085-97.

[3] Park SH, Kukushkin Y, Gupta R, Chen T, Konagai A, Hipp MS, et al. PolyQ proteins interfere with nuclear degradation of cytosolic proteins by sequestering the Sis1p chaperone. Cell. 2013;154:134-45.

[4] Prasad R, Kawaguchi S, Ng DT. A nucleus-based quality control mechanism for cytosolic proteins. Mol Biol Cell. 2010;21:2117-27.

[5] Rosenbaum JC, Fredrickson EK, Oeser ML, Garrett-Engele CM, Locke MN, Richardson LA, et al. Disorder targets misorder in nuclear quality control degradation: a disordered ubiquitin ligase directly recognizes its misfolded substrates. Mol Cell. 2011;41:93-106.

[6] Guo X, Engel JL, Xiao J, Tagliabracci VS, Wang X, Huang L, et al. UBLCP1 is a 26S proteasome phosphatase that regulates nuclear proteasome activity. Proc Natl Acad Sci U S A. 2011;108:18649-54.

[7] Burcoglu J, Zhao L, Enenkel C. Nuclear Import of Yeast Proteasomes. Cells. 2015;4:387-405.

[8] Dang FW, Chen L, Madura K. Catalytically Active Proteasomes Function Predominantly in the Cytosol. J Biol Chem. 2016;291:18765-77.

[9] Enenkel C, Lehmann A, Kloetzel PM. Subcellular distribution of proteasomes implicates a major location of protein degradation in the nuclear envelope-ER network in yeast. EMBO J. 1998;17:6144-54.

[10] Fabunmi RP, Wigley WC, Thomas PJ, DeMartino GN. Activity and regulation of the centrosome-associated proteasome. J Biol Chem. 2000;275:409-13.

[11] Wigley WC, Fabunmi RP, Lee MG, Marino CR, Muallem S, DeMartino GN, et al. Dynamic association of proteasomal machinery with the centrosome. J Cell Biol. 1999;145:481-90.

[12] Hedhli N, Wang L, Wang Q, Rashed E, Tian Y, Sui X, et al. Proteasome activation during cardiac hypertrophy by the chaperone H11 Kinase/Hsp22. Cardiovasc Res. 2008;77:497-505.

[13] Albert S, Schaffer M, Beck F, Mosalaganti S, Asano S, Thomas HF, et al. Proteasomes tether to two distinct sites at the nuclear pore complex. Proc Natl Acad Sci U S A. 2017;114:13726-31.

[14] Niepel M, Molloy KR, Williams R, Farr JC, Meinema AC, Vecchietti N, et al. The nuclear basket proteins Mlp1p and Mlp2p are part of a dynamic interactome including Esc1p and the proteasome. Mol Biol Cell. 2013;24:3920-38.

[15] Chen L, Madura K. Degradation of specific nuclear proteins occurs in the cytoplasm in Saccharomyces cerevisiae. Genetics. 2014;197:193-7.

[16] Freedman DA, Levine AJ. Nuclear export is required for degradation of endogenous p53 by MDM2 and human papillomavirus E6. Mol Cell Biol. 1998;18:7288-93.

[17] Wiechens N, Fagotto F. CRM1- and Ran-independent nuclear export of beta-catenin. Curr Biol. 2001;11:18-27.

[18] Bakhrat A, Baranes-Bachar K, Reshef D, Voloshin O, Krichevsky O, Raveh D. Nuclear export of Ho endonuclease of yeast via Msn5. Curr Genet. 2008;54:271-81.

[19] Rockel TD, Stuhlmann D, von Mikecz A. Proteasomes degrade proteins in focal subdomains of the human cell nucleus. J Cell Sci. 2005;118:5231-42.

[20] Kodadek T. No Splicing, no dicing: non-proteolytic roles of the ubiquitin-proteasome system in transcription. J Biol Chem. 2010;285:2221-6.

[21] Russell SJ, Johnston SA. Evidence that proteolysis of Gal4 cannot explain the transcriptional effects of proteasome ATPase mutations. J Biol Chem. 2001;276:9825-31.

[22] Russell SJ, Reed SH, Huang W, Friedberg EC, Johnston SA. The 19S regulatory complex of the proteasome functions independently of proteolysis in nucleotide excision repair. Mol Cell. 1999;3:687-95.

[23] Chen L, Romero L, Chuang SM, Tournier V, Joshi KK, Lee JA, et al. Sts1 plays a key role in targeting proteasomes to the nucleus. J Biol Chem. 2011;286:3104-18.

[24] Enenkel C, Lehmann A, Kloetzel PM. GFP-labelling of 26S proteasomes in living yeast: insight into proteasomal functions at the nuclear envelope/rough ER. Mol Biol Rep. 1999;26:131-5.

[25] Tatebe H, Yanagida M. Cut8, essential for anaphase, controls localization of 26S proteasome, facilitating destruction of cyclin and Cut2. Curr Biol. 2000;10:1329-38.

[26] Yano R, Oakes ML, Tabb MM, Nomura M. Yeast Srp1p has homology to armadillo/plakoglobin/beta-catenin and participates in apparently multiple nuclear functions including the maintenance of the nucleolar structure. Proc Natl Acad Sci U S A. 1994;91:6880-4.

[27] Conti E, Uy M, Leighton L, Blobel G, Kuriyan J. Crystallographic analysis of the recognition of a nuclear localization signal by the nuclear import factor karyopherin alpha. Cell. 1998;94:193-204.

[28] Chen L, Madura K. Yeast importin-alpha (Srp1) performs distinct roles in the import of nuclear proteins and in targeting proteasomes to the nucleus. J Biol Chem. 2014;289:32339-52.

[29] Takeda K, Yanagida M. Regulation of nuclear proteasome by Rhp6/Ubc2 through ubiquitination and destruction of the sensor and anchor Cut8. Cell. 2005;122:393-405.

[30] Romero-Perez L, Chen L, Lambertson D, Madura K. Sts1 can overcome the loss of Rad23 and Rpn10 and represents a novel regulator of the ubiquitin/proteasome pathway. J Biol Chem. 2007;282:35574-82.

[31] Zang ZJ, Gunaratnam L, Cheong JK, Lai LY, Hsiao LL, O'Leary E, et al. Identification of PP2A as a novel interactor and regulator of TRIP-Br1. Cell Signal. 2009;21:34-42.

[32] Lahaye F, Lespinasse F, Staccini P, Palin L, Paquis-Flucklinger V, Santucci-Darmanin S. hMSH5 is a nucleocytoplasmic shuttling protein whose stability depends on its subcellular localization. Nucleic Acids Res. 2010;38:3655-71.

[33] Ruggiano A, Foresti O, Carvalho P. Quality control: ER-associated degradation: protein quality control and beyond. J Cell Biol. 2014;204:869-79.

[34] Hood JK, Hwang WW, Silver PA. The Saccharomyces cerevisiae cyclin Clb2p is targeted to multiple subcellular locations by cis- and trans-acting determinants. J Cell Sci. 2001;114:589-97.

[35] Chen L, Madura K. Rad23 promotes the targeting of proteolytic substrates to the proteasome. Mol Cell Biol. 2002;22:4902-13.

[36] Chen L, Shinde U, Ortolan TG, Madura K. Ubiquitin-associated (UBA) domains in Rad23 bind ubiquitin and promote inhibition of multi-ubiquitin chain assembly. EMBO Rep. 2001;2:933-8.

[37] Schauber C, Chen L, Tongaonkar P, Vega I, Lambertson D, Potts W, et al. Rad23 links DNA repair to the ubiquitin/proteasome pathway. Nature. 1998;391:715-8.

[38] Watkins JF, Sung P, Prakash L, Prakash S. The Saccharomyces cerevisiae DNA repair gene RAD23 encodes a nuclear protein containing a ubiquitin-like domain required for biological function. Mol Cell Biol. 1993;13:7757-65.

[39] Bertolaet BL, Clarke DJ, Wolff M, Watson MH, Henze M, Divita G, et al. UBA domains mediate protein-protein interactions between two DNA damage-inducible proteins. J Mol Biol. 2001;313:955-63.

[40] Raasi S, Pickart CM. Rad23 ubiquitin-associated domains (UBA) inhibit 26 S proteasome-catalyzed proteolysis by sequestering lysine 48-linked polyubiquitin chains. J Biol Chem. 2003;278:8951-9.

[41] Chen L, Madura K. Evidence for distinct functions for human DNA repair factors hHR23A and hHR23B. FEBS Lett. 2006;580:3401-8.

[42] Sugasawa K, Ng JM, Masutani C, Maekawa T, Uchida A, van der Spek PJ, et al. Two human homologs of Rad23 are functionally interchangeable in complex formation and stimulation of XPC repair activity. Mol Cell Biol. 1997;17:6924-31.

[43] Neville M, Rosbash M. The NES-Crm1p export pathway is not a major mRNA export route in Saccharomyces cerevisiae. EMBO J. 1999;18:3746-56.

[44] Ortolan TG, Chen L, Tongaonkar P, Madura K. Rad23 stabilizes Rad4 from degradation by the Ub/proteasome pathway. Nucleic Acids Res. 2004;32:6490-500.

[45] Verma R, McDonald H, Yates JR, 3rd, Deshaies RJ. Selective degradation of ubiquitinated Sic1 by purified 26S proteasome yields active S phase cyclin-Cdk. Mol Cell. 2001;8:439-48.

[46] Kaplun L, Tzirkin R, Bakhrat A, Shabek N, Ivantsiv Y, Raveh D. The DNA damage-inducible UbL-UbA protein Ddi1 participates in Mec1-mediated degradation of Ho endonuclease. Mol Cell Biol. 2005;25:5355-62.

[47] Schlenstedt G, Saavedra C, Loeb JD, Cole CN, Silver PA. The GTP-bound form of the yeast Ran/TC4 homologue blocks nuclear protein import and appearance of poly(A)+ RNA in the cytoplasm. Proc Natl Acad Sci U S A. 1995;92:225-9.

[48] Maurer P, Redd M, Solsbacher J, Bischoff FR, Greiner M, Podtelejnikov AV, et al. The nuclear export receptor Xpo1p forms distinct complexes with NES transport substrates and the yeast Ran binding protein 1 (Yrb1p). Mol Biol Cell. 2001;12:539-49.

[49] Chen P, Johnson P, Sommer T, Jentsch S, Hochstrasser M. Multiple ubiquitin-conjugating enzymes participate in the in vivo degradation of the yeast MAT alpha 2 repressor. Cell. 1993;74:357-69.

[50] Corbett AH, Koepp DM, Schlenstedt G, Lee MS, Hopper AK, Silver PA. Rna1p, a Ran/TC4 GTPase activating protein, is required for nuclear import. J Cell Biol. 1995;130:1017-26.

[51] Ryan KJ, McCaffery JM, Wente SR. The Ran GTPase cycle is required for yeast nuclear pore complex assembly. J Cell Biol. 2003;160:1041-53.

[52] Hopper AK, Traglia HM, Dunst RW. The yeast RNA1 gene product necessary for RNA processing is located in the cytosol and apparently excluded from the nucleus. J Cell Biol. 1990;111:309-21.

[53] Elsasser S, Gali RR, Schwickart M, Larsen CN, Leggett DS, Muller B, et al. Proteasome subunit Rpn1 binds ubiquitin-like protein domains. Nat Cell Biol. 2002;4:725-30.

[54] Voloshin O, Bakhrat A, Herrmann S, Raveh D. Transfer of Ho endonuclease and Ufo1 to the proteasome by the UbL-UbA shuttle protein, Ddi1, analysed by complex formation in vitro. Plos One. 2012;7:e39210.

Tables

Table 1. *Saccharomyces cerevisiae* strains

Strain	Genotype	Source
NA10	*MAT***a** *leu2-3,112 trp1-1 ura3-1 his3-11,15 ade2-1 STS1*	F. Wyers
NA25	*MAT***a** *leu2-3,112 trp1-1 ura3-1 his3-11,15 ade2-1 sts1-2*	F. Wyers
FSY87	*MAT***a** *leu2-3,112 trp1-1 ura3-1 his3-11,15 ade2-1 rna1-1*	M. Roshbash

Table 2. Plasmids

Plasmid	Description		Source
LEP645	P_{CUP1}*-GFP-RAD23 URA3*	*CEN6*	This study
LEP52	P_{CUP1}*-FLAG-RAD23 LEU2*	*2μ*	This study
EOP34	P_{CUP1}*-FLAG-DDI1 LEU2*	*2μ*	This study
LEP155	P_{CUP1}*-FLAG-DSK2 LEU2*	*2μ*	This study
LEP97	P_{CUP1}*-FLAG-RPN10 LEU2*	*2μ*	This study
pYES2-GFP-Ho	P_{GAL1}*- GFP-HO URA3*	*2μ*	D. Raveh
Matα2-GFP	P_{CUP1}*-MATα2-GFP URA3*	*CEN*	U. Lenk
LEP778	P_{CUP1}*-MATα2-2HA LEU2*	*2μ*	This study
YCplac111	Empty vector *ARS LEU2*	*CEN4*	D. R. Gietz
EOP85	P_{GAL1}*-HO-2HA URA3*	*2μ*	This study
KEP443	P_{CUP1}*-myc-Ub TRP1*	*2μ*	This study
LEP846	P_{CUP1}*-GFP-Ub URA3*	*CEN6*	This study
LEP1008	P_{CUP1}*-RFP-ubΔRGG URA3*	*CEN6*	This study

FIGURE LEGENDS

Fig. 1: Rad23 interaction with polyubiquitylated proteins is increased in the nucleus. (a) GFP-Rad23 was expressed in wildtype yeast (*STS1*), and a mutant in which the proteasome is mislocalized to the cytosol (*sts1-2*) [23]. Cultures grown at the permissive (21°C) and non-permissive temperatures (37°C) were examined by microscopy. GFP-Rad23 is predominantly nuclear in *sts1-2* at 37°C. (b) (c) The stability of GFP-Rad23 was measured after the addition of cycloheximide to *STS1* and *sts1-2* cultures at 21°C (b) and 37°C (c). The levels of GFP-Rad23 and a proteasome subunit (Rpn10) are shown. (d) Flag-Rad23 was isolated from lysates prepared from *STS1* and *sts1-2*. (- and + indicate strains that lacked or contained FLAG-Rad23). An immunoblot containing total extract (lanes 6-11) was also reacted with anti-ubiquitin antibody. The amount of polyubiquitylated proteins co-purified with FLAG-Rad23 was similarly examined (lanes 1-5). The filters were also reacted with antibodies against FLAG and Rpn10. (e) The levels of polyubiquitylated proteins bound to FLAG-Rad23 (panel (d); lanes 2-5) were quantified. (These data are representative of four independent trials).

Fig. 2: Rad23 interaction with polyubiquitylated substrates is decreased in the cytosol**.** (a) GFP-Rad23 was expressed in *RNA1* and *rna1-1*, and cultures grown at either permissive (21°C) or non-permissive (37°C) temperatures were examined by microscopy. (b) (c) The stability of FLAG-Rad23 was tested in *RNA1* and *rna1-1* at 21°C and 37°C, following the addition of cycloheximide. The levels of Rpn10 are also shown as a loading control. (d) *RNA1* and *rna1-1* were grown at 21°C and 37°C and the level of polyubiquitylated proteins bound to Flag-Rad23 was tested. The filter was also incubated with antibodies against FLAG and Rpn10. Lanes 1, 4, 7 and 11 are extracts from cells that did not contain FLAG-Rad23 (-). (e) The level

of polyUb proteins isolated with FLAG-Rad23 (panel (d); lanes 2, 3, 5, and 6) was quantified by densitometry. These results are representative of four independent trials.

Fig. 3: Ubiquitin (GFP-Ub) accumulates in the nucleus in *sts1-2*. Based on the severe mislocalization of the proteasome in *sts1-2* [23], and nuclear accumulation of Rad23, we examined the localization of ubiquitin. (a) GFP-Ub was uniformly distributed in *STS1* at 37°C, but accumulated in the nucleus in *sts1-2*. Nup49-RFP was imaged to define the nuclear periphery. Control studies at 21°C (see Supplemental Results) showed no difference between *STS1* and *sts1-2*. (b) GFP-Ub was expressed in *rna1-1* and was detected primarily in the cytosol. (c) A ubiquitin mutant that cannot be conjugated ($ub^{\Delta RGG}$) is cytosolic in both *sts1-2*, and *rna1-1* (d).

Fig. 4: Rad23 is a major shuttle-factor for Ho endonuclease**.** (a) Wildtype cells expressing GFP-Ho endonuclease were co-transformed with constructs expressing different polyubiquitin chain binding proteins. The interaction between GFP-Ho and shuttle-factors FLAG-Rad23, FLAG-Ddi1, and FLAG-Dsk2, as well as a proteasome receptor FLAG-Rpn10 was investigated. Because the expression of GFP-Ho was regulated by the galactose-inducible *GAL1* promoter cultures were first grown in raffinose and then transferred to galactose medium. Protein extracts were prepared and resolved in a 12% SDS-polyacrylamide gel, and then transferred to nitrocellulose. FLAG-tagged proteins were purified and the bound proteins detected by immunoblotting to detect GFP, FLAG, Rpn12, and ubiquitin (not shown). (b) Total lysates were examined to gauge the expression level of the FLAG-tagged proteins and GFP-Ho. (c) Endonuclease Ho-HA was co-expressed with myc-ubiquitin in wildtype yeast. Cultures were grown in raffinose medium and then diluted into galactose-containing selective medium. Cells

were harvested after 2 hrs, and protein extracts were incubated with anti-HA antibodies. The level of myc-polyubiquitylated Ho-HA was also tested by immunoblotting (anti-myc).

Fig. 5: Ho-endonuclease accumulates in the nucleus in *sts1-2*. (a) GFP-Ho was expressed in *STS1* and *sts1-2* and the cells were examined at 23°C (left panel). Yeast cells were transferred to 37°C and GFP-Ho localization was re-examined (right panel). Unfixed cells were stained with Hoechst 33342 for 30 min. (b, c) The turnover of GFP-HO was tested in *STS1* and *sts1-2*, at both 21°C and 37°C. Cultures grown in raffinose medium were transferred to galactose-containing medium for 5 h. GFP-Ho synthesis was terminated following transfer to glucose-containing medium. Lysates were prepared at the intervals indicated and the levels of GFP-Ho and Rad23 were determined by immunoblotting. Rpn10 served as a loading control. (d) (e) Quantification of the results in panels (b) and (c).

Fig. 6: Ho-endonuclease is stabilized in *rna1-1*. (a) The sub-cellular localization of GFP-Ho was examined in *RNA1* and *rna1-1* at 21°C (left panel). The cultures were transferred to 37°C and GFP-Ho localization was re-examined (right panel). Punctate cytosolic aggregates of GFP-Ho were detected in *rna1-1*. (b, c) GFP-Ho stability was measured in *RNA1* and *rna1-1* at 21°C and 37°C. Yeast cultures were grown in galactose-containing medium to induce expression of GFP-Ho, and after 4 h glucose was added to block further expression of GFP-Ho. Protein lysates were prepared at the times indicated and immunoblots were reacted with antibody against GFP and Rpn10. (d) (e) GFP-Ho levels shown in panel (b) and (c) were quantified by densitometry.

Fig. 7: Matα2 is stabilized in *rna1-1*. (a) GFP-Matα2 was expressed in wildtype and *sts1-2* and its localization was examined at 21°C and 37°C. (b) GFP-Matα2 was expressed in *RNA1* and *rna1-1* at 21°C, and then transferred to pre-warmed medium at 37°C. The nuclear level of GFP-Matα2 was unchanged in *RNA1*. However, GFP-Matα2 was depleted from the nucleus in *rna1-1*, and was detected in cytosolic aggregates (see 90 min). (c) Protein lysates were prepared from cultures described in panel (b) at 21°C, and after 90 min incubation at 37°C. We examined GFP-Matα2 in the soluble (S) and insoluble (P) fractions. Ubc4 levels serves as a cytosolic loading control. (d) The same filter was stained with Ponceau S to examine protein loading. Lower protein levels are lower in *rna1-1* at both 21°C and 37°C (d), although the amount of GFP-Matα2 in the insoluble fraction was noticeably increased in the mutant (c; lane 8).

Fig. 8: The subcellular location of Rad23 affects its binding to Ho endonuclease. (a) Protein extracts were prepared from *STS1* and *sts1-2* that co-expressed FLAG-Rad23 and GFP-Ho. We expressed GFP-Ho at either 21°C or 37°C using the galactose-inducible *GAL1* promoter. Extracts were incubated with anti-FLAG agarose to isolate FLAG-Rad23. A nitrocellulose filter was treated with antibodies against GFP, FLAG, and Rpn10. A lysate prepared from a strain expressing GFP-Ho, but lacking FLAG-Rad23, is shown (lane 1). (b) Total protein lysates were separated in a 12% SDS-polyacrylamide gel, and characterized as described in (a). The expression levels of GFP-Ho, FLAG-Rad23, and Rpn10 are shown. (c) The results in panel (a) were quantified by densitometry, and the relative amount of GFP-Ho that was co-purified with FLAG-Rad23 is shown. The results were adjusted to the levels of FLAG-Rad23 detected. (d) GFP-Ho was also expressed in *RNA1* and *rna1-1* and cultured at 21°C in selective media containing 2% raffinose. Exponential-phase cells were diluted into selective media containing 2% galactose, and incubated at either 21°C or 37°C for 1hr. Yeast cells were collected and protein extracts were characterized by immunoblotting using antibodies against GFP, FLAG,

and Rpn10. Lane 1 is a strain expressing GFP-Ho, but lacks FLAG-Rad23. (e) Total protein extracts from the same lysates were similarly examined. (f) The results in panel (d) were quantified by densitometry, and adjusted to the levels of FLAG-Rad23 that was immunoprecipitated.

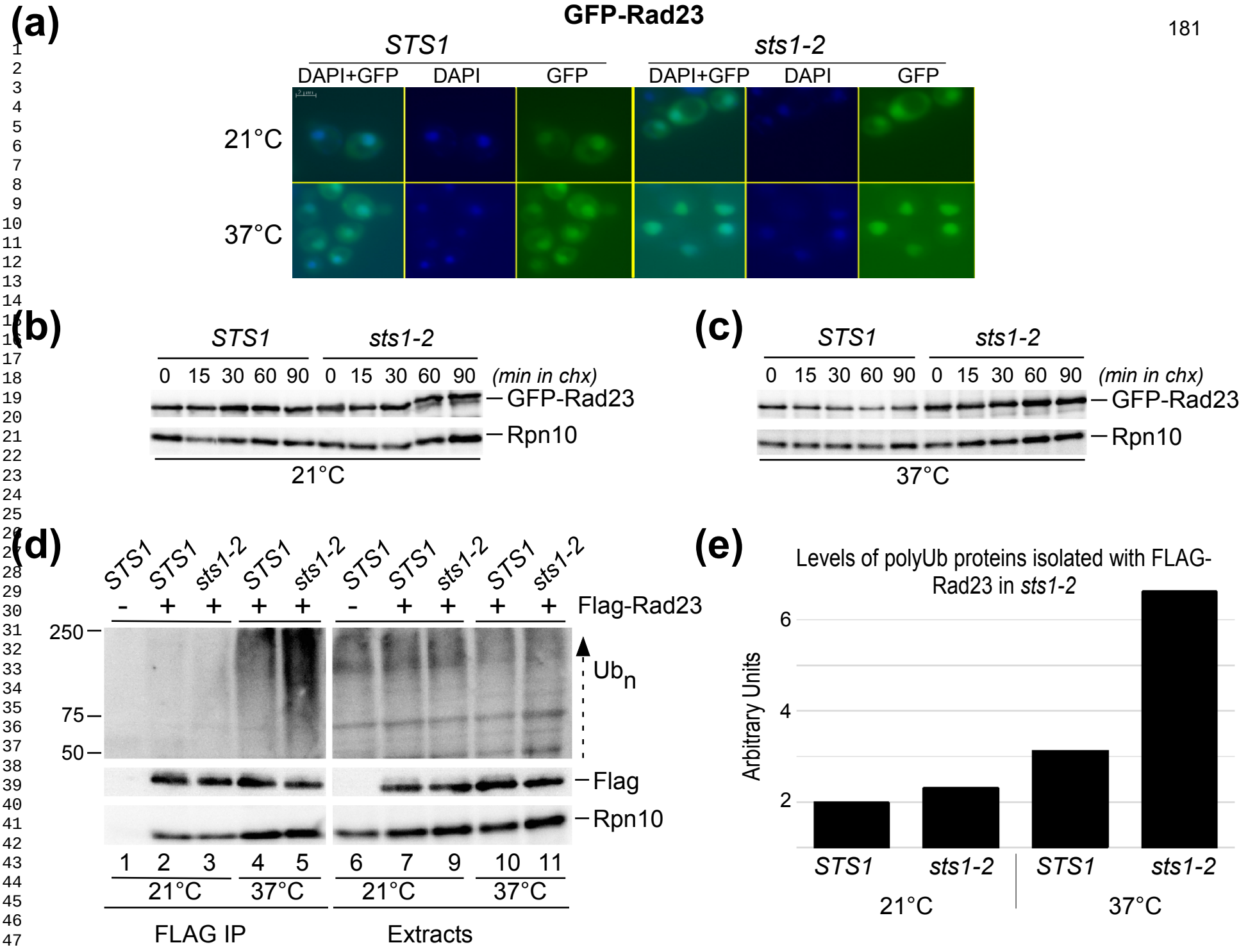
(a)
GFP-Rad23
STS1
sts1-2
DAPI+GFP
DAPI
GFP
DAPI+GFP
DAPI
GFP
21°C
37°C
(b)
STS1
sts1-2
0 15 30 60 90 0 15 30 60 90 (min in chx)
GFP-Rad23
Rpn10
21°C
(c)
STS1
sts1-2
0 15 30 60 90 0 15 30 60 90 (min in chx)
GFP-Rad23
Rpn10
37°C
(d)
STS1 STS1 sts1-2 STS1 sts1-2 STS1 STS1 sts1-2 STS1 sts1-2
- + + + + - + + + +
Flag-Rad23
250
75
50
Ub$_n$
Flag
Rpn10
1 2 3 4 5 6 7 9 10 11
21°C 37°C 21°C 37°C
FLAG IP
Extracts
(e)
Levels of polyUb proteins isolated with FLAG-Rad23 in sts1-2
Arbitrary Units
6
4
2
STS1 sts1-2 STS1 sts1-2
21°C 37°C

Figure 1

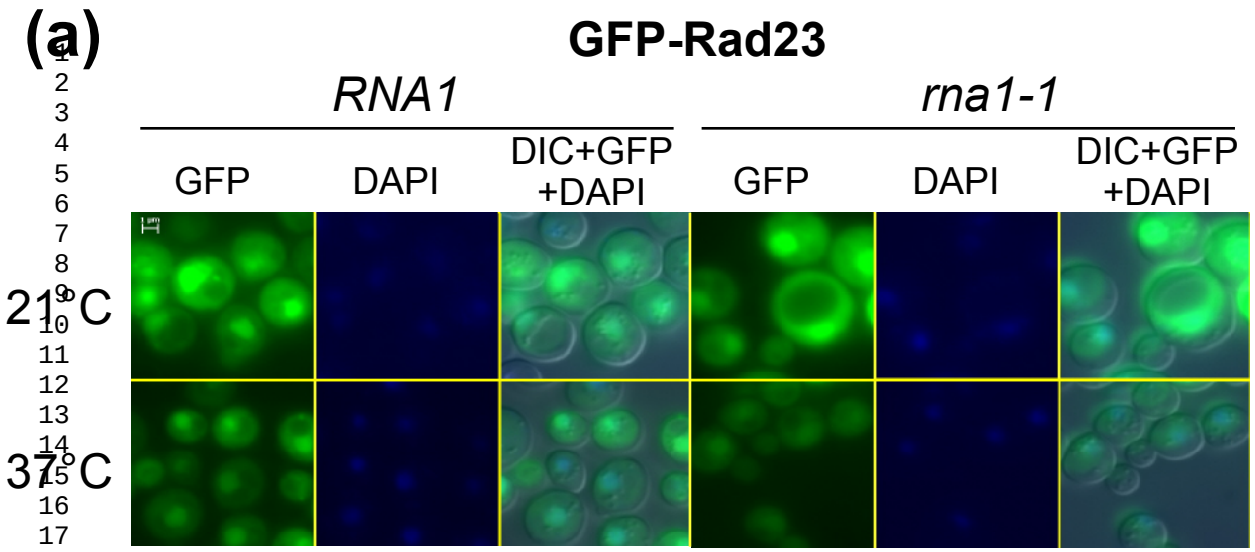
(a)
GFP-Rad23
RNA1
rna1-1
GFP
DAPI
DIC+GFP +DAPI
GFP
DAPI
DIC+GFP +DAPI
21°C
37°C

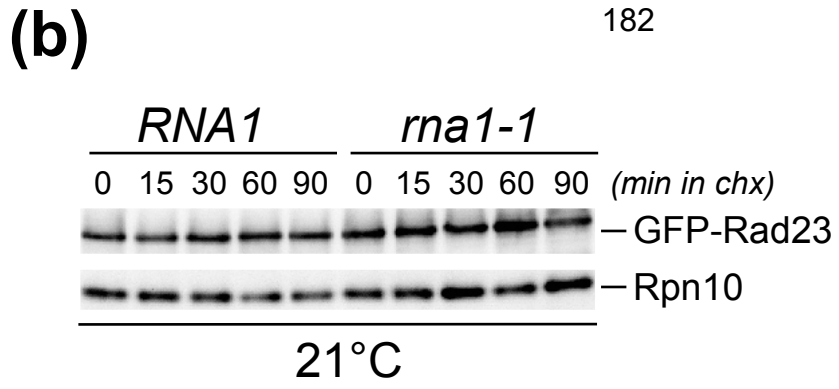
(b)
RNA1
rna1-1
0 15 30 60 90 0 15 30 60 90 (min in chx)
GFP-Rad23
Rpn10
21°C

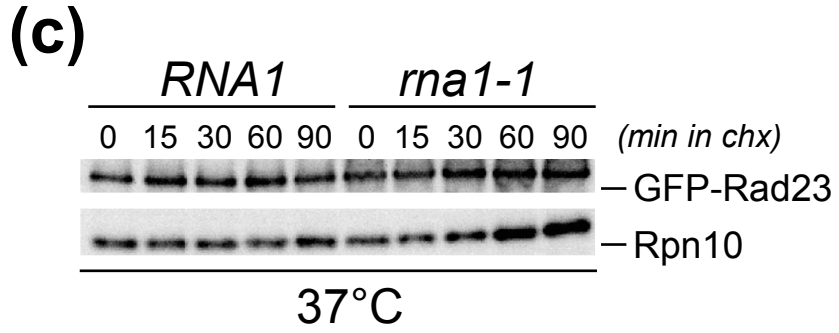
(c)
RNA1
rna1-1
0 15 30 60 90 0 15 30 60 90 (min in chx)
GFP-Rad23
Rpn10
37°C

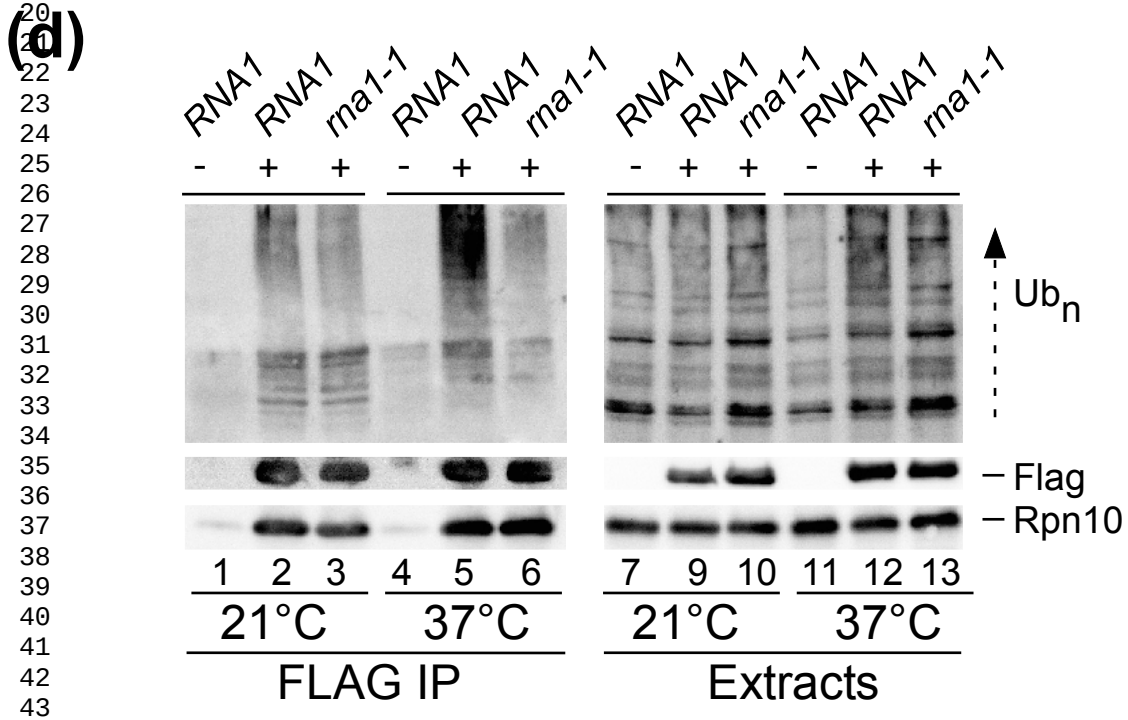
(d)
RNA1 RNA1 rna1-1 RNA1 RNA1 rna1-1 RNA1 RNA1 rna1-1 RNA1 RNA1 rna1-1
- + + - + + - + + - + +
Ub n
Flag
Rpn10
1 2 3 4 5 6 7 9 10 11 12 13
21°C 37°C 21°C 37°C
FLAG IP
Extracts

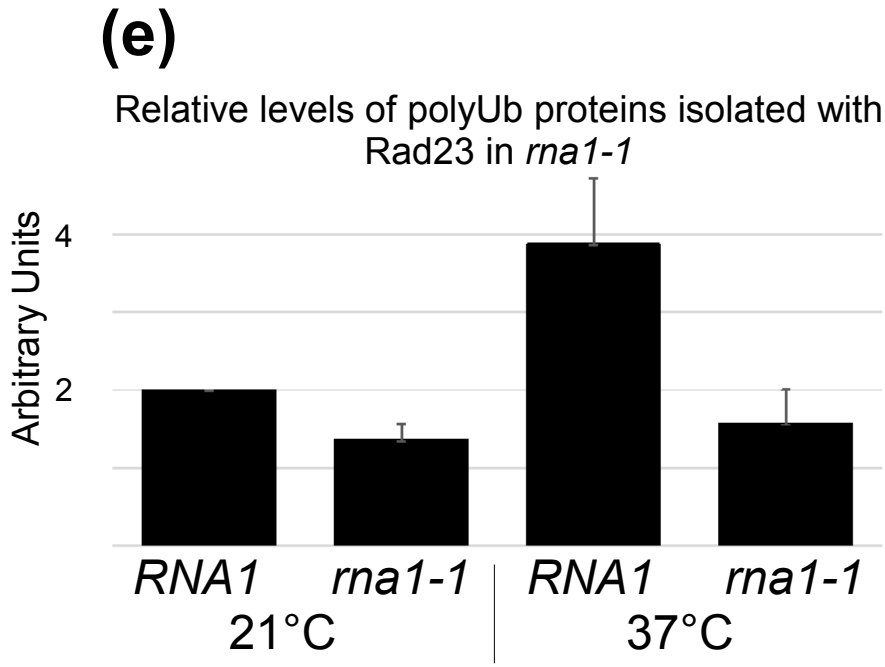
(e)
Relative levels of polyUb proteins isolated with Rad23 in rna1-1
Arbitrary Units
4
2
RNA1 rna1-1 RNA1 rna1-1
21°C 37°C

Figure 2

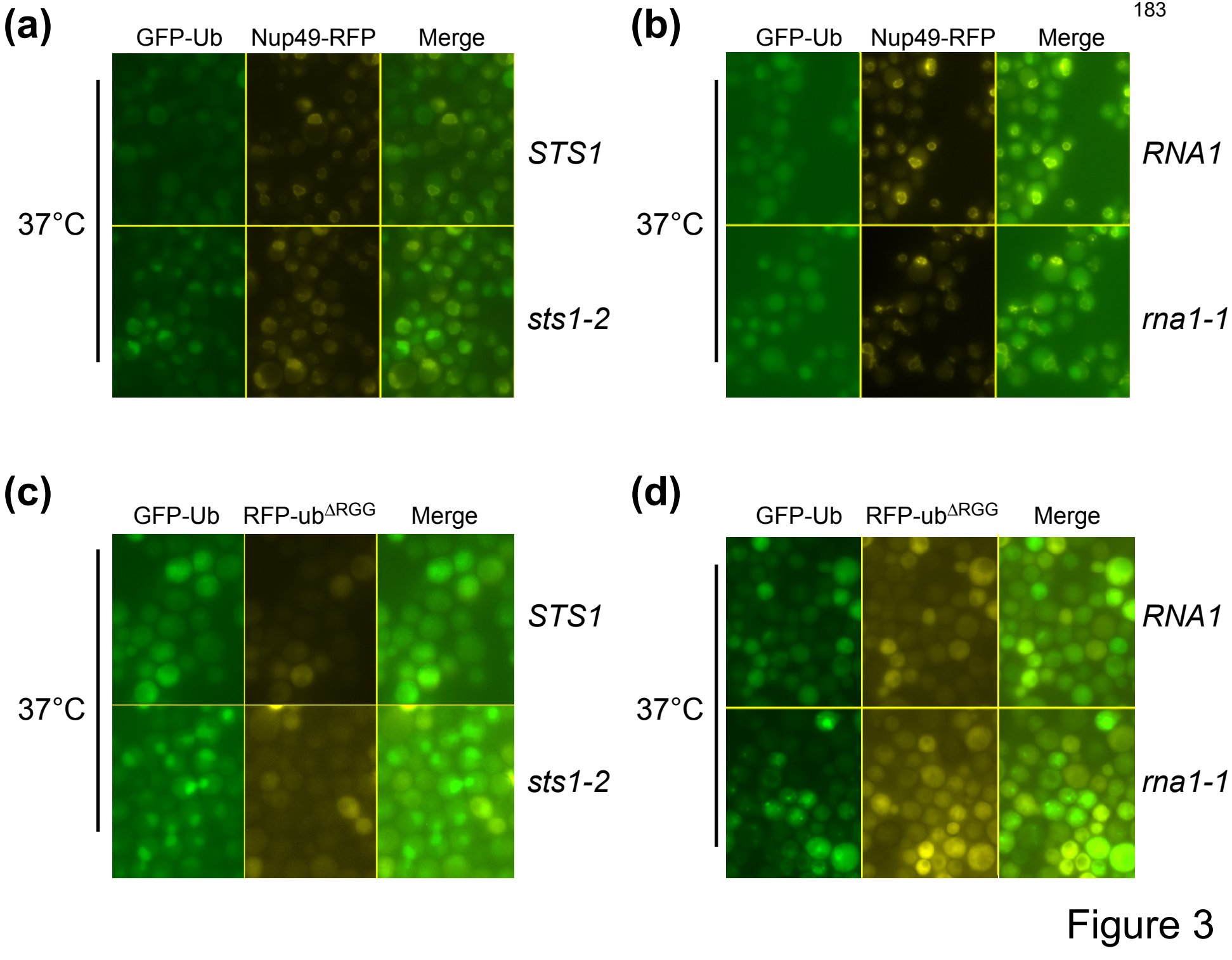
(a)
GFP-Ub
Nup49-RFP
Merge
37°C
STS1
sts1-2
(b)
GFP-Ub
Nup49-RFP
Merge
37°C
RNA1
rna1-1
(c)
GFP-Ub
RFP-ub^ΔRGG
Merge
37°C
STS1
sts1-2
(d)
GFP-Ub
RFP-ub^ΔRGG
Merge
37°C
RNA1
rna1-1

Figure 3

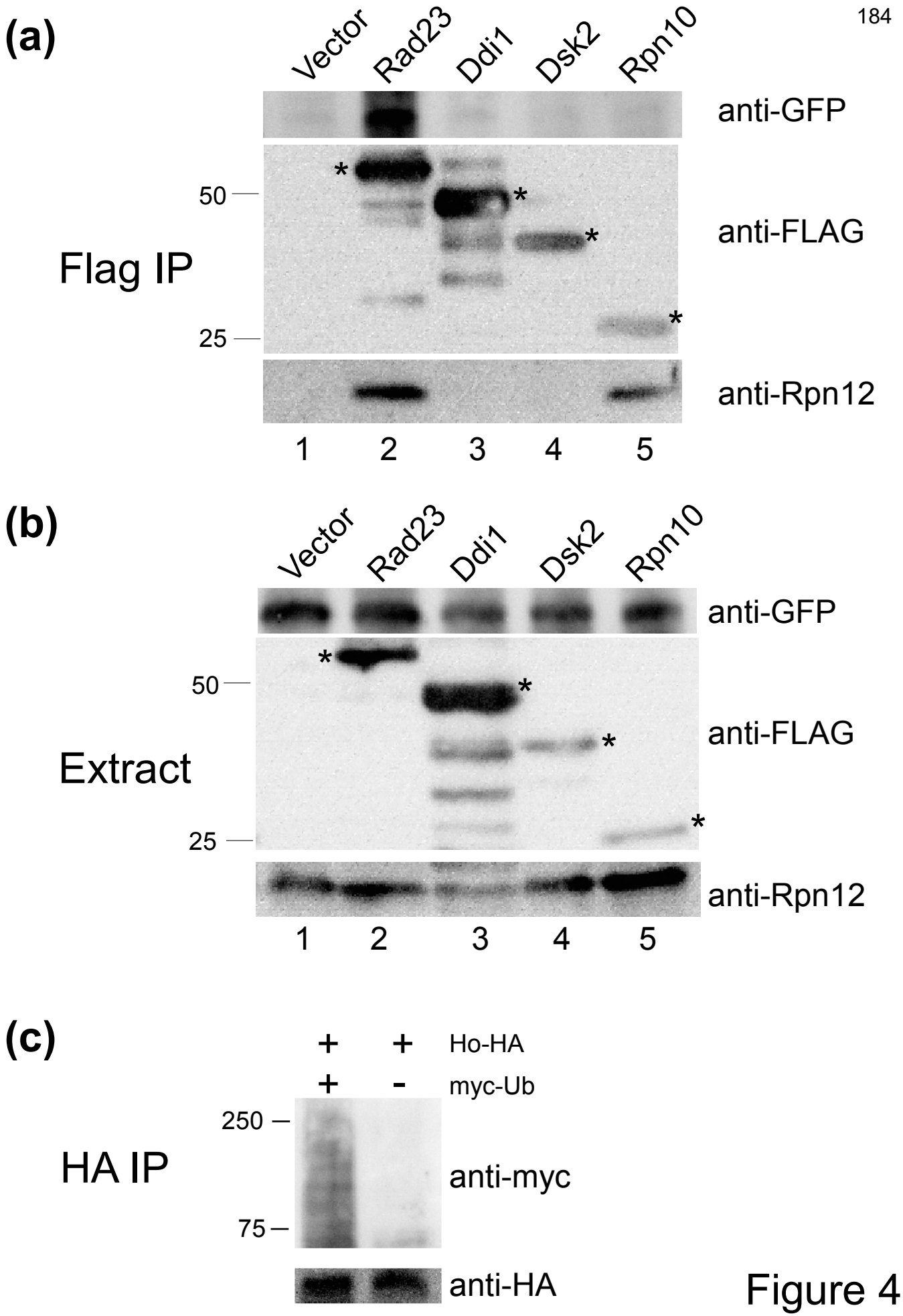
(a)
Vector
Rad23
Ddi1
Dsk2
Rpn10
anti-GFP
50
anti-FLAG
Flag IP
25
anti-Rpn12
1
2
3
4
5
(b)
Vector
Rad23
Ddi1
Dsk2
Rpn10
anti-GFP
50
anti-FLAG
Extract
25
anti-Rpn12
1
2
3
4
5
(c)
+
+
Ho-HA
+
-
myc-Ub
250
HA IP
anti-myc
75
anti-HA

Figure 4

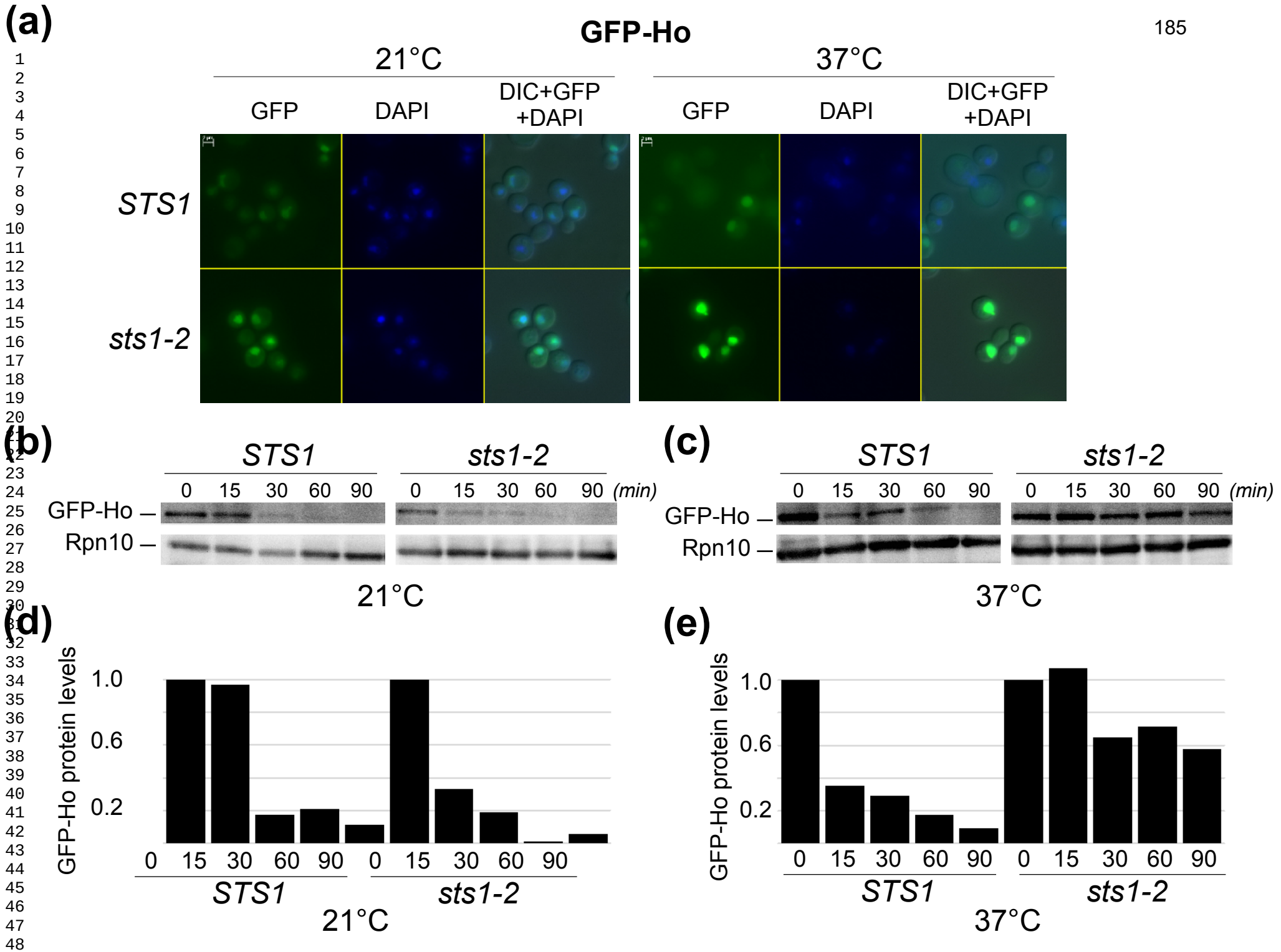
(a)
GFP-Ho
21°C
37°C
GFP
DAPI
DIC+GFP +DAPI
STS1
sts1-2
(b)
STS1
sts1-2
0 15 30 60 90 0 15 30 60 90 (min)
GFP-Ho
Rpn10
21°C
(c)
STS1
sts1-2
0 15 30 60 90 0 15 30 60 90 (min)
GFP-Ho
Rpn10
37°C
(d)
GFP-Ho protein levels
1.0
0.6
0.2
0 15 30 60 90 0 15 30 60 90
STS1
sts1-2
21°C
(e)
GFP-Ho protein levels
1.0
0.6
0.2
0 15 30 60 90 0 15 30 60 90
STS1
sts1-2
37°C

Figure 5

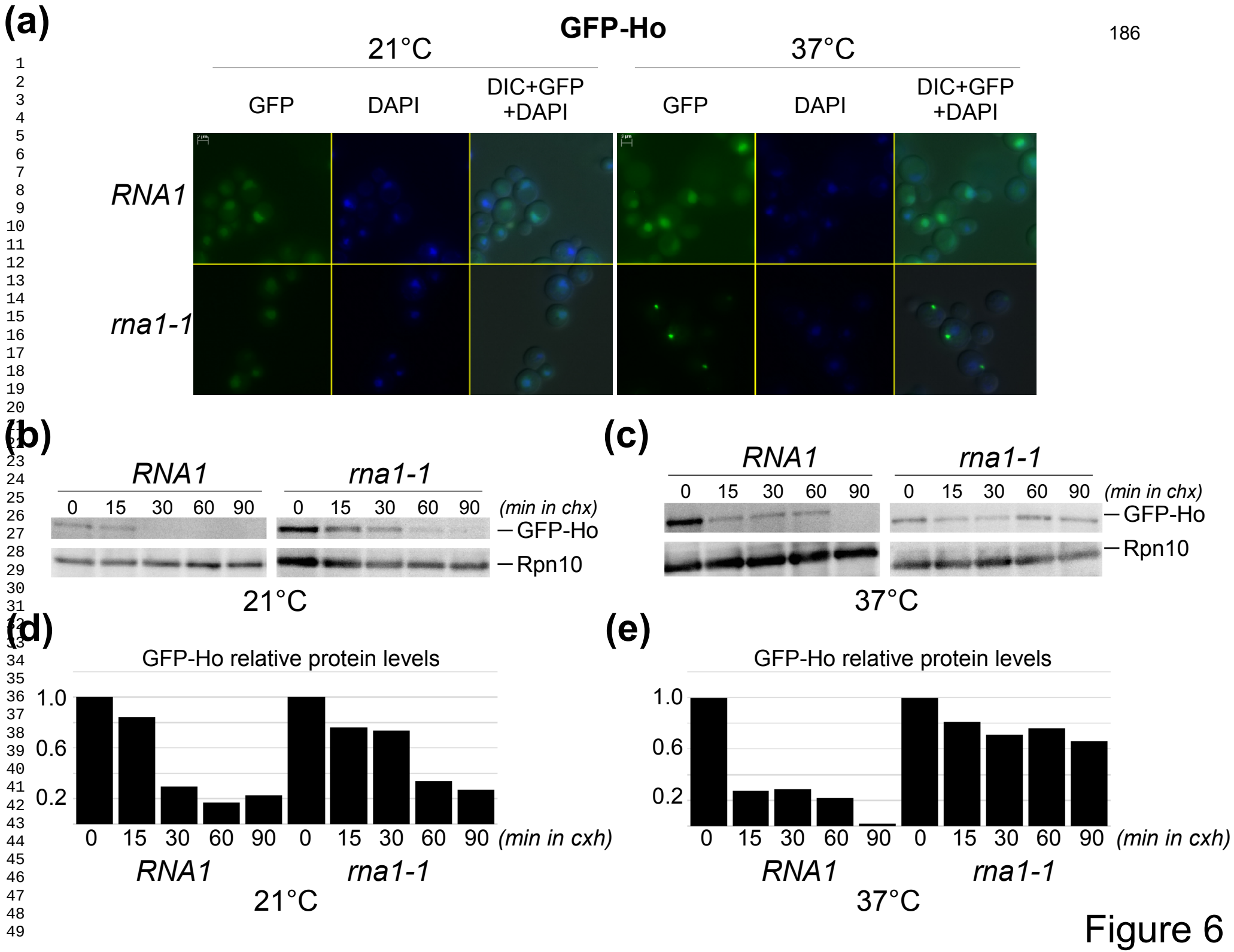
(a)
GFP-Ho
21°C
37°C
GFP
DAPI
DIC+GFP +DAPI
GFP
DAPI
DIC+GFP +DAPI
RNA1
rna1-1
(b)
RNA1
rna1-1
0 15 30 60 90
0 15 30 60 90
(min in chx)
GFP-Ho
Rpn10
21°C
(c)
RNA1
rna1-1
0 15 30 60 90
0 15 30 60 90
(min in chx)
GFP-Ho
Rpn10
37°C
(d)
GFP-Ho relative protein levels
1.0
0.6
0.2
0 15 30 60 90 0 15 30 60 90
(min in cxh)
RNA1
rna1-1
21°C
(e)
GFP-Ho relative protein levels
1.0
0.6
0.2
0 15 30 60 90 0 15 30 60 90
(min in cxh)
RNA1
rna1-1
37°C

Figure 6

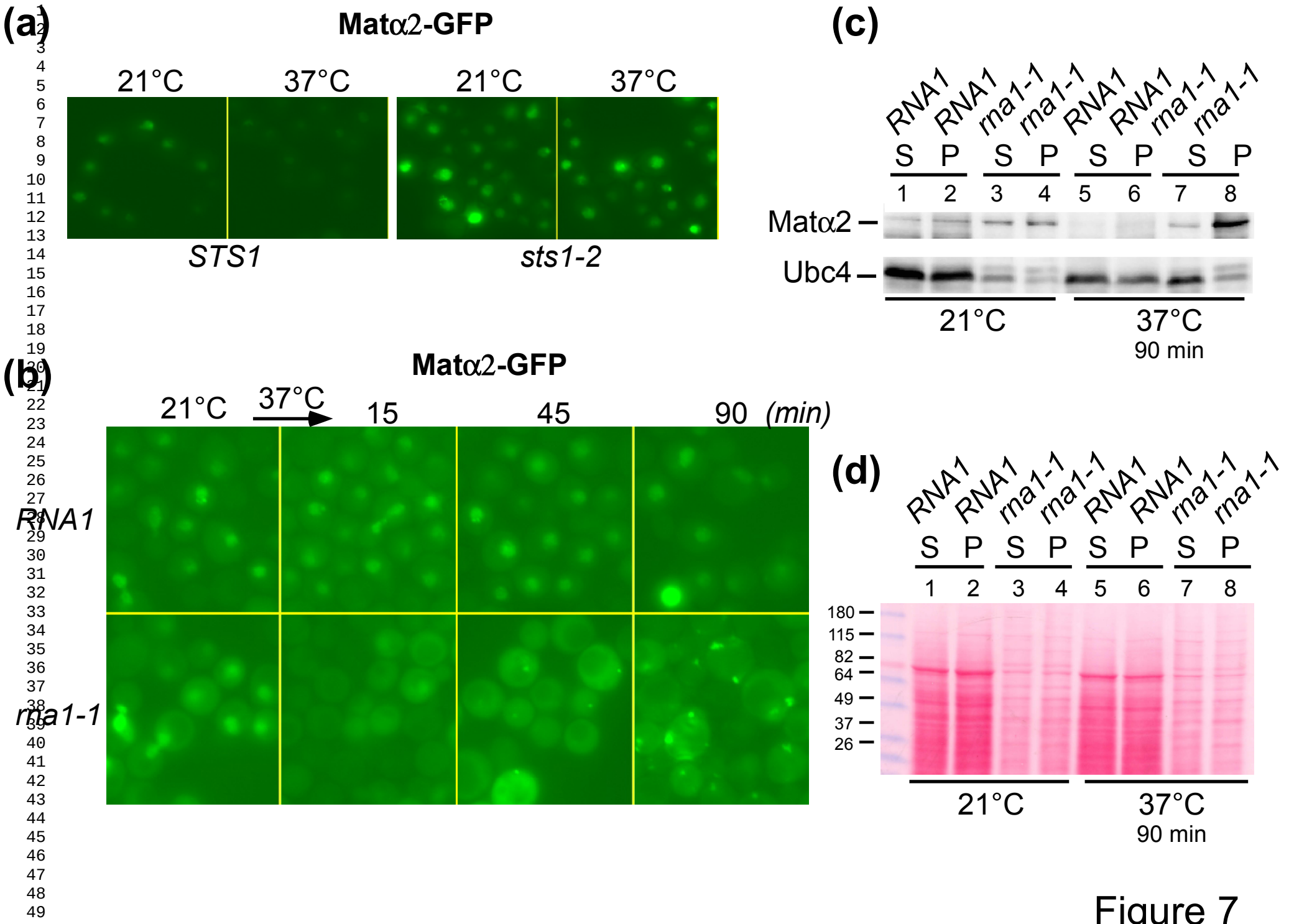
(a)
Matα2-GFP
21°C
37°C
21°C
37°C
STS1
sts1-2
(b)
Matα2-GFP
21°C
37°C
15
45
90
(min)
RNA1
rna1-1
(c)
RNA1
RNA1
rna1-1
rna1-1
RNA1
RNA1
rna1-1
rna1-1
S P S P S P S P
1 2 3 4 5 6 7 8
Matα2
Ubc4
21°C
37°C
90 min
(d)
RNA1
RNA1
rna1-1
rna1-1
RNA1
RNA1
rna1-1
rna1-1
S P S P S P S P
1 2 3 4 5 6 7 8
180
115
82
64
49
37
26
21°C
37°C
90 min

Figure 7

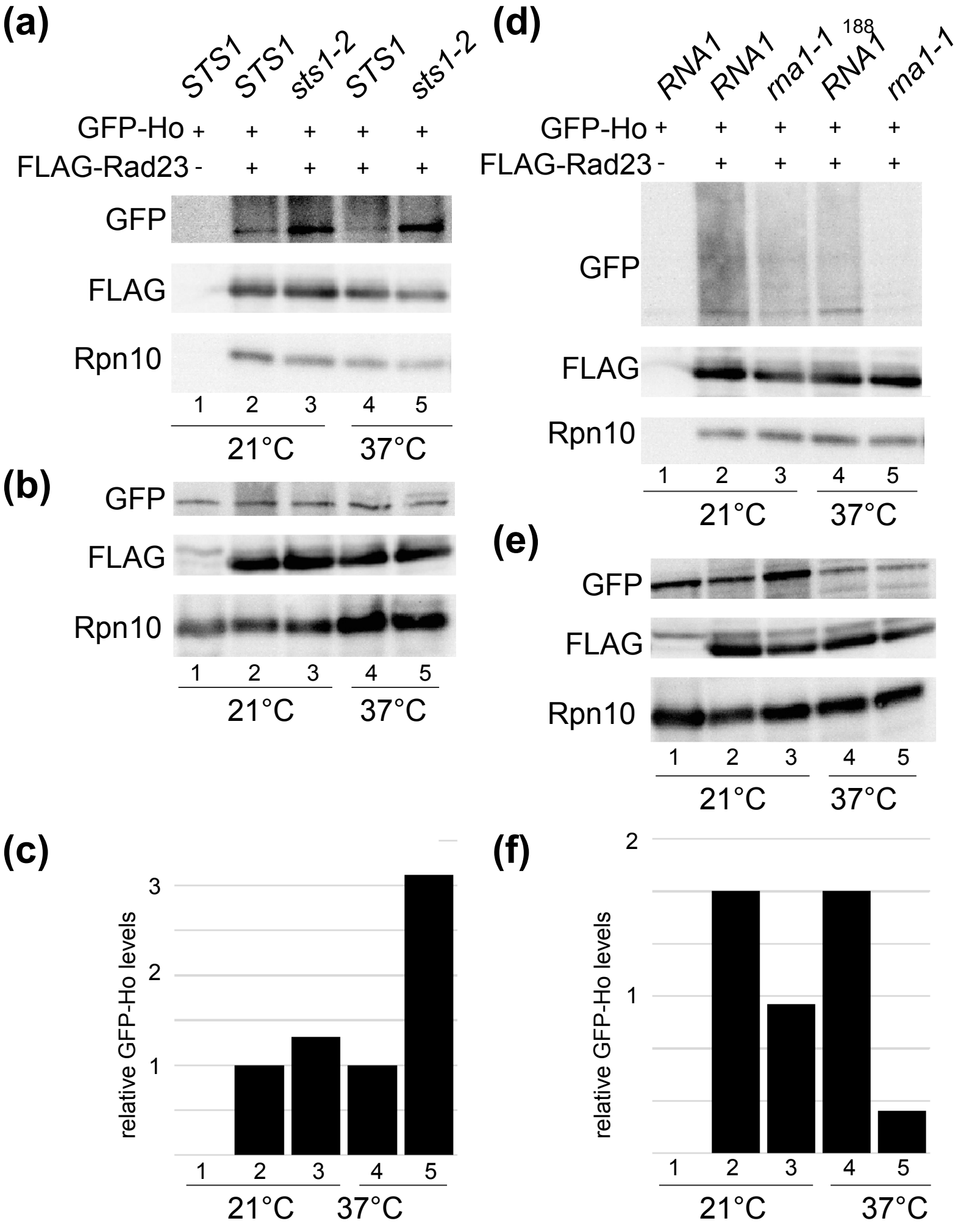
(a)
STS1
STS1
sts1-2
STS1
sts1-2
GFP-Ho + + + + +
FLAG-Rad23 - + + + +
GFP
FLAG
Rpn10
1 2 3 4 5
21°C 37°C
(b)
GFP
FLAG
Rpn10
1 2 3 4 5
21°C 37°C
(c)
relative GFP-Ho levels
3
2
1
1 2 3 4 5
21°C 37°C
(d)
RNA1
RNA1
rna1-1 188
RNA1
rna1-1
GFP-Ho + + + + +
FLAG-Rad23 - + + + +
GFP
FLAG
Rpn10
1 2 3 4 5
21°C 37°C
(e)
GFP
FLAG
Rpn10
1 2 3 4 5
21°C 37°C
(f)
relative GFP-Ho levels
2
1
1 2 3 4 5
21°C 37°C

Figure 8

Supplemental Data for Fig. 3

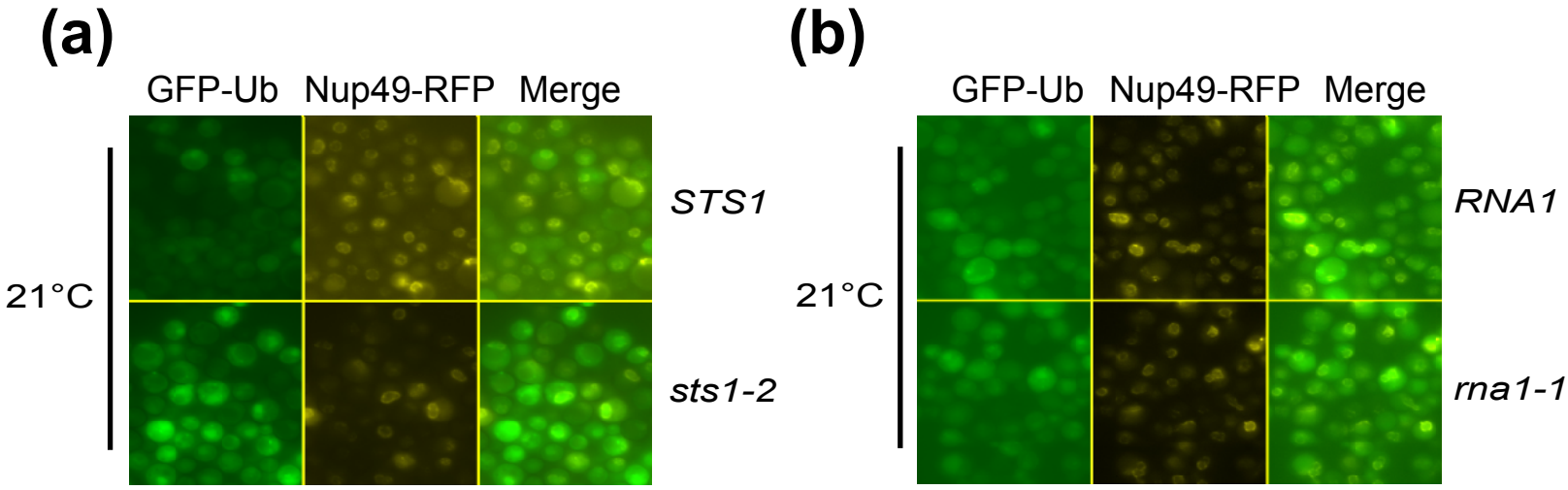

Figure Legend

(a) GFP-Ub was co-expressed with Nup49-RFP in *STS1* and *sts1-2*. Yeast cultures were grown at 21°C and examined by fluorescence microscopy. A merged image is shown in the right column.

(b) GFP-Ub was co-expressed with Nup49-RFP in *RNA1* and *rna1-1*. Yeast cultures were grown at 21°C and examined by fluorescence microscopy. A merged image is shown in the right column.